INNOVATIVE CATALYSTS FOR PROCESS INTENSIFICATION OF METHANE REFORMING AND PROPANE DEHYDROGENATION REACTIONS

Antonio Ricca

Unione Europea

Ministero dell'Istruzione, dell'Università e della Ricerca

UNIVERSITÀ DEGLI STUDI DI SALERNO

FONDO SOCIALE EUROPEO

Programma Operativo Nazionale 2000/2006
"Ricerca Scientifica, Sviluppo Tecnologico, Alta Formazione"
Regioni dell'Obiettivo 1 – Misura III.4
"Formazione superiore ed universitaria"

Department of Chemical and Food Engineering

Ph.D. Course in Chemical Engineering
(XII Cycle-New Series)

INNOVATIVE CATALYSTS FOR PROCESS INTENSIFICATION OF METHANE REFORMING AND PROPANE DEHYDROGENATION REACTIONS

Supervisor
Prof. Vincenzo Palma

Ph.D. student
Antonio Ricca

Scientific Referees
Prof. Vincenzo Palma
Prof. Paolo Ciambelli
Ing. Gaetano Iaquaniello

Ph.D. Course Coordinator
Prof. Paolo Ciambelli

To Milena, my wife

To Elio, my son

Acknowledgements

Il ringraziamento più grande va al prof. Vincenzo Palma, amico e collega oltre che tutor e guida scientifica in questo triennio. La sua esperienza e la sua genialità nell'approccio alla ricerca sono sempre stati il faro rassicurante della mia attività. Grazie a lui ho imparato a proiettare i risultati verso nuovi obiettivi, e a trasformare gli insuccessi in opportunità; da lui ho attinto la vera essenza della ricerca scientifica, e la passione verso questo mondo, passione che porterò sempre con me verso ogni destinazione futura.

Un doveroso ringraziamento va al prof. Paolo Ciambelli, coordinatore del corso di dottorato e membro del comitato scientifico, nonché luminare della catalisi industriale di riconosciuto prestigio internazionale. Aver lavorato con il prof. Ciambelli è stato per me un privilegio, vanto professionale che custodirò con orgoglio.

Un sentito ringraziamento alla Prof.ssa Diana Sannino, per la sua cordialità non disgiunta dalla sua impeccabile competenza, a completare un'equipe didattica e di ricerca di ineguagliabile talento e prestigio.

Un grazie di cuore va all'Ing. Gaetano Iaquaniello, che con la sua cortese disponibilità mi ha aiutato a proiettare il lavoro della ricerca scientifica verso la realtà dell'applicazione industriale.

Un dovuto ringraziamento è rivolto all'amico Antonio Mormile e alla sua "Officina Elettromeccanica", per il "sofferto" aiuto nella realizzazione degli impianti di laboratorio.

Ed al termine di questo percorso, come non esprimere tutta la mia riconoscenza ed ammirazione verso l'amica e collega Emma Palo, la cui professionalità è stata e sarà sempre per me l'orizzonte a cui tendere, e la cui vicinanza, dagli albori della mia carriera accademica sino a quest'ultimo traguardo, è stata sprone e gratifica negli alti e bassi di questi anni. Grazie di cuore, Emma, per tutto ciò che per me sei stata, e per ciò che sarai.

In questi tre anni ho avuto il privilegio di collaborare con tesisti eccezionali, ai quali va tutta la mia riconoscenza, e dei quali conservo in me ricordi straordinari: dalla briosità di Enrico alla travolgente vitalità di Donatella, dalla simpatia di Evrim alla straordinaria eccellenza di Marino, dalla paziente saggezza di Biagio alla freschezza di Erica. La qualità dei risultati illustrati in questa tesi è frutto anche del loro lavoro, ed a loro va tutta la mia gratitudine e stima.

Un ringraziamento speciale deve essere rivolto a Concetta, perché le ultime fasi di questo percorso di dottorato sono apparsi spesso buie e inconcludenti. La sua dolcezza e la sua pazienza mi hanno aiutato a superare le difficoltà e a ridare nuova forza alle mie giornate.

Un doveroso ringraziamento va poi a tutta la "popolazione" dei laboratori T1 e T3 del D.I.In. dell'Università di Salerno, a partire dal "capitano" Vincenzo Vaiano per proseguire con tutta la squadra, partendo dal caro Eugenio per poi passare a Daniela, Marco, Nico, Katty, Claudia, Anna, Olga, concludendo con il sempre disponibile Giuseppe. I risultati di un singolo non possono prescindere dalla buona organizzazione della squadra a cui si appartiene: grazie a tutti voi, ragazzi, per tutto il supporto che mi avete dato.

Ma in un periodo così lungo, può capitare che qualcuno abbandoni la squadra, lasciando nel cuore di chi ha avuto il privilegio di conoscerli un sentimento congiunto di gioia e malinconia. È per questo che mi piace condividere la gioia di questo traguardo con loro, partendo da Elvirosa, le cui doti umane hanno invaso il mio animo che tutt'ora non si rassegna alla sua lontananza. E come non rivolgere un pensiero a Laura, dolce e solare, sempre pronta ad un sorriso di conforto nei non rari momenti difficili. E mi si lasci condividere la soddisfazione di questi giorni con la cara Mena, uragano di dolcezza, allegria, spensieratezza, saggezza ed un pizzico di sana incoscienza; Amica con la "A" maiuscola, seppur lontana, ma sempre presente in un posto caldo del mio cuore.

Infine, voglio condividere la gioia di questo traguardo con Milena, mia moglie, ed Elio, mio figlio, perché loro più di tutti hanno sofferto la mia mancanza in questi lunghi anni di dottorato. Spero che il tempo vi permetterà di capire (e perdonare) l'assenza di un padre dalla propria famiglia, senz'altro io ho avuto modo di capire la straordinaria fortuna di avere una famiglia come voi, di avere te, Milena. questo intenso periodo di lavoro mi ha talvolta conferito una stanchezza alienante, ma non esiste migliore ricompensa dell'amore di una moglie che aspetta a casa, paziente, del sorriso di un figlio che corre tra le braccia chiamando: "Papà!".

The research leading to these results has received funding from the European Union Seventh Framework Programme FP7-NMP-2010-Large-4, under Grant Agreement n° 263007 (acronym CARENA).

Special thanks are due to Arend de Groot, Ca.Re.N.A. coordinator, to give me the possibility to be a part of this very amazing project.

Many thanks to Frans van Berkel, WP1a coordinator, of which I have appreciated the expertise in a wide range of scientific topics as well as his uncommon interpersonal skills, and which of course gave a great contribute to my scientific enrichment.

Publication List

Palma, V., Palo, E., Ricca, A., Ciambelli, P. Compact multi-fuel autothermal reforming catalytic reactor for H_2 production. *Chemical Engineering Transactions*, 25 (2011), 641-646.

Palma, V., Ricca, A., Ciambelli, P. Monolith and foam catalysts performances in ATR of liquid and gaseous fuels. *Chemical Engineering Journal*, 207–208 (2012), 577-586.

Palma, V., Ricca, A., Ciambelli, P. Structured Catalysts for Methane Auto-Thermal Reforming in a Compact thermal Integrated ATR Reformer. *Chemical Engineering Transactions*, 29 (2012), 1615-1620.

Palma, V., Ricca, A., Ciambelli, P. Fuel cell feed system based on H_2 production by a compact multi-fuel catalytic ATR reactor. *International Journal of Hydrogen Energy*, 38 (2013), 406-416.

Palma, V., Ricca, A., Ciambelli, P. Performances analysis of a compact kW-scale ATR reactor for distributed H_2 production. *Clean Technologies and Environmental Policy*, 15 (2013), 63-71.

Palma, V., Ricca, A., Ciambelli, P. Methane auto-thermal reforming on honeycomb and foam structured catalysts: The role of the support on system performances. *Catalysis Today*, 216 (2013), 30-37.

Palma, V., Ricca, A., Ciambelli, P. Structured catalysts for methane auto-thermal reforming in a compact thermal integrated reaction system. *Applied Thermal Engineering*, 61 (2013), 128-133.

Palma, V., Palo, E., Ricca, A., Ciambelli, P. Compact multi-fuel autothermal reforming catalytic reactor for H_2 production. *Conference PRES '11*, 2011, Florence (ITALY).

Palma, V., Ricca, A., Ciambelli, P. Catalytic multifuel ATR reformer for distributed H_2 production. *XXIV Congresso Nazionale della Società Chimica Italiana*, 2011, Lecce (ITALY).

Palma, V., Ricca, A., Ciambelli, P. High efficiency multi-fuel catalytic autothermal reformer for H_2 production. *8th European Congress of Chemical Engineering*, 2011, Berlin (GERMANY).

Palma, V., Palo, E., Ricca, A., Ciambelli, P. Fuel cell feed system based on H_2 production by a compact multifuel catalytic ATR reactor. *4th European Fuel Cell Piero - Lunghi Conference & Exhibition*, 2011, Roma (ITALY).

Palma, V., Ricca, A., Ciambelli, P. Compact multi-fuel auto-thermal reformer for H*2* production. *Fuel Cell 2012 - Science & Technology*, 2012, Berlin (GERMANY).

Palma, V., Ricca, A., Ciambelli, P. Methane auto-thermal reforming in a compact thermal integrated ATR reformer: monolith and foams structured catalyst performances. *The Energy and Materials Research Conference*, 2012, Torremolinos (SPAIN).

Palma, V., Ricca, A., Ciambelli, P. Structured catalysts for methane auto-thermal reforming in a compact thermal integrated ATR reformer. *Conference PRES'12*, 2012, Prague (CZECH REPUIBLIC).

Palma, V., Ricca, A., Ciambelli, P. Monolith and foam catalysts performances in autothermal reforming of liquid and gaseous fuels. *ISCRE22 - International Symposium on Chemical Reaction Engineering*, 2012, Maastricht (THE NETHERLANDS).

Palma, V., Ricca, A., Ciambelli, P. Methane auto-thermal reforming in a compact thermal integrated ATR reformer: monolithic catalysts performances. *IX International Conference on Mechanism of Catalytic Reaction*, 2012, St. Petersburg (RUSSIA).

Palma, V., Ricca, A., Ciambelli, P. Foam Catalysts performances in CH4 Auto-Thermal Reforming. *DEMCAMER & Ca.Re.N.A. Workshop*, 2013, Eindhoven (THE NETHERLANDS).

Palma, V., Ricca, A., Ciambelli, P. Auto-thermal reforming of methane: effect of catalytic support structure. *9th European Congress of Chemical Engineering ECCE9*, 2013, The Hauge (THE NETHERLANDS).

Palo, E., Iaquaniello, G., Cucchiella, B., Palma, V., Ricca, A., Ciambelli, P., Akporiaye, D., Tschentscher, R. Membrane assisted propane dehydrogenation for propylene production. 11th International Conference on Catalysis in Membrane Reactors, 2013, Porto (PORTUGAL).

Palma, V., Ricca, A., Ciambelli, P. Effect of catalyst support on methane processing in a compact thermally integrated ATR reactor. *XIth European Congress on Catalysis*, 2013, Lyon (FRANCE).

Palma, V., Ricca, A., Ciambelli, P. Methane autothermal reforming in a compact thermal integrated ATR reformer: monolithic catalysis performances *XVII National Congress of Catalysis*, 2013, Riccione (ITALY).

Palma, V., Ricca, A., Ciambelli, P. Effect of catalyst support on methane processing in a compact thermally integrated ATR reactor. *4th International Conference on Structured Catalysts and Reactors*, 2013, Bejing (CHINA).

Palma, V., Ricca, A., Ciambelli, P. Auto-thermal reforming of methane: the role of the catalyst support. *Conference Pres'13*, 2013, Rhodes (GREECE).

Palma, V., Ricca, A., Ciambelli, P. Hydrogen production by methane atr in a compact catalytic reactor thermally integrated: structured catalysts performances analysis. *5th European Fuel Cell - Piero Lunghi Conference*, 2013, Rome (ITALY).

Contents

Index of figures

Index of tables

Abstract

In the early decade, a rapid increase in oil consumption was recorded, that led to a widening between the predicted demand for oil and the known oil reserves. Such trend, mainly due to the growing new economies, is causing a quick increasing in oil price, that effect on European chemical industry competitiveness. In this dramatic scenario, characterized by higher cost of naphtha from crude oil, the ability to exploit novel feeds such as natural gas, coal and biomass may be the keystone for the chemical industry revival. Innovating chemical processes are thus essential for the future of the chemical industry to make use of alternative feedstock in the medium and long term future. In this direction, to open new direct routes with rarely used and less reactive raw feedstock such as short-chain alkanes and CO_2 appears one of the most promising breakthrough, since in one hand it may reduce the current dependency of European chemical industry on naphtha, in the other hand may reduce the energy use and environmental footprint of industry.

Despite light alkanes (C1–C4) and CO_2 are stable molecules hard to activate and transform directly and selectively to added-value products, these challenges could be overcome thanks to relevant process intensifications along with the smart implementation of catalytic membrane reactors. Process intensification consists of the development of novel apparatuses and techniques, as compared to the present state-of-art, to bring dramatic improvements in manufacturing and processing, substantially decreasing equipment size/production capacity ratio, energy consumption, or waste production. The past decade has seen an increase in demonstration of novel membrane technology. Such developments are leading to a strong industrial interest in developing membrane reactors for the chemical industry.

The main target of the CARENA is to address the key issues required to pave the way to marketing CMRs in the European chemical industry. The UNISA contribution in CARENA project is to study and optimize supported and unsupported catalysts in order to match to membrane reactors aimed to methane reforming and propane dehydrogenation processes. The guideline of this work was fully jointed to the UNISA involving in CARENA project.

The methane reforming routes (steam- and/or auto-thermal-) are processes widely analyzed in the literature, and many studies identified Ni and Pt-group as most active catalysts, as well as the benefits of bimetallic formulation. Moreover, the crucial role of ceria and zirconia as chemical supports was demonstrated, due to their oxygen-storage capacity. In this work, great effort was spent in the reforming process intensification, in order to maximize catalyst exploit in reforming process.

In order to minimize mass transfer limitations, without precluding the catalyst-membrane coupling, several foams were selected as catalytic support, and were activated with a catalytic slurry. The performances of such catalysts

in the auto-thermal reforming and steam reforming of methane were investigated. Catalytic tests in methane auto-thermal reforming conditions were carried out in an adiabatic reactor, investigating the effect of feed ration and reactants mass rate. Tested catalysts showed excellent performances, reaching thermodynamic equilibrium even at very low contact time. By comparing foams catalyst performances to a commercial honeycomb catalyst, the advantages due to the foam structure was demonstrated. The complex foam structure in one hand promotes a continuous mixing of the reaction stream, in the other hand allows conductive heat transfer along the catalyst resulting in a flatter thermal profile. As a result, the reaction stream quickly reaches a composition close to the final value.

Steam reforming catalytic tests were carried out on foam catalysts at relatively low temperature (550°C) and at different steam-to carbon ratios and GHSV values. The catalytic tests evidenced the relevance of heat transfer management on the catalytic performances, since the samples characterized by the highest thermal conductivity showed the best results in terms of methane conversion and hydrogen yield. The beneficial effect was more evident in the more extreme conditions (higher S/C ratios, higher reactants rates), in which the heat transfer limitations are more evident.

The selective propane dehydrogenation (PDH) was one of the most attractive challenges of the CARENA project, that points to insert a membrane-assisted PDH process in a wider scheme characterized by the process stream recirculation. This approach requires to minimize inerts utilization and side-products formation. Moreover, no papers are present in literature on the concentrated-propane dehydrogenation, due to the severe thermodynamic limitations. A wide study is present in this work aimed to identify and select an optimal catalytic formulation and the appropriate operating conditions that allows the process intensification for the PDH reaction by means of a membrane reactor.

In a first stage, the relevance of side-reactions in the catalytic volume and in the homogeneous gas phase was analyzed, resulting in the optimization of the reaction system. Platinum-tin catalysts were prepared, in order to study the role of each compound on the catalytic performances and lifetime. Preliminary studies have defined the optimal operating conditions, able to minimize the coke formation and then to slow down catalyst deactivation. Several studies on catalyst support highlighted the requirement to use a basic supports with a high specific surface, able to minimize cracking phenomena.

Basing on such indications, CARENA partners provided two catalytic formulations optimized with respect the indicated operating conditions, that showed excellent activity ad selectivity. On these catalyst, the effect of the water dilution, the operating pressure and the presence of CO and CO_2 was investigated, in order to understand the catalytic formulation behavior in the real scheme conditions.

Chapter I
Introduction

I.1 Propane to Propylene

The synthesis of olefins, "building-blocks" in the chemical industry, is nowadays realized by the steam-cracking technology (for the production of ethylene from ethane or naphtha), catalytic cracking (used for the formulation of gasoline, where the olefins are by-products of the process), and catalytic dehydrogenation (for the selective production of propylene and isobutene). They are well-established processes, but which are characterized by very high operating costs, due mainly to the energy needed to provide heat to the highly endothermic reactions. In addition, for these processes exist the concept of economies of scale, therefore the production is cost effective only if made in large plants, for which high investment costs are needed.

I.1.1 The propylene

The propylene (CH_3-CH=CH_2) at room conditions appears as a colorless, odorless and higher density than air (1.915 gL^{-1}). It is not a toxic substance. It shows a high degree of flammability with a flash point of 455°C. Propylene can also generate explosive mixtures with air within the following limits: 2.0 vol% (35 g/m^3) - 11.1 vol% (200 g/m3).

The propylene was one of the first products in the field of petrochemical to be used on industrial scale: in its first employment in the 40s, it was used in the production of isopropanol.

Today it is the second largest commodity in the world and it is used in the production of many important intermediates in the primary chemistry, including polypropylene, acrylonitrile, cumene (in Europe), and propylene oxide.

In 2009, 87.4 million tons of propylene were produced in the world (Davanney, 2009). Since its demand is increasing, an annual production speed growth of 10% is expected, which in 2020 will lead to a production of 120 million tons. As a consequence, the propylene price (Figure I.1) had a constant increasing that led to a quadrupling from 2009 to 2011 (Lemos, 2011).

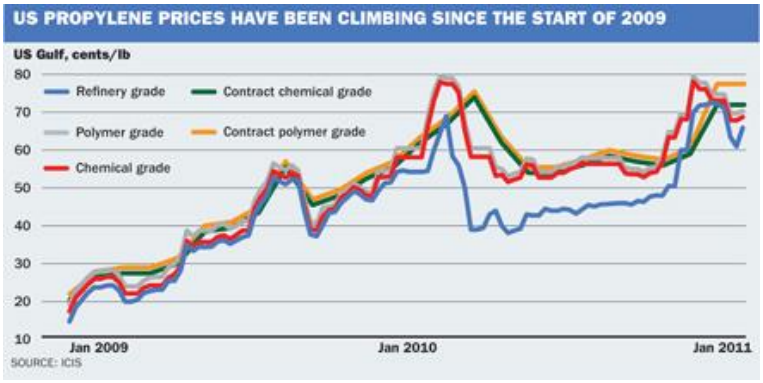

Figure I.1 *Worldwide Propylene price trend from 2009 to 2011 (Lemos, 2011)*

In Europe in 2012 the production capacity was about 15 million tons per year, and the price in Europe was around 1.4 $/tons (Egoy, 2012).

There are three commercial grades of propylene, which differ in the impurities content (usually propane) and are used in different applications (thermal or chemical).

The refinery-grade (which has a minimum propylene content of 65% by weight) is produced from refinery processes and is used primarily as fuel in Liquid Petroleum Gas (LPG) or to increase the octane number in gasoline for cars; can also be used in some syntheses, e.g. for the production of cumene and isopropanol.

The chemical grade (must contain 90-99.8% of propylene) is used in the production of many chemical derivatives such as acrylonitrile and oxo-alcohols.

The polymer grade (which can have no more than 0.5% of impurities) is used in the synthesis of polypropylene and propylene oxide.

Essentially all of the propylene produced for chemical purposes is consumed as a chemical intermediate in other chemical manufacturing processes, aimed to produce polypropylene, acrylonitrile, oxo-chemicals, propylene oxide, cumene, isopropyl alcohol, acrylic acid, and other chemicals.

I.1.2 Propylene production

The annual production of propylene in 2009 reached 87.4 million tons. Of these, 61.4% was obtained from steam-cracking process, 33.18% Fluid Catalytic Cracking (FCC), and only 3.3% from the catalytic dehydrogenation of propane (Nexant, 2009).

I.1.2.1 Steam-cracking

The steam-cracking is the main petrochemical process used to convert paraffins to the corresponding olefins, the primary building blocks of

chemistry. The main product of this process is ethylene, but other important co-products are propylene, butadiene and pyrolysis gas.

It consists of the pyrolysis, in presence of steam, of saturated more or less long hydrocarbons chains, at a temperature of 800-850 °C.

Fed hydrocarbons molecular weight is variable: from light paraffins to gasoline and diesel, according to the geographical areas of production. In the United States is fed primarily ethane (natural gas), while in Europe and Japan, the most widely used feed is naphtha, (naphta-cracking).

The amount of produced propylene, ethylene, butenes changes with the composition of the feed, and percentage of propylene and butenes is much greater in the case of steam cracking of naphtha (Table I.1).

Table I.1 *Main steam-cracking products*

	Feed	
	Naphta	Ethane
Feed Conversion(%)	94	69
Ethylene yield (wt%)	23.52	50.10
Propylene yield (wt%)	16.15	1.67
Butenes yield (wt%)	5.44	0.25

This is an endothermic reaction ($\Delta H°$=124.4 *kJ/mol*), promoted at high temperatures and low pressures, due to the increase in the number of moles. The process is conducted at about 800°C, but at atmospheric pressure: Instead of working in a vacuum system, it's preferable to to use steam as diluent to lower the partial pressure of the feed.

The industrial process must satisfy several requirements. First of all, the reaction heat must be introduced in a very warm system; the partial pressure of the feed mist be reduced and the reaction must occur in less than 1 second. Moreover the product must be captured, in order to promote reaction balance.

The reaction mixture (hydrocarbon and water vapour) passes through a series of pipes placed in a furnace heated by combustion of natural gas or fuel. The contact time in the pipes does not exceed the second, and at the furnace output the separation of the products is realized.

I.1.2.2 FCC (Fluid Catalytic Cracking)

The FCC is a petrochemical process that brings out the heavy fractions of oil to produce gasoline and diesel, but also produces gaseous light fractions C_2, C_3, C_4.

Heavy fuels, vacuum gasoils and deasphalted oils are fed; in Table I.2 a typical product distribution obtained from the FCC is reported. The conversion of the feed reaches values of 78-80%.

Table I.2 *Typical FCC production*

Product fraction	$C_{1,2}$	C_3	C_4	C_5	C_6	Light gasoil	Heavy gasoil	Coke
% wt	1	4	10	9	48	15	8	5

The C3 fraction is composed by 76 wt% of propylene and 24 wt% of propane. The reaction is quite endothermic, is carried out at 400-500°C in the presence of amorphous silica-aluminate catalysts and zeolites in a circulating fluidized reactor. To encourage the production of short chain alkenes, small amounts of zeolite ZSM-5 zeolite in addition to the conventional Y was used.

I.1.2.3 Catalytic dehydrogenation

In the recent years, propylene and butadiene demand is increased more fastly than ethylene, therefore the traditional refinery processes are not able to satisfy the global demand. So the research activity is shifted toward solutions able to produce the only desired olefins. The most important of these is the catalytic dehydrogenation.

The catalytic dehydrogenation (DH) is realized by paraffin reduction in the corresponding olefin, by the subtraction of a molecule of hydrogen.

$$CH_3 - CH_2 - CH_3 \;\rightleftarrows\; CH_3 - CH = CH_2 + H_2$$

Since the reaction is endothermic and associated at an increasing of the number of moles, is favored at high temperatures and low pressures. However, the temperature increase promotes the formation of by-products such as coke and other products of thermal cracking, thermodynamically more stable. To optimize the olefin yield and minimize unwanted by-products is therefore necessary to work in conditions close to atmospheric pressure and at temperatures not exceeding 700°C.

Compared to the steam-cracking, the catalytic dehydrogenation of propane is much more selective toward propylene, although the conversion must be controlled and maintained at lower values necessarily to prevent unwanted parallel reactions. A better selectivity, despite the lower conversion, leads to an increase in yield per cycle, reaching conversion values of 20-40% for the catalytic dehydrogenation, considerably higher than values obtained in the steam-cracking (about 15% weight in the case of naphtha cracking).

The first process of catalytic dehydrogenation of butane to produce butenes has been developed and marketed since 1940 by UOP (Universal Oil Products) in the United States and by ICI in England. The butene was then converted into aviation fuel. In 1943 Phillips Petroleum performed a multi-tubular reactor for dehydrogenation in Texas. At the end of the Second World War, Houdry developed the first low-pressure process for increasing the conversion per cycle. The used catalysts were chromium and alumina based.

In 1959 in the Soviet Union an alternative technology to the Houdry's one had been developed: the process was conducted in a fluidized bed reactor, similar to the FCC, with a continuous recirculation of the catalyst.

Since 1980, the consolidated Houdry technology was also applied to propane for the production of propylene in a process named CATOFIN.

Today there are numerous processes in the world: Oleflex UOP, ABB Lummus Crest Catofin, STAR Phillips Petroleum and FBD-4 licensed by Snamprogetti are the most important.

I.1.2.4 Olefllex UOP

The Oleflex UOP process is industrially used for the dehydrogenation of paraffins C3 and C4. In Figure I.2 is shown a process scheme, which is divided into a reaction section and a separation and products recovery section. The reaction section consists of a series of four adiabatic-stage moving bed reactor and a CCR (Continuous Catalyst Regeneration) for regeneration of the platinum based catalyst. Propane is fed in presence of hydrogen, to facilitate the removal of coke deposited on the catalyst, that causes the deactivation, but the reaction is thermodynamically disadvantaged. The reaction heat is provided by water vapour. At the exit of the reactor the zone of separation of the reaction mixture is placed: unreacted propane is recycled with an amount of hydrogen. The catalyst used is Pt, Sn, K based, supported on Al_2O_3.

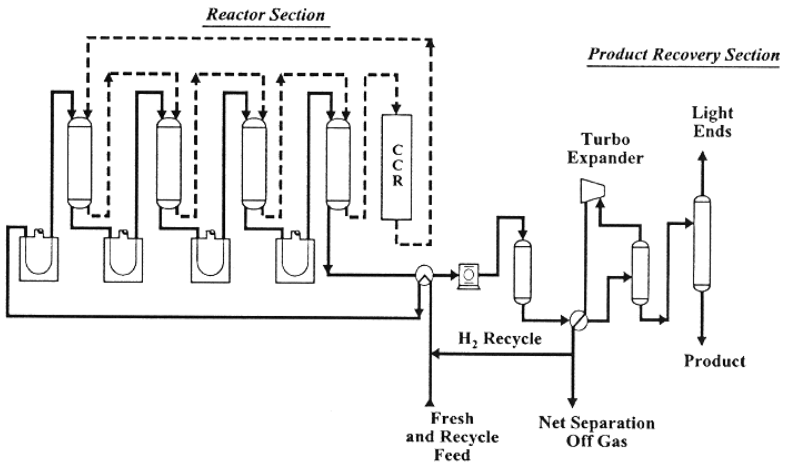

Figure I.2 *UOP Oleflex Process*

I.1.2.5 Catofin ABB Lummus

The Catofin technology was initially developed by Houdry, and is currently owned by United Catalysts Inc. and licensed by ABB Lummus

Crest. In Figure I.3 the process flow-sheet is shown. The system which operates under vacuum conditions (0.5 atm) with a system of multiple fixed-bed adiabatic reactor. It is a batch process with alternating cycles of reaction and regeneration of the catalyst in a flow of steam. The reactors that alternate are five: in two of which the reaction occurs, in other two the regeneration phase takes place, and the last one is in reclamation. The total cycle has a duration of 15-30 min. The used catalyst is based on chromium oxide supported on alumina. The supplied propane is preheated with the heat produced by combustion of coke in the regeneration phase.

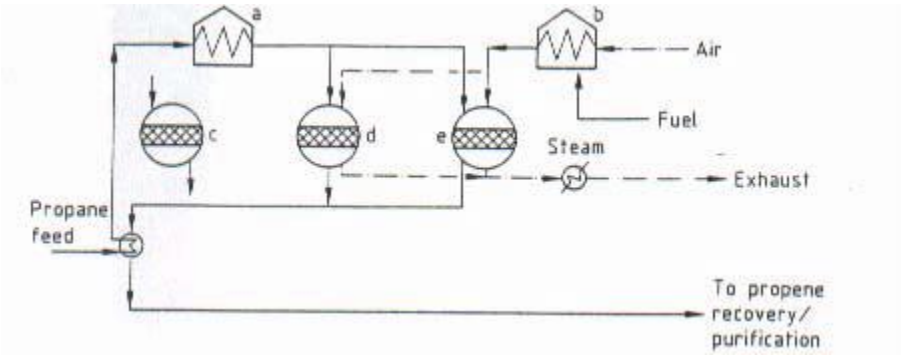

Figure I.3 *Catofin Process: (a) feed pre-heating; (b) air heating; (c) cleaning fixed bed reactor; (d) working reactor; (e) regenerating reactor.*

I.1.2.6 STAR Phillips Petroleum

The STAR process (Steam Active Reforming) developed by Phillips Petroleum is used for the dehydrogenation of light paraffins and the dehydrociclization of C6 and C7 paraffins.

In Figure I.4 a process scheme is shown. It is a fixed bed multi-tube isothermal reactor in which simultaneously steam and propane are fed. In this way the necessary heat to the reaction is provided and the reagent is diluted to limit the formation of coke. It's so possible to work with high total pressure to increase the conversion, but at the same low partial pressure of reagent to limit by-products production.

The catalyst, Pt promoted by Sn supported on $ZnAl_2O_3$, requires a periodic regeneration: normally after 7 hours of reaction a regeneration is needed. Therefore for continuous operations, several reactors are needed: 7 normally operate for reaction and one in regeneration.

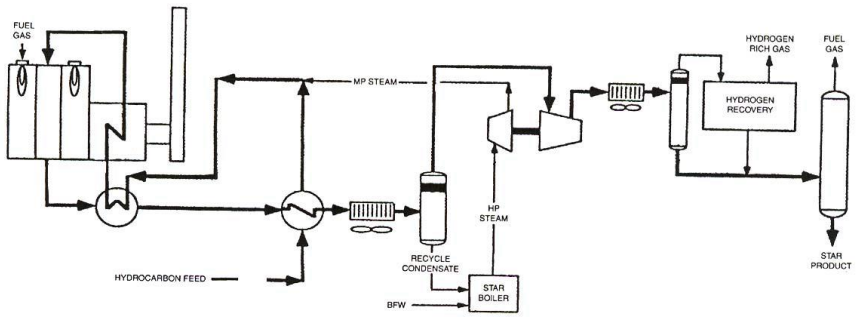

Figure I.4 *Phillips Star process layout*

I.1.2.7 FBD-4 Snamprogetti

This process works with a fluidized bed reactor. The catalyst is realized by chromium oxide supported on alumina with an alkaline promoter. The reaction heat is supplied by the circulation of hot regenerated catalyst (Figure I.5). In general this process is very similar to the FCC.

Since back-mixing phenomena occur that have a negative effect on the yield of propylene, horizontal baffles are inserted in the reactor to limit the back-flow of the catalyst. The latter circulates continuously from the reactor to the regenerator, where deposited coke is removed. Fuel is fed to the regenerator to develop heat enough to warm up the catalyst.

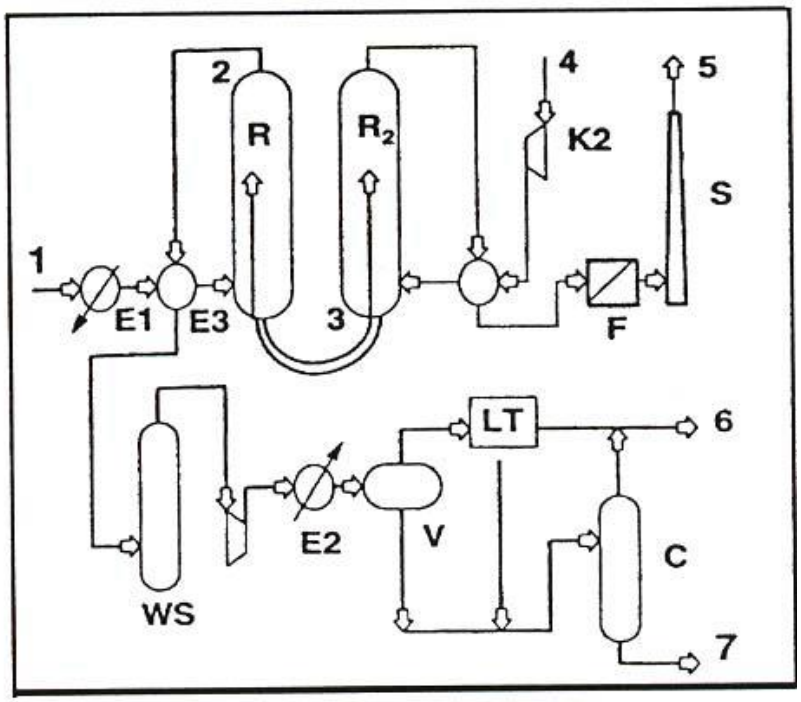

Figure I.5 *Snamprogetti catalytic dehydrogenation process layout: R: Reactor; R2: Regenerator; C: Depropanizer; 1: Propane; 2: reactor effluent; 3: catalyst recirculating; 4: air regeneration; 5: flue gas; 6: light ends; 7: propylene*

I.1.3 Catalyst

The main catalytic systems with dehydrogenation activity reported in the scientific literature and patents are:

- the Group VIII metals (mainly platinum with tin) supported on alumina with promoters;
- chromium oxides on alumina or zirconia, with promoters;
- supported iron oxides, with promoters;
- gallium oxide as a supported or included in zeolite structures: Gallium, in / on mordenite on SAPO-11, on MCM-41, of TiO_2, Al_2O_3 on copper, for the dehydrogenation of alcohols to aldehydes.

Including the most recent literature, the scenario of catalytic dehydrogenation and their applications are configured as shown in Table I.3.

Table I.3 *Dehydrogenation catalyst performances*

Catalyst Active Compound	Light paraffins dehydrogenation	C10-C14 Paraffins dehydrogenation	Ethylbenzene-styrene dehydrogenation

Pt/Sn	excellent	excellent	poor
Cr oxides	excellent	weak	good
Fe Oxides	poor	not available	excellent
Ga systems	excellent	not available	excellent

Commercial applications have restricted potential catalysts to those listed below:

- for ethyl-benzene dehydrogenation to styrene: Fe oxides as the only choice;
- for long-chain paraffins for labs: Pt/Sn promoted on Al_2O_3;
- for light paraffins to olefins: Pt/Sn promoted on Al_2O_3 and Cr_2O_3 on Al_2O_3.

The two great families of catalysts for the dehydrogenation of paraffins (based on Pt and Cr) have been developed in parallel. These two families did not differ substantially in terms of activity and selectivity, but rather in terms of quality of some products and processes needed to complete the regeneration after the combustion of coke. Moreover, the phenomena that lead to irreversible deactivation (sintering, volatilization of the active components and morphological or phase transformations of the substrate) are typically associated with chemical species that characterize the various catalysts.

I.2 Methane and hydrogen production

Hydrogen is the lightest and the most plentiful chemical element of the universe: it's present in the water and in all the organic compounds. It may be considered as the optimal fuel: it presents the highest energetic density, and don't produce pollutant gases. From these considerations, we can conclude that hydrogen must be the only world energetic source, but it's not the real situation. The motivation of this apparent contradiction is due to the fact that hydrogen is not present in the nature in free form, but it may be extracted (more or less expensively) from the substance in which it's contented (mainly water, but also from organic compounds, alcohols, etc.). For this reason, hydrogen can't be considered as an energetic source, but properly an energetic vector for transfer and/or stock energy. In this direction, hydrogen may be considered as the only theoretically inexhaustible energetic vector, able to satisfy the world energy demand for the next years. Moreover, it's a zero-carbon fuels: hydrogen combustion produces steam only.

I.2.1 Hydrogen production technologies

Hydrogen may be produced mainly by 2 methods: hydrocarbons reforming (steam reforming, partial oxidation and auto-thermal reforming), or water electrolysis. Due the widespread fossil fuels distribution pipelines and their relatively low costs, the former method is preferred than the latter. Actually, only 4% of hydrogen production is obtained by electrolytical way, while hydrocarbons reforming still remain the favorite choice, and results as the most viable solution in the short and middle term.

I.2.2 Steam Reforming

The steam reforming is a chemical process in which hydrocarbons, by reacting with high temperature steam, are oxidized by extracting oxygen from water molecules and so releasing hydrogen molecules.

The process may be divided in 4 main phases:

- Feed purification;
- Methane Steam Reforming (SR);
- Further CO oxidation to produce CO_2 (well note as CO-Shift or Water-Gas-Shift);
- Product purification.

Reactants purification is needed because some components (like sulphur compound) may poison catalysts used in the next stages. Instead in products purifications several by-products are removed, such as steam in excess, CO_2, CO, non-converted hydrocarbon and eventually nitrogen: the purification degree strictly depend on the further hydrogen uses.

The steam reforming is substantially exploited in the 3rd and 4th pints, described by the following reactions:

$$CH_4 + H_2O \rightleftarrows CO + 3H_2$$
$$CO + H_2O \rightleftarrows CO_2 + 3H_2$$

The steam reforming is an very endothermic equilibrium reaction, so external heat must be provided to the system. Further, in order to achieve high hydrocarbon conversion, high operating temperature (higher than 700°C) is needed. Too high temperature is not a viable solution, because, in order to sustain the endothermic reaction, external heat must be supplied at a very warm system, by using heater means warmer than system, and so several problems due to the material thermal resistance may occur. Therefore, in the industrial processes, the steam reforming reaction is performed in 2 stages: in a first stage methane and steam react at 700-800°C, so obtaining a hydrocarbon conversion up to 90%. In the second stage, an amount of air (or oxygen) is added to the reforming gas, that reacts with a part of produced hydrogen. The heat generated to this reaction increase reaction mixing temperature op to 1000-1200°C, so allowing a quasi-complete hydrocarbon conversion. This process is carried out a very high temperature, and therefore don't undergoes to kinetic limitations, and it easily reach thermodynamic equilibrium. However, the steam reforming reaction may be followed by several side-reactions, that lead to the coke formation:

$$2CO \rightleftarrows CO_2 + C$$
$$CO + H_2 \rightleftarrows C + H_2O$$
$$CH_4 \rightleftarrows C + 2H_2$$

The steam reforming is a catalytic reaction: the most common catalysts are Nickel or Platinum supported on calcium aluminate, that assure a good selectivity towards the reforming reactions and avoid coke formation. The support has the twice function of improve the mechanical properties of cat6alytic system and of increase the surface/mass ratio.

The steam reforming reaction is characterized to an increase in total molar number and therefore it's favored in low pressure conditions. Steam-to-carbon ratio must be as higher as possible, both to favor products formation and to avoid coke formation. However, too high steam-to-carbon ratio results as a non-ideal operating condition, mainly because to the expensive pre-heating of the fed steam.

The "top-fired" are the most common steam reforming reactors, designed as a tube-shell heat exchanger, in which tube-side reactants flow, on the top of the shell a burner is placed to the heat generation, and combustion gas flows shell-side so providing heat to the reactants in the tubes. Naturally, catalyst is placed inside the tubes. This systems have very large sizes (e.g. in order to produce 5000 Nm^3/h of syngas a plant sized 3 x 6 x 11 m is required), and hardly may be scale-based realized.

A little innovation is achieved by the using of plate-exchangers reactors: this solution lead to great benefits for the reduction in plant size, while several problems due to pressure drop and operating limitations may be exceeded.

I.2.3 Partial Oxidation

The methane partial oxidation consists on a hydrocarbon oxidation with an oxygen content less than stoichiometry.

$$CH_4 + \frac{1}{2}O_2 \rightleftarrows CO + 2H_2 \qquad \Delta H^0_{reac} = -35.6kJ/mol$$

It's an exothermic reaction, characterized by a very fast kinetic, that assures contact time very low: this feature allows reaction plants very smaller than steam reforming.

However, partial oxidation implies a lower hydrogen yield, in fact e moles of hydrogen are achieved from a mole of methane, while in the case of steam reforming 3 moles of hydrogen are achieved.

In a mechanistic hypothesis, the methane partial oxidation results as the following of several reactions. In a first time, the total oxidation of an amount of hydrocarbon occurs:

$$CH_4 + 2O_2 \rightleftarrows CO_2 + 2H_2O$$

The combustion heat is partially used to supply steam reforming and dry reforming reactions:

$$CH_4 + H_2O \rightleftarrows CO + 3H_2$$
$$CH_4 + CO_2 \rightleftarrows 2CO + 2H_2$$

The partial oxidation reaction don't need any catalysts, showing good performances for temperatures between 1300 and 1500°C, assuring in the selected conditions a full hydrocarbon conversion and decreasing coke and soot production. The absence of catalysts allows to avoid feed desulphurization, with a notable cost saving. However, such high temperatures make the process hardly controllable, therefore lower temperatures (800-1000°C) are preferred, by using a catalytic system. In these conditions we have a fast reaction kinetic, and side-reactions are avoided. The most common catalyst is nickel or rhodium based: the first one don't exclude coke formation, while the second is very more expensive.

Downstream the partial oxidation reactor, as in the case of steam reforming, a Water-Gas-Shift stage is needed, followed by a product stream purification stage.

I.2.4 Auto-thermal Reforming

The auto-thermal reforming results as a compromise solution between steam reforming and partial oxidation, in which both reactions occurs. By this process from one hand well product composition and hydrocarbon conversion are achieved, from the other no external heat must be supplied.

Fuel (methane), steam and air (or oxygen) are inserted in the reactor. The oxygen reacts with the hydrocarbon in combustion and partial oxidation reactions, so generating an amount of energy further used from the system for the steam reforming reaction between steam and remaining methane. So, the heat produced for the one reaction is used to by the second in the same reactor, so no external heat is needed.

Globally, the reaction may be summarized as:

$$CH_4 + xO_2 + yH_2O \rightleftarrows aCO + bCO_2 + cCH_4 + dH_2O + eH_2 + fC_{(s)}$$

Obviously, d represents the excess water and (a+b+c)=1. The reaction enthalpy ($\Delta H°_{react}$) depends of feed parameters (x, y).

The auto-thermal reforming reaction is very flexible and controllable, by varying x and y parameters as needed. Moreover, between the fuel processes analysed for the hydrogen production, the auto-thermal reforming has the lowest coke formation.

Because of no external heat must be provided to the system, no heat exchangers, steam generators or burners are needed; this feature allows very smaller plants than the former systems, and scale-sized plants are easier to realize.

Auto-thermal reforming is a catalytic process: because it's the synthesis of steam reforming and partial oxidation, the selected catalyst must either favour hydrocarbon oxidation and assure high reforming degree. Conventionally nickel oxide based catalysts based on alumina, calcium oxide and magnesium oxide are used.

I.2.5 Water-Gas-Shift

Downstream all the three analysed processes, a further purification stage is needed: it's the water-gas-shift (WGS) reaction. Mainly, carbon monoxide must be removed from the stream outgoing to the reforming stages, by reacting with steam: by this reaction a further mole of hydrogen was produced for each mole of CO converted.

$$CO + H_2O \rightleftarrows CO_2 + H_2 \qquad \Delta H^0_{reac} = -41 kJ/mol$$

The reaction is weakly exothermic, and is thermodynamically favoured at relatively low temperature (< 200°C). But low temperatures implies slow kinetics, therefore catalysts are needed in the process. Since it's an exothermic

reaction, by using an adiabatic reactor, CO conversion develop a reaction heat that increase reaction stream temperature, so decreasing thermodynamic CO conversion. In order to reduce this phenomenon, preferentially the process is split in in 2 stages, separated by a stream cooling.

The first stage, known as high-temperature water-gas-shift (WGS-HT), is performed at about 350°C, by using an iron-chrome based catalyst.

The second stage, known as low-temperature water-gas-shift (WGS-LT), is performed at about 220°C, by using a copper-zinc based catalyst.

I.3 The membrane reactors

Membrane reactors facilitate simultaneous rate based reactive separation schemes. In addition to the key attributes of membrane technology such as membrane stability, lower catalyst deactivation, higher selectivity and yield, and low cost, the optimal performance of a membrane reactor involves the combinatorial selection of key process variables such as reaction and permeation temperatures, retentate and permeate zone pressures, membrane area per unit volume and membrane thickness. The capability of membrane reactors to enhance reactor conversions has been demonstrated experimentally for different schemes such as dehydrogenation and hydrogenation, oxidative dehydrogenation and other reversible reaction schemes. Based on experimental study of membrane reactors, several literatures attempt to aggrandize the economic potential of membrane reactors, with a basic rule of thumb that enhancement of reactor conversions directly translate into higher profit margins and hence economic competitiveness.

Nonetheless, the admirable characteristics for membrane reactors in process industries have been summarized by Armor (1998), who indicated several materials performance issues for their industrial applicability. These have been summarized as fabrication of crack free thin composite membranes with materials not susceptible to poisoning or fouling, developing compatible membrane-support combinations that can resist temperature cycling, balance between catalyst and membrane distributions for optimal heat and mass transport. Therefore, a first step towards the selection of membrane reactors for industrial schemes involves a mandatory exercise on the materials performance issues.

Based on simulations conducted for various process schemes associated to fluidized membrane reforming, Roy et al. (1998) concluded that the cost of producing hydrogen from membrane integrated fluidized reformers was 5% lower than the cost affordable to produce hydrogen by best configurations deploying conventional reactor technology only. Petersen et al. (1998) concluded that the membrane integrated reforming process is not competitive to the traditional steam reforming process and only with exceptional unit costs of power and membranes could make the membrane integrated reforming process an inexpensive and attractive alternative for reforming.

A number of metal membranes are highly hydrogen selective at higher temperatures. Especially palladium and platinum can therefore be used for the production of highly purified hydrogen from steam reforming of gases. Ultra-pure hydrogen, generated from these reactions, is extracted by use of thin dense metallic membranes that are 100% selective to hydrogen. The mechanism of the transport is the separation of hydrogen into protons and electrons at the surface and recombination on the filtrate or raffinate side.

Hydrogen selective membranes offer the possibility of combining reaction and separation of the hydrogen in a single stage at high temperature and

pressure to overcome the equilibrium limitations experienced in conventional reactor configurations for the production of hydrogen. The reforming reaction is endothermic and can, with this technique, be forced to completion at lower temperature than normal (typically 500-600°C). The shift reaction being exothermic can be forced to completion at higher temperature (300-450°C). Membrane reactors allow one-step reforming, or a single intermediate water gas shift reaction, with hydrogen separation (the permeate) leaving behind a retentate gas which is predominantly CO_2 and steam, with some unconverted methane, CO or H_2. After clean-up, condensation of the steam leaves a concentrated CO_2 stream at high pressure, reducing the compression energy for transport and storage. The need for multiple shift reaction stages is avoided. Moreover, process intensification with membrane reactors allows for more compact units, lower investment cost, higher yields and reduced energy cost. In the same way, hydrogen removing from the products may force dehydrogenation reactions, thermodynamically limited, towards further hydrogen production, and therefore increase hydrocarbon conversion.

However, some problems must be exceeded to obtain a stable and optimal membrane using. The greatest limit of membrane reactors concerns the operating temperature of a membrane. Previous studies have demonstrated that high temperature reduces the membrane life, as well as the membrane perm-selectivity. By working to temperature typical of reforming or dehydrogenation processes, not only hydrogen permeates the membrane, but also other stream components, so reducing the desired benefits.

I.4 The CARENA project

(CAtalytic membrane REactors based on New mAterials for C1-C4 valorization)

The last decade has seen an increase in dempstration of novel membrane technology, mainly in the carbon capture and fuel cell fields, bringing this technology out of the labs. Dense conducting membranes have been demonstrated at pilot-scale. These developments are leading to intensified industrial interest in developing membrane reactors for the chemical industry. The objective of the CARENA project is to develop and implement novel nano-structured materials and optimized chemical processes to enable the efficient conversion of light alkanes into higher value chemicals resulting in the reduction in the number of process steps and increase in feedstock flexibility for the European chemical industry.

CARENA aims to achieve break-through in catalytic membrane materials and processes at 3 levels:

1. Enable selective conversion of raw feedstock such as light alkanes (C1-C3) by generating in situ active species). The integration of catalyst and membrane will be optimized.

2. Develop reactor concepts, that match and control highly intensified rates of mass and heat transfer resulting from application of novel materials and architectures. Process intensification combining in-situ reaction and reparation will be designed for equilibrium-limited reaction for high industrial relevance.
3. Create novel process schemes, that translate novel materials and reactions concepts into innovative industrial processes that exploit the opportunities, such as reduction of the number of process steps and elimination of energy intensive separations.

CARENA focuses on the activation of three specific primary feedstock: methane, propane and CO_2. The integrated scheme of process is shown in Figure I.6.

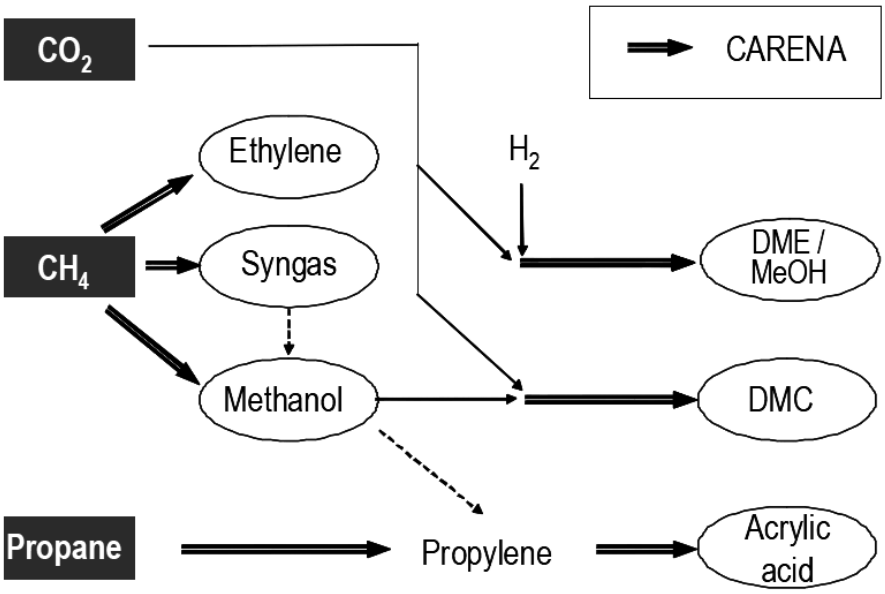

Figure I.6 *CARENA's integrate scheme of process*

The main routes are:

a) Indirect and direct route for conversion of methane into olefins and methanol
b) (Oxidative) dehydrogenation of propane and subsequent selective oxidation of a propane/propylene mixture to acrylic acid.
c) Direct conversion of CO_2 into dimethyl carbonate (DMC) and dimethylether (DME) and methanol (MeOH).

To achieve competitiveness and sustainability of new chemical processes through the development of highly innovative nano-structured materials and optimized membrane-reactors, scientific excellence needs to be combined

with industrial know-how of leading businesses. CARENA brings together companies and institutes from 8 European countries. European chemical companies as AkzoNobel and Arkema ensure a strong industrial leadership to the project. Technology providers and developers include Johnson Matthey, StGobain, Technip KTI, Linde, Acktar and PDC. Scientific excellence is strengthened with top-level academic partners and research institutes: CEA, ECN, SINTEF, CNRS-IEM, CNRS-IRCE, Diamond, Technion, Universities of Salerno, Twente and Hannover. As a very complex and effective operating network, activities of each partners are arranged in a multi-level and multi-task scheme (Figure I.7) able to exploit the skills of the involved partners in a common research pathway.

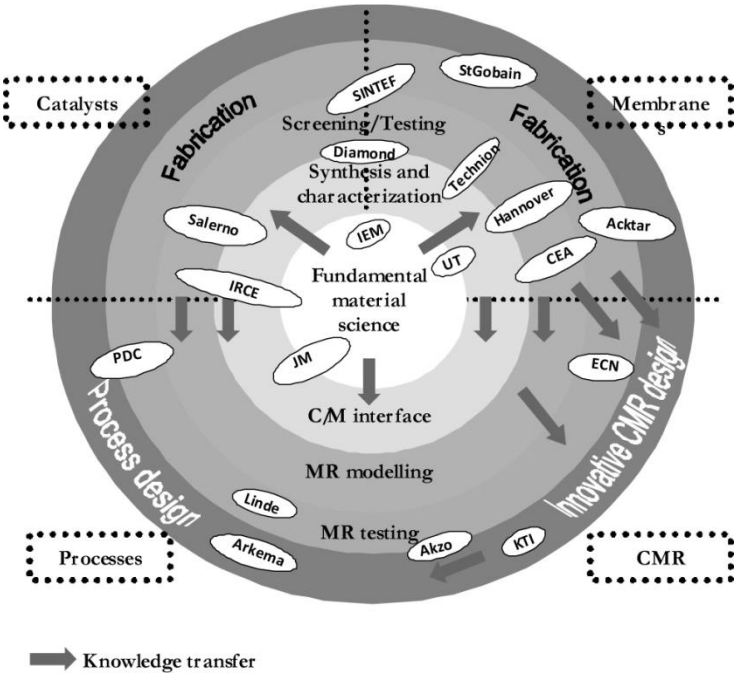

Figure I.7 *CARENA knowledge transfer scheme*

I.4.1 UNISA in CARENA

In order to contribute in the CARENA project, the University of Salerno will perform several tests on the catalytic activity in some of the selected process in the project.

As a first, reforming of methane will be studied. The screening of different structured catalyst supports (ceramic and metal substrates, like honeycomb, foam and wires) covers great importance in the process intensification. The individuation of optimal support to couple to a membrane reactor results as a fundamental step in the catalyst preparation. Long term tests will be performed

with the selected coated catalyst samples at reforming conditions, in order to evaluate the support efforts and the stability of the system.

Great attention was aroused on the propane dehydrogenation, in order to obtain high selective processes by starting from pure propane. The formulation of novel catalyst-support combination, active in the selected operating conditions, results as a starting point towards novel membrane catalytic reactors. In this objective, UNISA should understand the effect of the operative conditions in the PDH performances, by validating and supporting numerical evaluations carried out by partners. In this aim, UNISA will test catalysts prepared by partners, so understanding any weakness of the formulations and eventually suggesting appropriate modifications.

Chapter II
State of the art

II.1 Methane reforming: state of the art

In the methane auto-thermal reforming, the catalyst selection is of great importance. An optimal catalytic system play a crucial role both in hydrocarbon conversion and in the reaction selectivity; so the choice of a catalyst rather than another can lead to different product compositions. Naturally, the active species be selected on the basis of the operating conditions and the used hydrocarbon. As seen, auto-thermal reforming is composed at least by two reaction: the steam reforming and the partial oxidation. Therefore, the selected catalyst must assure an high selectivity toward these two reactions, and must avoid other side-reactions, first of all the hydrocarbon cracking.

By several studies performed several decades ago, nickel (JR-Rostrup-Nielsen, 1975) and cobalt (JR-Rostrup-Nielsen, 1993) supported on alumina or magnesia spinel, often promoted by alkaline compounds (Bharadwaj SS, 1995) to remove carbonaceous compounds, or supported on rare metals oxides, especially cerium oxide (Craciun R, 2002) , result as the favorite catalytic systems for steam reforming reactions. In the other hand, partial oxidation is a very quick process, and so smaller reactors are needed. By using nickel based catalyst on alumina, the coke deposition on the catalyst surface was reported (Dhammike Dissanayake, 1991), that produces catalyst pores clogging and so catalyst deactivation. Moreover, by working with molar feed ratio $C/O_2>2$ catalyst break-up in very fine powders was observed. A complex study (Ruckenstein and Hu, 1999) concluded that nickel oxide supported on magnesium oxide (NiO-MgO) show both a promising catalytic activity and a high selectivity, in solid solution; while, as a mechanic mixture, an evident decreasing of these features are reported. However both activity and selectivity may be improved by increasing calcination time. Moreover, a better activity, stability and selectivity were remarked for NiO loaded between 9.7 and 35 $\%_{mol}$: too low concentrations lead to a decrease in activity and stability; concentration too high lead to low stability.

The improvement in methane conversion obtained by adding noble metals as rhodium, platinum and palladium to a NiO-NgO solid solution was reported(M. Nurunnabi, 2006): such benefits result more evident even by using very poor content (0.035%). It's demonstrated that the presence of such noble metals holds nickel in the reduced state, so improving methane conversion. Moreover, in pressurized conditions, it's observed that rhodium and platinum reduce coke formation.

In a comparative study (S. Ayabe, 2003) the catalytic behavior of several metals supported on alumina was reported for auto-thermal reforming of methane and propane. As results of this analysis, an activity classification may be defined: Rh>Pd>Ni>Pt>Co. Moreover, in rich steam operating conditions, no coke formation was observed in methane processing, while in propane auto-thermal reforming more evident coke compounds were achieved.

In study on the effects of ceria (CeO_2) (Trovarelli, 1996), especially in platinum group metal (PGM) catalysts, as Pt, Rh, Pd, was reported that ceria leads to an increase in catalytic activity toward hydrocarbon and CO, due to its oxygen storage capacity. This behavior was more marked for ceria-zirconia mixtures(S. Bedrane, 2002). The improvement achieved by adding zirconia (Roh et al., 2002) may be due to its high stability at high temperature, as well as to its high surface area; moreover, Hori et al (X. Wu, 2004) in their studies have observed the very high oxygen storage capacity in CeO_2-ZrO_2 mixtures.

The behavior of a 1% platinum based catalyst supported on ZrO_2-Al_2O_3 in the auto-thermal reforming of methane was analyzed(M. M.V.M. Souza, 2005), by comparing the obtained results with Pt/Al_2O_3 and Pt/ZrO_2 catalysts. An higher activity and stability of the former was observed by performing an auto-thermal reforming test at 800°C. The high stability may be due to the avoiding to coke formation, due in turn to Pt-Zr interaction on the metal-support interface.

The effect of some transition metals (Cu, Co, Fe) on $Ni/Ce_{0.2}Zr_{0.1}Al_{0.56}O$ catalysts in the methane auto-thermal reforming was studied(X. Dong, 2007). The performed tests show that by adding copper and cobalt lead to an increasing on catalyst activity for low temperature, while by adding iron a decrease in catalytic activity was observed. The authors conclude that the presence of copper leads to a high nickel oxide dispersion, so inhibiting the formation of species as $NiAl_2O_4$.

Nickel based catalyst supported on CeO_2-ZrO_2/SiO_2 (silica spheres impregnated with a ceria-zirconia mixture) was tested in a fluidized bed (J. Gao, 2008). Such catalyst, due to the presence of silica, is characterized by a very higher surface area (300 m^2/g) than for the only ceria and zirconia supported (6 m^2/g): this feature leads to an higher activity. Moreover, in the selected catalyst a high active species dispersion is observed, so making nickel highly reducible and giving to the catalyst a great capacity to activate the methane.

Methane auto-thermal reforming tests by using nickel base catalysts supported on α-Al_2O_3, on Y_2O_3 or a combination of both were performed (D.C.R.M. Santos, 2009). Naturally, the presence of yttrium oxide implies a strong surface area increasing (8%Ni/α-Al_2O_3 = 3.9 m^2/g; 8%Ni/5%Y_2O_3/α-Al_2O_3 = 18.6 m^2/g). Best performance, in order to both conversion and stability, are obtained by 8%Ni/5%Y_2O_3/α-Al_2O_3 configuration; the configuration without Y_2O_3 showed very low stability, the configuration without α-Al_2O_3 showed low activity. The benefit leaded by adding yttrium oxide may be explained in the formation of a Ni-Y_2O_3 intermediate on the surface, that preserve nickel toward coke deposition.

II.2 Propane dehydrogenation: state of the art

Paraffin dehydrogenation for the production of olefins has been in use since the late 1930s. During World War II, catalytic dehydrogenation of butanes over a chromia-alumina catalyst was practiced for the production of butenes, which were then dimerized to octenes and hydrogenated to octanes to yield high-octane aviation fuel.

In the dehydrogenation process using chromia-alumina catalysts, the catalyst is contained in a fixed shallow bed located inside a reactor that may be either a sphere, a squat vertical cylinder, or a horizontal cylinder. The actual design reflects a compromise between gas flow distribution across a large cross-sectional area and the need to maintain a low pressure drop. A significant amount of coke is deposited on the catalyst during the dehydrogenation step, therefore, a number of reactors are used in parallel. The dehydrogenation reactions are strongly endothermic, and the heat is provided, at least in part, by the sensible heat stored in the catalyst bed during regeneration (carbon burn); additional heat is provided by direct fuel combustion and also by heat released in the chromium redox cycle. The length of the total reactor cycle is limited by the amount of heat available, and can be as short as 10–20 min.

The Houdry Catadiene process was used extensively for the production of butadiene, either by itself (n-butane to butadiene) or in conjunction with catalytic oxydehydrogenation of n-butene to butadiene. The latter was commercialized by the Petro-Tex Chemical Corp. (Waddams, 1980) and was called the Oxo-DTM process. A similar oxydehydrogenation approach for the production of butadiene was also practiced by Phillips Petroleum (Waddams, 1980). Large quantities of butadiene have become available over the past 30 years, mostly as a by-product from the thermal crackin g of naphtha and other heavy hydrocarbons. This market shift has resulted in the shutdown of all on-purpose catalytic dehydrogenation units for butadiene production in North America, western Europe, and the far East.

In the late 1980s, the application of chromia-alumina catalysts was extended by Houdry to the dehydrogenation of propane to propylene and

isobutane to isobutylene. The new process application called CatofinTM (Weiss, 1970, Graig and Spence, 1986) operates on the same cyclic principle as in the former Catadiene process. The Catofin process technology is currently owned by Sud-Chemie and is offered for license by ABB Lummus.

In 1959, an alternative chromia-alumina catalytic dehydrogenation process was developed in the former Soviet Union. This process avoided the use of the cyclic operation by using a fluidized bed reactor configuration similar to the fluidized catalytic cracking (FCC) process used in refineries (Sanfilippo et al., 1998). However, back-mixing common to dense fluidized bed operations results in poor selectivity and increases the formation of heavies, sometimes called "green oils". Circulating regenerated catalyst is used to provide the heat of reaction in the riser and spent catalyst is reheated by carbon burn in the regenerator.

A different approach to catalytic dehydrogenation was first introduced in the mid-1960s for the supply of long-chain linear olefins for the production of biodegradable detergents. The work on catalytic reforming with noble metal (Pt) catalysts done in the 1940s by Haensel clearly demonstrated that Pt-based catalysts had high activity for the dehydrogenation of paraffins to the corresponding olefins(Haensel, 1952). In the 1960s, Bloch (Bloch, 1969) further extended this thinking by developing Pt-based catalysts that could selectively dehydrogenate long-chain linear paraffins to the corresponding internal mono-olefins with high activity and stability and with minimum cracking. This was the basis for the UOP PacolTM process for the production of linear olefins for the manufacture of biodegradable detergents (Berg and Vora, 1982). In 1999, there were more than 30 commercial Pt-catalyzed dehydrogenation units in operation for the manufacture of detergent alkylate.

Long-chain paraffins are both valuable and highly prone to cracking. Therefore, in order to maintain high selectivity and yield, it is necessary to operate at relatively mild conditions, typically below 500°C, and at relatively low per-pass conversions. While this is economical for the production of heavy linear olefins, it is not for the production of light olefins.

Paraffin dehydrogenation is an endothermic reaction that is limited by chemical equilibrium and, according to Le Chatelier's principle, higher conversion will require either higher temperatures or lower pressures.

Literature propose some kinetics approach to the reactions involved in the propane dehydrogenation process (Farjoo et al., 2011), underlining that an optimal management of residence time may maximize selectivity to propylene vs others side-products

Detailed studies (Kumar et al., 2009) were carried out on the influence of tin in platinum based catalysts. The active species are supported on SBA-15, a mesoporous silica-based material with high surface area and high thermal stability. Dehydrogenation of propane over these catalysts was studied at 793 K. Sn results in higher Pt dispersion by alloy formation in Pt-Sn-SBA-15. This leads to the formation of smaller Pt particles in Pt-Sn-SBA-15-IW than in Pt-

SBA-15. Catalytic properties of Pt sites are influenced by modification of electronic properties of the same sites by Sn in bimetallic Pt–Sn alloy particles. Higher propane conversion and higher amount of coke formation on smaller Pt particles (Pt-Sn-SBA-15) than on the larger (Pt-SBA-15) are due to higher surface roughness of the former than that of the latter. Tin addition so leads to an higher selectivity to propylene and superior catalyst stability due to weaker adsorption affinity of hydrocarbons on the surface Pt sites in Pt-Sn bimetallic particles.

Further studies (Vu et al., 2011a) indicated the role of tin in coke formation. The increasing of tin loading on a Pt-Al2O3 catalyst effects on the electronic properties of Pt allowing better coke tolerance and a catalytic performance. In particular, the tin presence induced the shift of coke oxidation temperature to higher because Sn addition accelerates the transfer of coke to the support. Tin addition leads to transfer of coke from the metal to the support, with the ratio of coke fraction on the metal to support deceasing significantly.

A similar result was observed by studying the Indium effect on a Pt/Mg(Al)O catalyst in ethane and propane dehydrogenaiton (Sun et al., 2011). For both reactants, maximum activity was achieved for a bulk In/Pt ratio of 0.48, and at this In/Pt ratio, the selectivity to alkene was nearly 100%. Coke deposition was observed after catalyst use for either ethane or propane dehydrogenation, and it was observed that the alloying of Pt with In greatly reduced the amount of coke deposited. While the amount of coke deposited during ethane and propane dehydrogenation are comparable, the effects on activity are dependent on reactant composition. Coke deposition had no effect on ethane dehydrogenation activity, but caused a loss in propane dehydrogenation activity. This difference is attributed to the greater ease with which coke produced on the surface of PtIn nanoparticles migrates to the support during ethane dehydrogenation versus propane dehydrogenation.

The effect of sodium on Pt-Sn catalyst was investigated in the literature (Duan et al., 2010), remarking that the presence of sodium modified the properties of the Pt metal phase. The Pt dispersion, combined with interaction between metal and support, were effected by the sodium content,which may be responsible for catalytic properties. The sodium existence also neutralized the strong acidic sites of catalysts, thus reduced the formation of coke effectively. However, the incorporation of excessive sodium prompted the reduction of Sn species to Sn°, which may be alloyed with Pt, leading to a decrease in catalytic activity.

An interesting coke formation mechanism was proposed in the literature (Li et al., 2011), that identify the coke formation starting by a coke precursor. The coke precursor formed on the metal may migrate to the support and then undergoes subsequent polymerization/oligomerization, condensation and so on. Thus, increasing the partial pressure of propane would increase the rate of coke formation on the support. Sn in the Pt catalyst will weaken the binding of hydrocarbon to the metal, and promote the migration of the coke precursor

from the metal to the support. The presence of hydrogen will weaken the acidity of the support by converting Brønsted acid sites to Lewis acid sites and thus reduce the coke formation rate Propane is firstly dissociated on the metal and the coke precursor is formed through dehydrogenation; then the "soft coke" is generated on the metal from the coke precursor. As schematized in Figure II.1, the coke precursor generated on the metal will also migrate to the acid sites. On these acid sites, the coke precursor and the adsorbed propylene undergo polymerization/oligomerization, condensation, cyclization and hydride transfer, etc., resulting in the formation of "hard coke" (Bai et al., 2011).

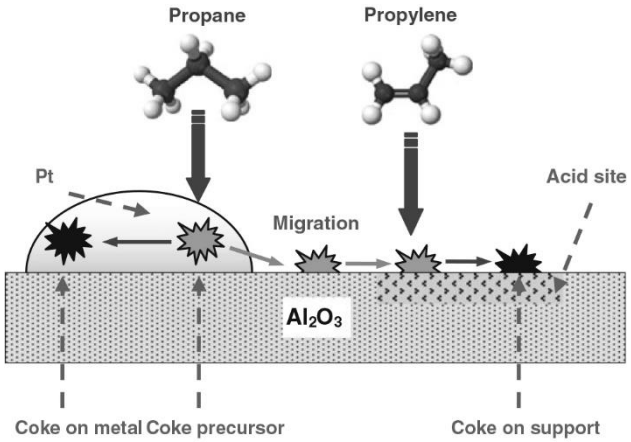

Figure II.1 *Coke formation mechanism (Bai et al., 2011)*

Other studies (Vu et al., 2012) concluded that the stability of Pt–Sn/xAl–SBA-15 catalysts is inversely proportional to the aluminum content in the SBA-15 support. The role of Sn as a promoter in the supported Pt–Sn catalysts can be enhanced by the weak interaction between SnOx species and supports. Weaker interactions between SnOx species and supports result in easy formation of Pt–Sn alloys, which are necessary for high catalyst stability.

An hypotesis on the reaction pathway of the PDH reaction in the presence of CO_2 on cromium based catalysts was proposed in the literature (Shishido et al., 2012). It was found that the activity for the dehydrogenation of C_3H_8 with CO_2 over Cr/SiO_2 was enhanced with increasing the partial pressure of CO_2, while the activity of Cr/Al_2O_3 was remarkably reduced by the addition of a small amount of CO2. It was supposed that the promotion effect of CO_2 on the activity of Cr/SiO_2 is caused by the oxidative dehydrogenation of C_3H_8 over Cr(VI) regenerated by the oxidation of Cr(III) to Cr(VI) with CO_2 (Figure II.2). In the case of Cr/Al_2O_3, although CO_2 could oxidize Cr(III) to Cr(VI), strongly adsorbed CO_2 on Al_2O_3 inhibited the adsorption of C_3H_8, resulting in the reducing the activity.

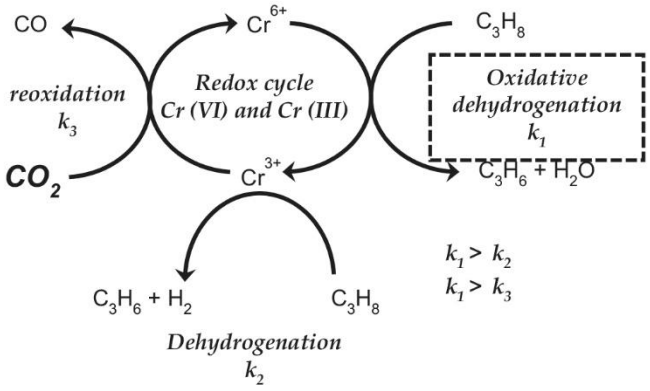

Figure II.2 *Proposed reaction mechanism of dehydrogenation of C_3H_8 in the presence of CO_2 (Shishido et al., 2012)*

Interesting studies (Yu et al., 2007) on propane dehydrogenation and the catalytic role in the process. The tests are performed by using a feed mixture C_3H_8:H_2:Ar = 1:1:5, in a isotherm reactor at 576°C at 1 atm. The hydrogen in the feed current have the role to avoid coke deposition during the reaction. Pt, Sn, and Zn are selected as active species, and were deposed on α-Al_2O_3 in several compositions (Pt/α-Al_2O_3; Sn-Pt/α-Al_2O_3; Zn-Pt/α-Al_2O_3; Zn-Sn-Pt/α-Al_2O_3). A great improvement in dehydrogenation selectivity is obtained over both zinc-doped Pt and PtSn catalysts. However, the performance of zinc-doped PtSn catalysts is strongly dependent on the sequence of zinc deposition and the zinc content. High activity and selectivity and the lowest activity loss are obtained over the Zn(0.5%)–Sn–Pt/Al catalyst. The high performance must be related to the low amount of coke and high thermal stability of platinum particles. The authors demonstarte that zinc increases the platinum particles dispersion.

In a further studies (Yu et al., 2010), Pt, Sn and Zn catalytic activity were tested; the active species were supported on SBA-15. The activity tests are peroformed by feeding a propane-hydrogen-helium mixture (feed ratio 1:1:3). The high-dispersed tri-metallic PtZn-Sn catalyst shows high activity, stability, and selectivity in propane dehydrogenation reaction. The low acidity of support is the main reason for the low coke. Moreover, the presence of zinc can increase the dispersion of platinum and decrease the electronic density of platinum metal, and then remarkably increase the stability and selectivity of catalyst in the dehydrogenation of propane to propylene.

Further studies (Vu et al., 2011b) on Pt-Sn catalysts supports for propane dehydrogenation were carried out, in which the active species are dispersed in Al_2O_3 or $ZnAl_2O_4$ supports. A propane-nitrogen mixture is used as feed, and the reaction was conducted in a isotherm reactor at 600°C. Both Pt–Sn/Al and Pt–Sn/ZnAlO catalysts exhibited deactivation with time on the stream; however, the Pt–Sn/ZnAlO catalyst showed a higher tolerance for

deactivation than the Pt–Sn/Al catalyst. By catalysts analysis, the authors noticed the formation of Pt-Sn alloys especially in alumina supported catalysts. Therefore, the dominant Pt_3Sn alloy was likely responsible for faster deactivation of the Pt–Sn/Al than that of the Pt–Sn/ZnAlO catalyst. The amount of coke accumulated on the Pt–Sn/ZnAlO was slightly less than that on the Pt–Sn/Al catalyst, and the transport of the coke from metallic sites to the support on Pt–Sn/ZnAlO became easier than that on the Pt–Sn/Al catalyst.

In other studies (Sokolov et al., 2012) the catalyst deactivation mechanism was investigated, concluding that not only the amount of surface carbon species, but also their nature may determine the deactivation rate. The phenomena is highlighted in the regeneration procedures, in which the catalyst oxidation may lead to several oxidized metals sites, that may have a role in the catalytic process. In particular, it was demonstrated that vanadium oxide was less active towards coking than PtO_2 and Cr_2O_3, therefore despite the latters have an high activity in the fresh state, after several regeneration cycles the vanadium based catalyst showed an higher stability and selectivity.

A very complex study on indium oxide based catalysts (Chen et al., 2010) analyzed the influence of adding several metal oxides, as well as the indium oxide content were analyzed. A propane-carbon dioxide was used as reactant (in the ratio 1:4), diluted in helium.. Best activity an stability was observed by using In_2O_3-Al_2O_3 at 20% of indium oxide content. which allows the steady formation of a maximum propylene yield of ca. 27% in the catalytic dehydrogenation of propane at 873 K. The high catalytic activity of the present In_2O_3–Al_2O_3 catalysts has been attributed to the favorable creation of surface stabilized metallic In° nanoclusters as a consequence of in situ reduction of well-dispersed surface indium sites during the induction period.

A similar study was conducted (Ren et al., 2009), in which ZnO_2 was selected as active specie, and zeolite (HZSM-5) at several Si/Al ratio were studied as support, for propane dehydrogenation. A propane – carbon dioxide – nitrogen mixture at a feed ratio of 5:10:185 was used as reactant. The initial activity of HZSM-5 supported zinc oxide catalysts decreases with increasing the Si/Al ratio, while the stability and the propene selectivity improve. The ZnO/HZSM-5 catalyst at Si/Al=160 exhibits the best performance at steady state. The enhancement of the catalyst stability with increasing the Si/Al ratio of the HZSM-5 support originates from the decrease in acidity of the catalysts, which leads to the suppression of the side reactions, such as cracking, oligomerization and aromatization. The promoting effect of CO_2 on the dehydrogenation reaction is observed over ZnO/HZSM-5 catalyst. Results of the influence of CO_2 partial pressure on the dehydrogenation reaction suggest that there are two roles of CO_2: a positive role by transforming H_2 with CO_2 into CO and H_2O through the reverse water-gas shift reaction, and a negative role by blocking the dissociative adsorption of propane on the catalyst surface. The catalytic stability is also improved by the addition of CO_2 to the feed gas due to the suppression of coke formation.

Further studies (Wang et al., 2012) confirmed the negative effect of the CO_2 in the diluted propane dehydrogenation on a gallium oxide on zeolite supports. The paper demonstrated that a relevant selectivity to aromatics compounds, other than methane and ethylene and coke, occurred in the investigated operating conditions (600°C). However the study also highlighted that the reduction of the Brønsted and Lewis acid sites resulted in a reduction in cracking phenomena.

The negative influence of acid sites was demonstrated by several tests (Kley and Traa, 2012), in which the zeolite acid sites were reduced by sodium borohydride.

The role of SBA-15 modified with γ-Al_2O_3 as a support for Pt-Sn based catalysts was investigated (Huang et al., 2008). A propane-hydrogen mixture in feed ratio of 1:4 was used as reactant current. The tests results show how the PtSn catalyst supported on Al_2O_3-modified SBA-15 (Al_2O_3/SBA-15) exhibits higher activity than the PtSn/SBA-15 catalyst and higher stability than conventional PtSn/γ-Al_2O_3 catalyst for propane dehydrogenation. The higher catalytic activity and stability of PtSn/Al_2O_3/SBA-15 catalyst can be correlated to the nature of interaction between Pt–Sn-support as well as the mesoporous structure of the support used.

A similar study (Duan et al., 2012) revealed that the SBA-15 support modification may contribute in the Pt dispersion. The modification may in turn improve the platinum dispersion on the support and promote interaction between Pt and support resulting less sensible to the coke deposition and so increasing in catalyst stability. The improvement in Pt dispersion on zeolitic supports may be achieved by using HCl adsorbate in the preparation, resulting also in enhanced interaction between platinum and tin (Bai et al., 2011).

The role of the support on the nature of PtSn alloys formation was reported in the literature (Vu et al., 2011c), in which the addition of lanthanum, cerium and yttrium on an al based support was investigated. The formation and stability of the Pt–Sn alloy in the catalysts were remarkably influenced by the addition of La, Ce, or Y. Compared to pure Al_2O_3 supports, La-doped Al_2O_3 promoted the formation of PtSn, while Ce- and Y-doped Al_2O_3 promoted the formation of $PtSn_2$ alloy on reduced catalysts. Moreover, La-, Ce-, and Y-doped Al_2O_3 increased the Pt dispersion and decreased the reduction temperature of the Pt–Sn species However, the stability of Pt–Sn alloy during the reaction exhibited different tolerances according to the catalyst used. Compared to those of the Pt–Sn/Al and Pt–Sn/Y–Al catalysts, Pt–Sn/La–Al and Pt–Sn/Ce–Al catalysts showed superior catalytic performances and stabilities because of the lower coke contents, higher stabilities of PtSn and $PtSn_2$ alloys, and smaller losses of Pt dispersion. Moreover, the oxygen mobility of the support may lead to a lower oxidation temperature during regeneration of spent catalysts (Vu and Shin, 2010), so enhancing the overall catalyst life

A complex study on Pt-Sn catalysts supports were carried out (Nawaz et al., 2009). Very concentrated feed was used, by supplying propane and hydrogen at a feed ratio of 4:1. The superior catalytic performance of Pt–Sn/SAPO-34 was obtained due to weak acid sites that can convert propyl cation to propylene selectively. Moreover SAPO-34 was almost inert to dehydrogenation and cracking, and their shape selectivity effect which only allowed propylene to form. The SAPO-34 supported catalyst was much better than a ZSM-5 supported bimetallic catalyst. Both Lewis and Brönsted acid sites were exist on SAPO-34 supported catalysts and these were stable after metal incorporation. However, deactivation also occurred due to the loss in active metallic sites with time-on-stream. The presence of Sn improved the reduction of Pt. In the propane dehydrogenation mechanism over Pt–Sn/SAPO-34, only one hydrogen attached to a b-carbon in propane was available for attack by Pt, to form the propoxy species ($Z–O–C_3H_7$). These propoxy species were selectivity converted to propylene over SAPO-34.

Other tests on propane dehydrogenation over Pt-Sn /Al_2O_3 catalysts, in a temperature range of 575-620°C, were found in the literature (Fattahi et al., 2011). A propane-hydrogen mixture was fed to the test plant, with a feed ratio H_2:HC = 0.8; moreover, the addition of several oxygenate compounds (water or methanol) is analyzed. The addition of oxygenates to the feed in dehydrogenation of propane over commercial Pt–Sn/γ-Al_2O_3 catalyst showed beneficial effects on catalyst performance. The oxygenates improve propylene yield when added in appropriate amounts. There is an optimum level of oxygenate, depending on oxygenate type and operating conditions. Methanol is a more effective modifier, compared to water, which can be accounted for by the simple mechanism presented. Finally, the oxygenate modifier increases the catalyst lifetime as well, through reducing coke formation on the catalyst.

A similar conclusion was obtained by another study (Samavati et al., 2013) focused on water addition effect on PDH catalyst performances. The increasing in water content led as expected to an increasing in propane conversion due in one hand to the hydrocarbon dilution, and so to the decreasing of its partial pressure, in the other hand to the coke gasification by steam presence. However, an excessive water content increasing led to the Platinum sintering in the PtSn/Al_2O_3 catalyst, that causes the catalyst deactivation. Therefore, an optimal steam content value was achieved, that increase in the operating temperature increasing. The same conclusion was extracted by another paper in the literature (Barghi et al., 2012), that get a model tool to predict the catalyst behavior in the presence of oxygenated compounds.

A complex analysis on the support influence on oxidative dehydrogenation of propane over low-loaded vanadia catalysts was reported in literature (Dinse et al., 2008). Several metal oxide supports are tested, as ceria, titania, alumina, zirconia and silica. The catalytic performance seems to depend on a complex interplay of vanadium surface species and bulk supporting material. All

catalysts expose differently structured and/or distributed vanadium surface sites (monomers/oligomers). V-ZrO_2 undergoes structural changes under reaction conditions. To improve selectivity towards the desired product, high temperatures seem to be appropriate, independent of the nature.

A comparison between non-oxidative and oxidative (lean oxygen) propane dehydrogenation (Ovsitser et al., 2012) highlighted that in one hand the non-oxidative process have a very high selectivity to propylene, in the other hand the oxidative process resulted clearly more stable and one magnitude order faster.

Monolithic Pt-Sn based catalysts (2-3 wt%) (Pavlova et al., 2003) was studied for the propane oxidative dehydrogenation. C_3H_8 and O_2 are selected as reactants, and diluted with nitrogen. In the reaction of the autothermal propane oxidative dehydrogenation at short contact times on monolithic supported catalysts, a substantial impact of the homogeneous gas-phase reactions on the propane conversion and product selectivity is demonstrated. A share of those reactions is shown to strongly depend upon the longitudinal temperature gradient within the monolithic layer which is determined by its design, operation parameters (feed rate and composition) and a nature of the active component. The yield of propylene is improved when the temperature maximum is shifted to the monolith inlet, and undesired endothermic reactions of cracking or steam reforming are suppressed.

An interesting study on the effect of support morphology in the oxidative dehydrogenation of ethane to ethylene was performed (Donsì et al., 2005). $LaMnO_3$ and Pt based catalysts were used as active species, while 400 cpsi honeycomb and 45-80 ppi foam monoliths are used as mechanical support. Experimental results showed that, even though ethylene formation occurs in the gas phase, the catalyst composition outscores any morphological consideration. $LaMnO_3$-based catalysts always give higher performance than Pt-based ones independently on the support. Nevertheless, support morphology and cell density may affect ethylene selectivity for more than 10 points%. It can be generally stated that foams perform better than honeycombs thanks to the higher geometrical surface and to the high degree of tortuosity and randomness of the pores, which drastically increase the heat and mass transfer rate. The 45 and 60 ppi foams gave the highest ethylene selectivity and yield, even though the performance of 400 and 600 cpsi honeycomb monoliths is only slightly lower. Hence, at increasing cell density above these optimal values both for foams and for honeycombs, the performance decreases. Based on the evaluation of the performance, it appears that 45 and 60 ppi foam monoliths are the optimal supports for the ODH reaction. Nevertheless, honeycomb monoliths guarantee significant advantages with respect to foams in terms of pressure drops, structural strength and easier catalyst deposition, resulting only in a minor reduction in performance for 400 and 600 cpsi cell density.

A very interesting study on the heat transfer in catalytic metallic foams as catalysts support in the oxidative dehydrogenation of hydrocarbons is carried out (Löfberga et al., 2011). Several tests are performed by comparing VO_x/TiO_2 catalytic activity as powder or supported on foams, in the oxidative propane dehydrogenation. The solid foam improves the radial bed conductivity and decreases the thermal gradients. Using a catalytic stainless steel foam in the exothermic oxidative dehydrogenation of propane to propene was clearly responsible for increasing the yield of propene when compared to catalytic powder. It is assumed that hot spots were reduced, leading to more isothermal the operation. The isothermicity due to more efficient heat transfer has to be confirmed by measuring the temperature gradient between the center of the foam and the wall of reactor.

Some approaches to the membrane assisted propane dehydrogenation were found in the literature. The use of the membrane led to an increasing in propane conversion due to the hydrogen removal from the products stream, however several problems due to the coke formation on the membrane surface and structure causes a rapid membrane plugging and to a loss in the achieve advantages (Didenko et al., 2013), more evident at the highest temperatures.

As an innovative configuration, a Two-Zone Fluidized Bed Membrane Reactor was proposed in the literature (Medrano et al., 2013) for the PDH reaction of a 50% propane stream. The system, schematized in Figure II.3, was composed by two zones aimed to the PDH reaction and to the catalyst regeneration. Such arrangement assured a continuous regeneration loop for the catalytic powder, as well as the direct catalyst heating by the catalyst oxidation. The reactor architecture of the reaction system allowed a significant improvement in propane conversion and catalyst stability, however a sensible decreasing in propylene selectivity due to the oxygen use.

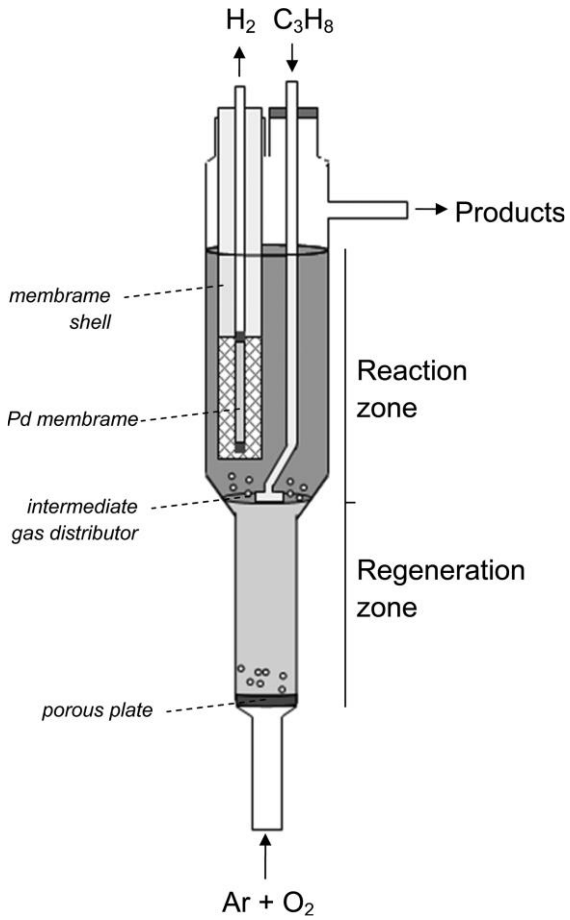

Figure II.3 *Schematic drawing of the TZFBR with two sections and membrane (Medrano et al., 2013)*

Chapter III
PDH thermodynamic analysis

In order to investigate the effect of operating conditions in PDH performances, a thermodynamic analysis was carried out for propane dehydrogenation. In this phase, the variation of thermodynamic equilibrium conditions by varying system macroscopic operating parameters was realized.

The analysis was conducted with the GasEq software.

Is worth to underline that pure propane at high temperature will involves in cracking reactions, so according with the Francis diagram, in the thermodynamic point of view propane will convert in methane and coke. Therefore thermodynamic analysis will be carried out by supposing that no side reactions were involved, in order to evaluate the propylene productivity limitations in the propane dehydrogenation reaction.

$$C_3H_8 \rightleftarrows C_3H_6 + H_2$$

III.1 Pure propane dehydrogenation

III.1.1 Pressure influence

A first approach towards the thermodynamic analysis of propylene selective PDH reaction was carried out by evaluating the operating pressure and temperature effect on hydrocarbon conversion.

In Figure III.1 the thermodynamic propane conversion trend was reported on temperature at several operating pressure values. The propane conversion increases by increasing operating temperature, due to its endothermic nature; on the other hand, as the PDH reaction generates an increasing in mole number, the reactants conversion decreases by increasing the operating pressure. The thermodynamic analysis underlines that the propane dehydrogenation is promoted only at very high temperature: by referring to the atmospheric pressure conditions, below 600°C the propane conversion was not higher than 50%. If in one hand to operate at pressure below 1 bar is not convenient in an economical point of view, to increase the process temperature promotes side products. Of course, to operate at pressure as low

as possible leads to the higher conversions, so all analyses carried out in the following will be evaluated at atmospheric pressure.

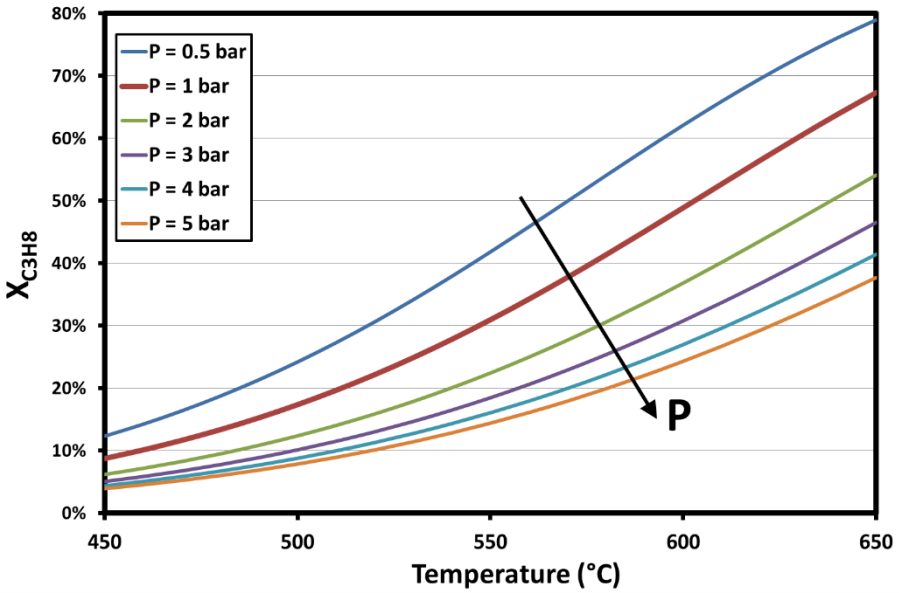

Figure III.1 *Thermodynamic equilibrium propane conversion vs operating temperature and pressure*

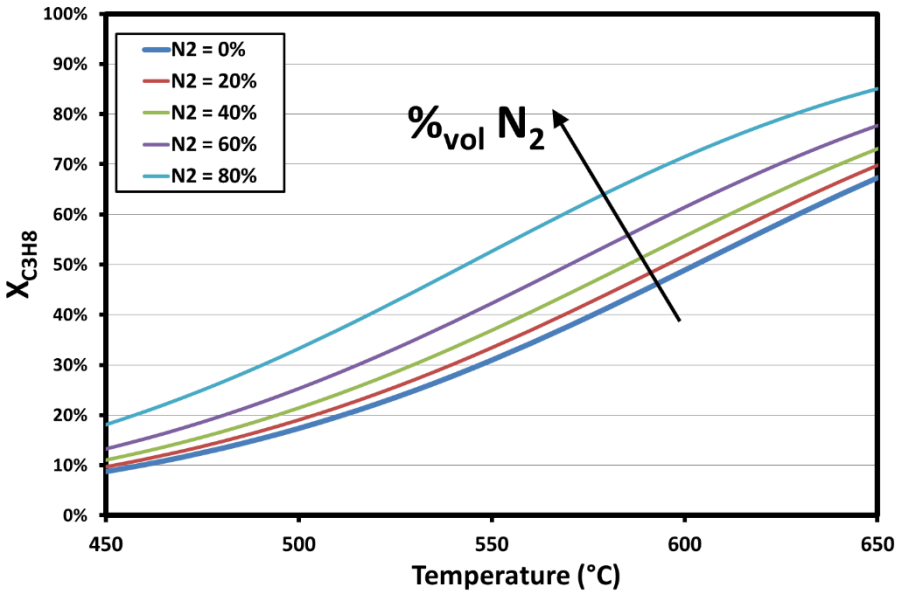

Figure III.2 *Thermodynamic equilibrium propane conversion vs operating temperature and inert dilution*

III.1.2 Inert dilution effect

The influence of the presence of an inert gas (in this case nitrogen) in the reaction stream was evaluated. Several composition was considered, and the propane conversion trend respect to the temperature was reported in Figure III.2.

Since the reaction results in an increasing of the number of moles, the propane partial pressure reduction due to the presence of an inert gas in the reaction stream results in a clear increasing of hydrocarbon conversion. The conversion percent increasing was more evident at lower temperature, for which the highest dilution lead to a double conversion if propane. On the other hand, the absolute highest conversion increment was recorded for a temperature of about 580°C.

Of course, the advantages of a massive dilution, demonstrated by the thermodynamic analysis, should be compared to the relevant increasing on operative and plant costs, due to the increasing in the process stream and to the separation stages.

III.1.3 Hydrogen dilution effect

One of the most common procedure used in the industrial processes pointed to the reduction of cracking phenomena, and therefore to the increasing in catalyst lifetime, consist in the adding of hydrogen in the fed stream. The hydrogen presence reduces the formation of coke precursors (e.g. ethylene). The influence of hydrogen in the thermodynamic conversion was then investigated; the thermodynamic analysis was summarized in Figure III.3.

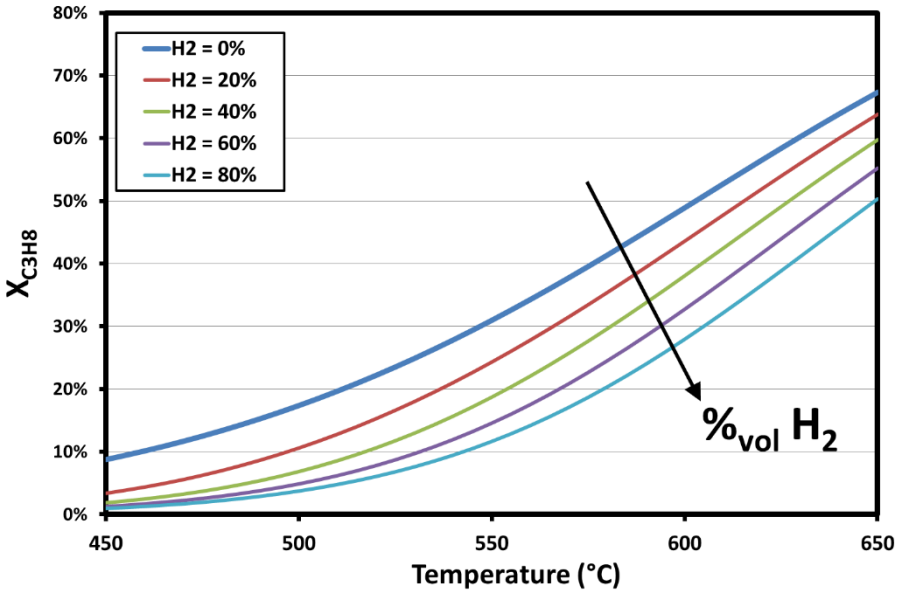

Figure III.3 *Thermodynamic equilibrium propane conversion vs operating temperature and hydrogen dilution*

As expected, since H_2 is one of the products of the PDH reaction, by adding hydrogen results in a reduction of the thermodynamic propane conversion. In particular, by referring to the process temperature of 550°C, the dilution of 20% of H_2 causes a conversion drop from 31% 24%; by using a dilution of 40% of H_2 the conversion was 19%. Moreover, the presence of hydrogen in fed stream will be also detrimental in a membrane reactor context, since causes an increasing in the needed membrane area

Since the presence of hydrogen is often needed in order to reduce the catalyst deactivation, its presence should be restricted to contents below 10%.

III.2 Water dilution effect

A really interesting chance, often found in the available literature as well as in the industrial scenario, was to add steam in the fed mixture. The water has two main role: in one hand, it is a reactant diluent, on the other hand the well note cracking inhibition properties were exploited, so assuring a longer catalyst lifetime. Of course, by considering steam as a diluent, no variations are expected with respect to the nitrogen dilution; therefore, also the reforming and water-gas shift reactions were considered in the thermodynamic equilibrium evaluations.

$$C_3H_8 + 3H_2O \rightleftarrows 3CO + 7H_2$$

$$CO + H_2O \rightleftarrows CO_2 + H_2$$

Therefore, beside the propane conversion, also selectivity to propylene should be taken in account. The selectivity was defined as

$$S_{C_3H_6} = \frac{N_{C_3H_6}^{out}}{N_{C_3H_8}^{in} - N_{C_3H_8}^{out}}$$

where $N_{C_3H_6}^{out}$ are the produced moles of propylene, $N_{C_3H_8}^{in}$ are the fed moles of propane and $N_{C_3H_8}^{out}$ are the non-converted moles of propane.

Thermodynamic analysis was carried out by varying water content in the reactants stream, and by considering several operating temperature values at atmospheric pressure. The thermodynamic propane conversion was analysed.

The main result highlighted in the Figure III.4 is of course the initial decreasing trend of propane conversion by adding water, for each investigated operating temperature. The reduction in propane conversion is more evident for the lowest temperatures, while for the highest temperature the lack of conversion is extended for a wider water content range. The effect should be due to the reforming reactions, that even in one hand results in a propane conversion, in the other hand causes H_2 production, that as observed had a detrimental effect on hydrocarbon conversion. The dot-line fits for each isotherm curve the points in which the wet conversion is equal to the dry conversion. In a thermodynamic point of view, it is not convenient to operate in conditions resulting on the left side of the dot line, since the adding of water will lead (at the thermodynamic equilibrium conditions) to a less propane conversion.

For a wet fed stream, it is clearly important to understand the thermodynamic trend of selectivity to propylene, resumed in the Figure III.5.

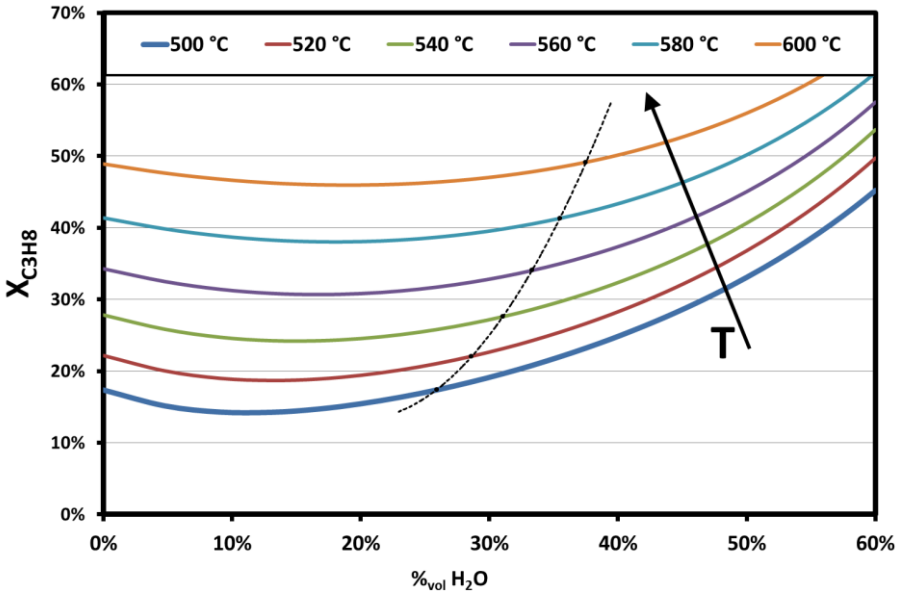

Figure III.4 *Thermodynamic equilibrium propane conversion vs water content and operating temperature*

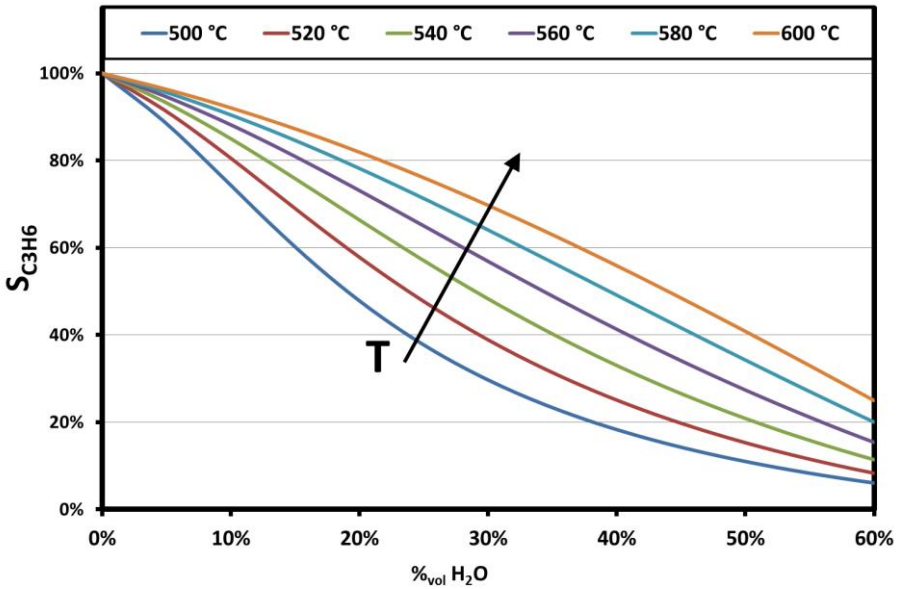

Figure III.5 *Thermodynamic equilibrium selectivity to propylene vs water content and operating temperature*

As expected, by adding water in the reactants results in a reduction of selectivity to propylene. The water content effect is stronger for the lowest

temperature, since the reforming reactions have a weaker dependence by temperature than propane dehydrogenation reaction.

The thermodynamic analysis is concluded by the thermodynamic propylene yield analysis for fed propane:

$$Y_{C_3H_6} = \frac{N_{C_3H_6}^{out}}{N_{C_3H_8}^{in}}$$

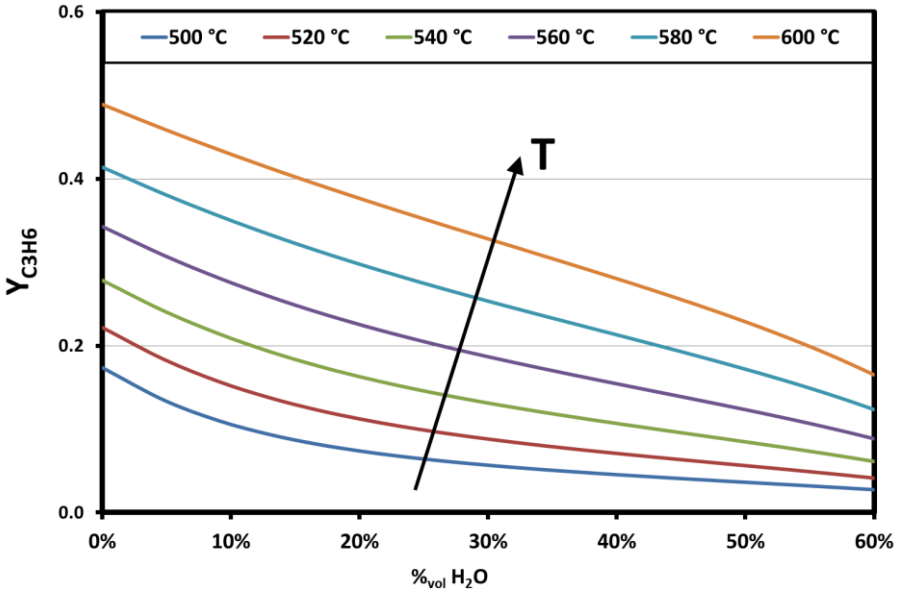

Figure III.6 *Thermodynamic equilibrium propylene yield vs water content and operating temperature*

By analyzing thermodynamic trend of propylene yield by varying operating temperature and water content (Figure III.6), it's worth to note that the highest propylene productivity is obtained at the highest temperature (propane conversion promoted) and lowest water content (reduced contribution of reforming reactions).

Is anyway crucial to underline again that the presence of steam in the fed stream results in a better catalyst stability, and for this reason is often accepted to reduce the propylene yield and operate in wet conditions.

Chapter IV
Experimental apparatuses

IV.1 Auto-thermal Reforming

Experimental tests are conducted in a laboratory scale plant designed and realized in the Industrial Engineering Department of University of Salerno. The reaction system consists in three main modules: a thermal exchange module in which reactants are pre-heated by heat recovery from exhaust gas, a mixing module in which a homogeneous mixture of reactants was realized and a reaction module in which reactants pass through the catalytic bed and ATR reaction occurs.

IV.1.1 Reactants delivery system

In experimental tests, methane as fuel, air instead of oxygen, and distilled water were used. Methane and air, supplied from Sol S.p.a., are delivered to the system by means of mass flow controllers (Brooks); distilled water is stocked in a 10 atm pressurized vessel, and delivered by means of a Coriolis based mass flow controller (Quantim, Brooks): air and water are fed to the heat recovery module for pre-heating, while methane are fed directly in the reaction module. In this way, the risk of methane cracking is very small: methane is fed in the mixing chamber at room temperature, where is mixed with superheated steam and air, thus avoiding coke formation risk.

IV.1.2 Heat exchange module

Heat recovery from reactants streams was achieved by means of heat exchangers, that consists of a series of rectangular coils realized with stainless steel tubes (o.d. 1/8”, thickness 0,74*mm*) and mounted in parallel ways on two manifolds (in and out) in order to distribute uniformly the reactants stream in all coils (Figure IV.1).

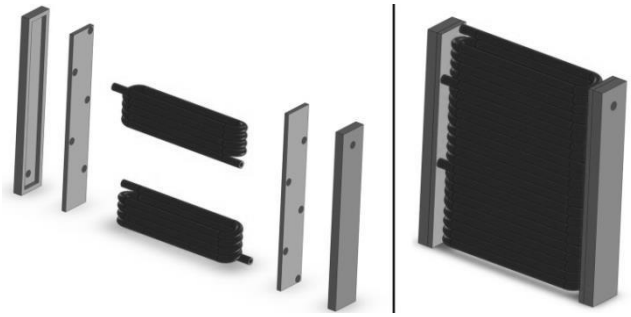

Figure IV.1 *Heat exchanger: disassembled and assembled views*

The heat exchangers are mounted in a rectangular module, in transversal-way respect to the exhaust gas flux, to create a uniform cross section and thus to maximize the overall heat transfer. It was so created a tube-shell like heat exchangers: the reactants flow in the tube-side, and the exhaust gas flow in the shell-side. Different configurations were realized for each reactant, in terms of number of tubes per coil and number of coils per manifold: for all the configurations, the number of tubes per manifold is fixed, to achieve a uniform cross section along the module. In order to strike a balance between pressure drops and heat exchange efficiency, water vaporization and steam superheating were split in two stages.

The heat exchange system was designed for a hydrogen production of 5 Nm^3/h from a reactant mixture composed by methane, air and water, (feed ratio $CH_4/O_2/H_2O$ = 1/0.6/1.2) ™(Palma et al., 2011). In order to maximize heat recovery efficiency, the heat exchangers are disposed as indicated in Figure IV.2.

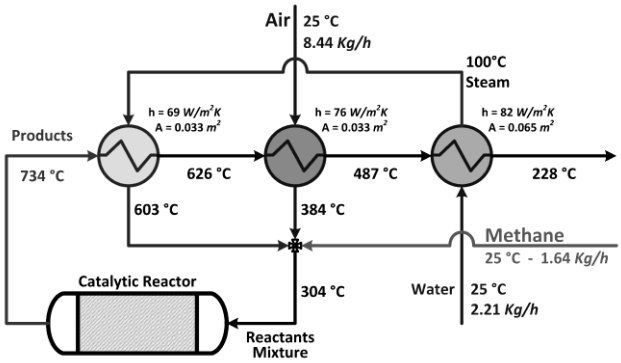

Figure IV.2 *Heat recovery module scheme*

Water was vaporized in the downstream heat exchanger, and then was super-heated in the first one: this disposition assures the best temperature profile along the heat recovery module. A simulation of different

configurations was performed for 2 different operating conditions, to check the heat exchange efficiency for each configuration. As reported in Table IV.4, the selected modules disposition (steam – air – liquid water) assures the highest efficiency for both feed ratio.

Table IV.1 *Heat exchange efficiency for the different heat exchange module configurations*

	$O_2/H_2O/C$ 0.6/1.2/1	0.6/1.2/1
Steam - Air - Water	71.4%	53.0%
Air - Steam - Water	71.0%	48.4%
Steam - Water - Air	64.8%	44.1%
Water - Steam - Air	60.1%	50.9%
Water - Air	60.3%	52.3%
Air - Water - Steam	60.3%	52.3%

IV.1.3 Mixing module

After pre-heating, reactants are provided to mixing module: superheated steam and air and cold methane are fed. The special shape of the module, showed in Figure IV.3, with subsequent section expansions and constrictions, allows the formation of eddies and whirlpools that allow to achieve a very high reactant mixing. Homogeneous temperature and composition realized my means of mixing module assure uniform conditions along the whole section of catalytic bed, so avoiding cracking reactions.

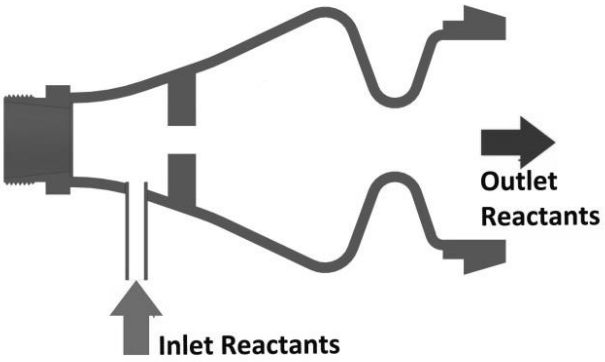

Figure IV.3 *Schematic shape of mixing module*

IV.1.4 Reaction module

After mixing stage, reactants are provided to reaction module. It's a short tube with a rectangular section (60 x 80mm), in which catalytic bed is placed.

The module walls are realized by 5mm thickness stainless steel foils; a special flange on the top of reactor allows a quick access to the catalytic volume. System start-up is realized by means of an electrical resistance mounted just before the catalytic zone. The whole system is wrapped in a layer of insulating material in order to achieve an adiabatic system.

Mixing module, reaction module and heat recovery module are fixed together by means of flanges, so assuring a quick disassembly for maintenance procedures. In Figure IV.4 a 3D image of the reaction system (realized by SolidWorks© software) is reported: external dimensions (without pipes and sensors) are within 45 x 13 x 13 mm.

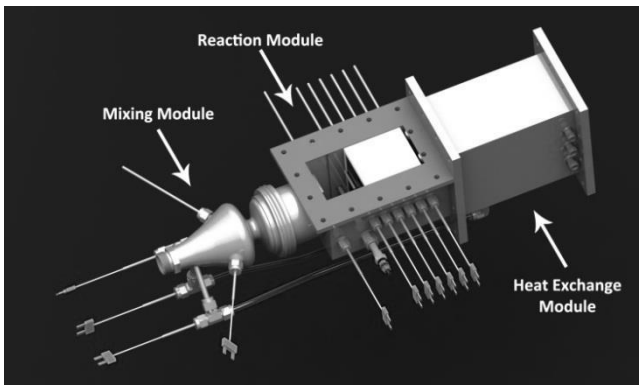

Figure IV.4 *Assembled reaction system*

IV.1.5 Analysis system

A complex analysis system was adopted for monitoring the overall process trend. 10 K-type thermocouples are used for control temperature in some crucial points of the system. Catalyst temperature profile was recorder by measuring the temperature in the inlet section, in the outlet section and in 4 points inside catalytic bed at a distance of 14 mm between them. The temperature in the mixing volume was also measured. In order to control heat exchangers efficiency, the exhaust gas temperature downstream the heat recovery module as well as air and steam temperature just before inlet in the reaction module was monitored. A scheme of sampling configuration

Reaction progress along the catalyst bed was monitored by means of a series of sampling lines for gas composition analysis. Gas concentration was analyzed in the mixing chamber, in order to verify the fed gas composition and the mixing efficiency, just before the first catalyst brick, and after every catalyst brick. Sampling lines are provided to a Hiden Analytics mass spectrometer, equipped with a Proteus multi-valve able to switch between sampling lines. In this way a complete control of reaction trend was obtained, by recording both temperature and composition after each catalytic brick. Furthermore, this analysis system allow in one test to achieve test results in

terms of concentration and temperature for 5 different GHSV (gas hourly space velocity) values and without varying other parameters (reactants rate, Reynolds number, etc.).

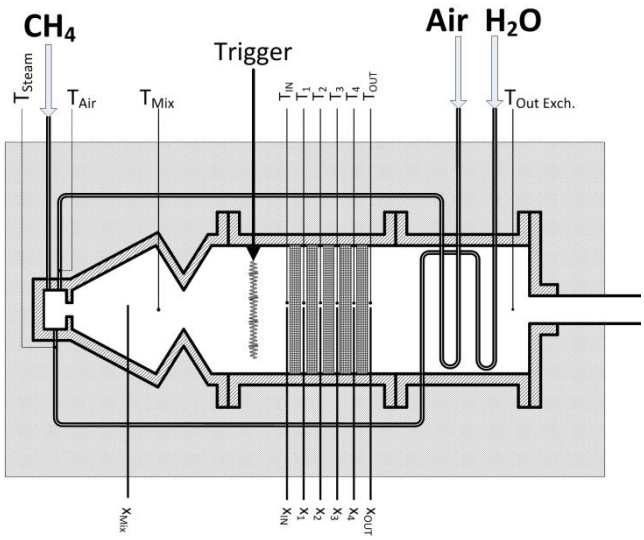

Figure IV.5 *Analysis system scheme of ATR reformer thermally integrated*

In Figure IV.5 the disposition of thermocouples and composition sampling along the system is reported.

GHSV is defined as (4): by feeding a global reactants rate of 4.8 m^3/h, since catalytic bricks have a volume of $V_{brick} = 24\ cm^3$, after each brick the following space velocities are calculated and reported in Table IV.2.

$$GHSV = \frac{F_{Tot}\left[Nm^3/h\right]}{V_{cat}\left[m^3\right]}$$

Table IV.2 *Relationship between number of catalytic bricks and space velocity (GHSV)*

N. of bricks	Total volume of catalyst	GHSV
1	24 cm^3	200000 h^{-1}
2	48 cm^3	100000 h^{-1}
3	72 cm^3	66667 h^{-1}
4	96 cm^3	50000 h^{-1}
5	120 cm^3	40000 h^{-1}

In order to evaluate the proper overall functioning of the integrated reaction system, the thermal efficiency of reaction η was monitored, where N_{H2} is

moles of hydrogen produced per 1 mole of methane and LHV is lower heating value of H_2 or CH_4.

$$\eta = \frac{N_{H_2} \cdot LHV_{H_2}}{LHV_{CH_4}}$$

Methane conversion (X_{CH4} or X_CH4) was defined, where $N°_{CH4}$ is moles of methane fed to the system, and N_{CH4} is moles of methane out of the system.

$$X_{CH_4} = \frac{N^0_{CH_4} - N_{CH_4}}{N^0_{CH_4}}$$

Gas composition detected downstream the catalyst bed was compared to thermodynamic equilibrium values: these compositions were calculated by GasEq software as an isotherm reaction at the outside section temperature of each catalyst brick. GasEq is a Windows software based on the minimization of Gibbs free energy, able to find thermodynamic equilibrium condition in gas-phase reactions.

IV.1.6 Catalysts

Supported catalysts were selected for catalytic tests. In order to strike the requirements of high thermal transfer and low pressure drops along the catalytic structure, foam catalysts was selected as the optimal catalytic system. Within the CARENA project purposes, Johnson Matthey will activate these foams with a catalytic slurry.

IV.1.6.1 Support

3 different kinds of foams are selected as catalytic support:

- **AL 513150** - 65 PPI - **AL92**
- **AL 513148** - 65 PPI - **OBSiC**
- **AL 513315** - 65 PPI - **PSZM**

All foams are characterized by a cell density of 65ppi. In the Table IV.3 the main characteristics are summarized:

Table IV.3 *Foam characteristics*

Sample Name	Material Code	Composition	Material thermal conductivity (W/mK)	Foam Density (g/cm^3)
AL 513150	AL92	100% Al_2O_3	35	0.63
AL 513148	OBSiC	50% Al_2O_3 40% SiC 10% SiO_2	16	0.54
AL 513315	PSZM	100% ZrO_2	2	0.99

The foams were sized in disks of D29 x 15 mm, and are sent to Johnson Matthey for the active phase deposition.

IV.1.6.2 Catalyst arrangement

5 coated catalytic disks are attached to realize cylindrical mono-blocks, sized D29 x 75 mm, so obtaining a catalytic volume of 50 cm^3. The catalyst is inserted in an insulating brick sized H80 x W60 x L75 mm, in order to reduce heat loss in the catalytic volume. The brick was then wrapped in a thin layer of thermal expanding foam, in order to avoid bypass phenomena.

The prepared catalyst was then inserted in the reaction module, and then is drilled radially in the correspondence of sampling lines and thermocouples inserting.

Foam catalysts performances were compared to a commercial honeycomb monolith (provided by BASF), in order to evaluate the gain (or the drop) generated by the foam structure. Honeycomb was cut in 5 bricks each sized L x H x W = 36 x 27 x 11 mm (total catalytic volume 55 cm^3) and distanced each other 3 mm, in order to allow reaction stream mixing in the catalytic volume after each brick.

IV.1.7 Experimental procedure

Preliminary tests were conducted on AL92 catalyzed foam, in order to understand the operating conditions suitable for further activity tests. In the tests, space velocity was hold (GHSV = 80,000 h^{-1}), as well as the reaction pressure was fixed in 2.5 bar while feed ratios varied both In terms of oxygen-to-carbon and steam-to-carbon ratios as reported below:

1. $H_2O:O_2:C = 0.49:0.56:1$
2. $H_2O:O_2:C = 1.50:0.56:1$
3. $H_2O:O_2:C = 1.50:0.30:1$
4. $H_2O:O_2:C = 2.00:0.30:1$

Activity tests were then repeated on the honeycomb and the 3 different foam samples by fixing the feed ratio (H_2O:O_2:C = 0.49:0.56:1) and operating pressure (p = 2.5 bar) and by varying the feed flow rate (GHSV = 80,000 – 120,000 h^{-1}).

IV.2 Steam Reforming

The experimental tests were conducted in a lab scale plant, schematized in Figure IV.6, consisting in 3 main sections:

- Feed section
- Reaction section
- Analysis section

The experimental apparatus is available in ProCEED – Industrial Chemistry and Catalysis labs in the Department of Industrial Engineering of University of Salerno.

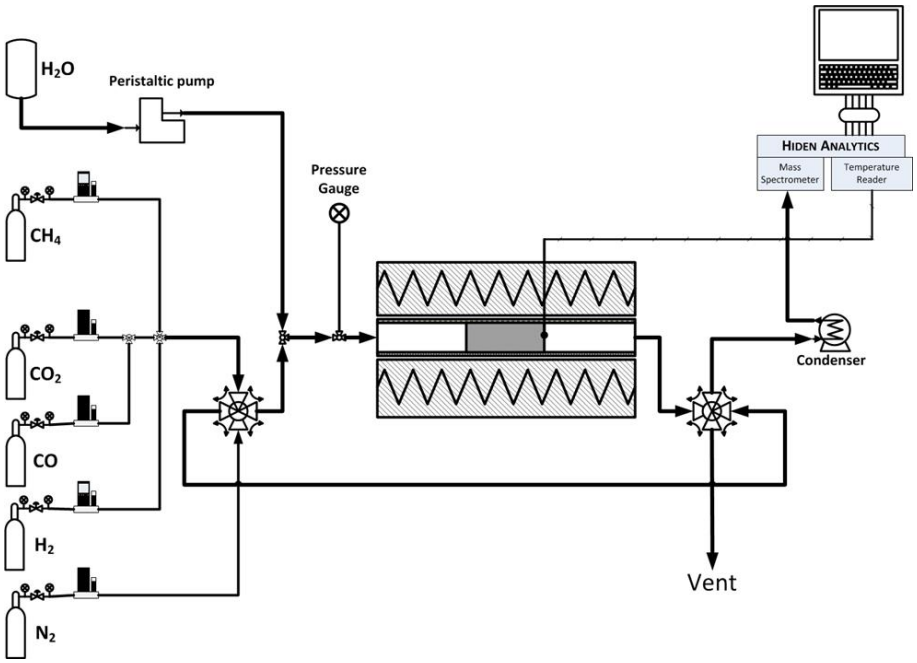

Figure IV.6 *Steam reforming lab-scale plant scheme*

Gaseous and liquid reactant delivery was assured by means of a series of mass flow controllers (MFC). A series of pure gases (precision gas purity), supplied by SOL S.p.a, was used to calibrate analysis system. A couple of 4-way valves allows delivered stream to by-pass reaction system, for preliminary calibration operations. In this phase, an equivalent He stream was fed to the reactor, in order to stabilize temperature in the initial period of the catalytic tests, assuring a constant heat flux.

Products composition was evaluated by means of a Hiden Analytical mass spectrometer. The analyzed stream was dried by means of a cooled vessel before to be delivered to the analyzer, in order to avoid water condensing in the lines.

IV.2.1 Tubular reactor

A tubular AISI 310 stainless steel reactor was designed and realized, with a length of 38 cm, inner diameter of 18 mm and wall thickness of 4 mm (Figure IV.7); the two ends are fixed by compressed flanges easy disassembling procedure, leakage was assured by means of graphite seals. AISI 310 stainless steel is suitable to operating conditions at high temperature in both oxidant and reducing environment.

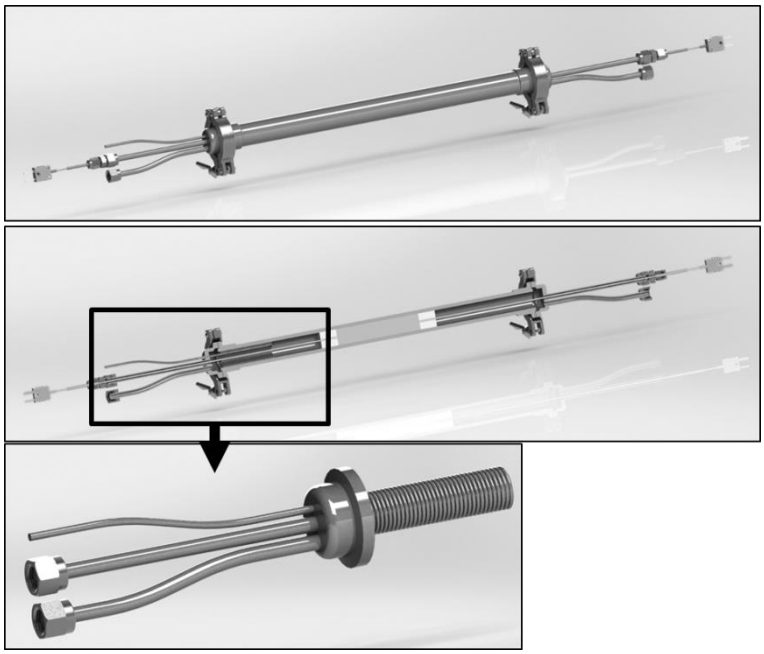

Figure IV.7 *Tubular reactor*

The inlet section was provided by 3 tubes, aimed respectively to the gas feed, liquid feed and thermocouple housing. The gas inlet was connected to a pressure transducer in order to monitor the inlet section pressure. The water was delivered in liquid state to the system. A special coil placed just in the first zone of the tubular reactor was designed to vaporize water before to be mixed with the gaseous reactants. Finally, a K-type thermocouple was used in order to evaluate the gas temperature just before the catalytic bed, as well as in correspondence of the outlet section.

IV.2.2 Electrical oven

Reaction temperature control is realized by placing the reactor in a 4kW annular oven, supplied by "Officina Elettromeccanica Mormile": it consists in an open oven with 3 heating sections, each driven by means of a TLK38 controller that allows to realize a controlled heat increasing in the reaction

system; the temperature in the different sections is measured by means of 3 thermocouples, able to measure temperature on the external wall of the reactor. In Figure IV.8 a screenshot of the oven is reported.

Figure IV.8 *Electrical oven*

Oven wall are realized in ceramic material, to avoid high axial an radial temperature gradients, so improving isothermal behavior. The oven has an inner channel of 55mm diameter, in order to easily place the reactors. A relevant amount of quartz wool was placed around the reactor in the left and right side of the oven, in order to minimize thermal dispersion in the surrounding, and to assure a coaxial alignment between reactor and oven channel.

The electrical oven should be able to assure a constant reaction temperature (up to 600°C) inside the reactor, and to hold a flat axial thermal profile. Therefore, before start catalytic tests, oven thermal profile was verified, by setting oven zone controllers to 600°C and by sliding a k-type thermocouple along the oven channel. The achieved results are summarized in Figure IV.9.

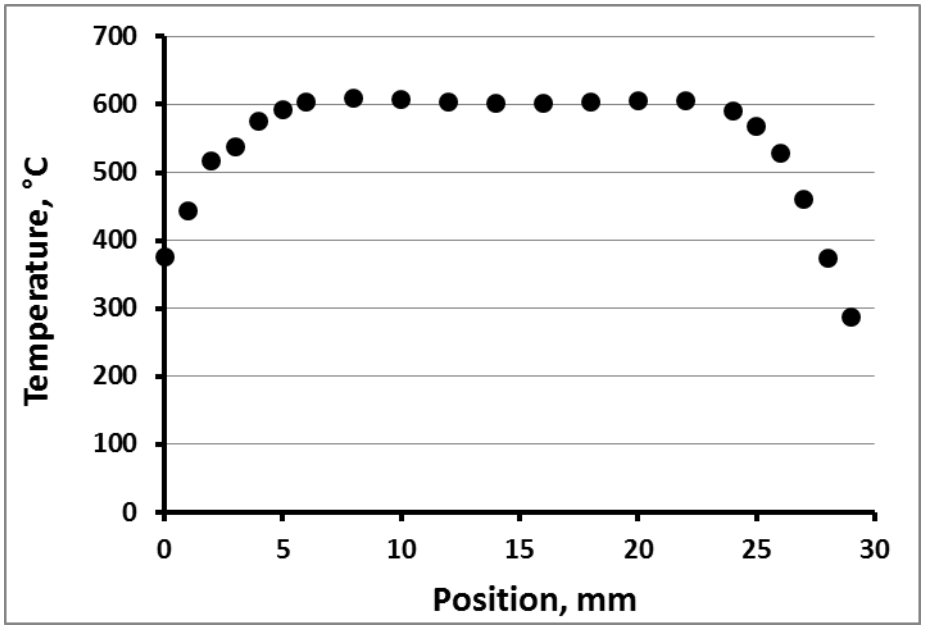

Figure IV.9 *Oven thermal profile*

As reported in the diagram, the electrical oven shows a wide isothermal zone. In fact, apart the external 6 cm, there is a 18cm length zone in which temperature appears constant: this is the zone in which catalyst should be placed, to assure an effective isothermal reaction.

However, is important to underline that thermal profile was verified without any flux or chemical reactions. In the facts, inside the oven will be delivered a reaction mixture at room temperature, and inside the oven an endothermic reaction occurs. Therefore the oven should be able at same time to supply the heat needed to reactants preheating and to sustain chemical reaction endothermicity.

IV.2.3 Catalysts

The catalytic performances of the samples used in the ATR tests () were evaluated in the steam reforming conditions. The catalytic foams were cut as cylinders sized D15 x 15 mm, and 2 disks were attached in order to obtain a catalytic cylinder sized D15 x 15 mm resulting in a total catalytic volume of 5.3 cm^3. The catalysts were then wrapped in a thin layer of inert expanding foam and then inserted in the tubular reactor.

IV.2.4 Experimental procedure

Catalysts were tested in methane steam reforming conditions. In order to evaluate the coupling of such catalysts in a membrane integrated reactor, the catalytic tests were carried out by feeding methane and water (Steam-to-

Carbon ratio = 3 and 4) at 550°C. Furthermore, the influence of operating pressure on the catalyst performances was also evaluated. The effect of reactants rate was also investigated, by varying GHSV value between 10,000 and 40,000 h^{-1}.

The performances analysis was completed by comparing results with thermodynamic equilibrium compositions.

IV.3 Propane Dehydrogenation

IV.3.1 Catalytic reactor

IV.3.1.1 Tube-shell reactor

The first approach toward the study of the dehydrogenation reaction involved the use of a quartz reactor, at the disposal of laboratory, consisting of a tubular part, open at both ends, to be inserted in a shell, closed at one end. Figure IV.10 shows the two parts of the reactor.

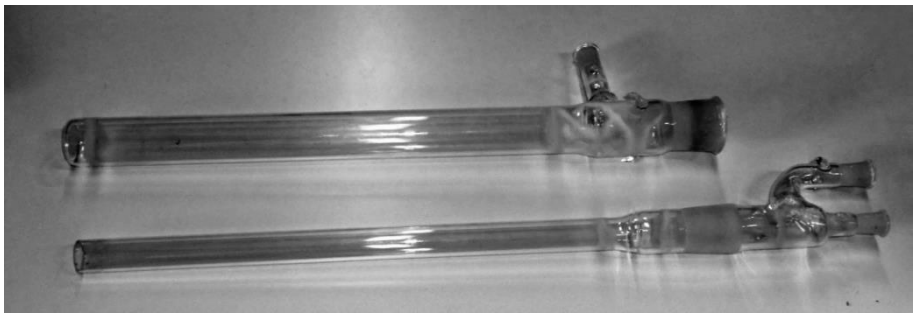

Figure IV.10 *Tube-shell reactor parts*

The shell have a lateral opening decentralized in which a graft steel is inserted to connect a Teflon tube to 1/8", used for the feed mixture. The reactants flux flows through the reactor shell side, so preheating, and, subsequently, flux through the reactor tube side where the catalytic bed is placed, locked between two layers of glass wool. Finally, the flow escapes from the system, after passing through the final area of the tube containing filling quartz, whose role is to avoid that pressure flux drags the catalytic bed. The quartz tube has two outlets: one is used to connect the output line of the stream, and the other is used to insert the thermocouple to measure the temperature at the exit of the catalytic bed. The main reactor features are summarized in Table IV.4.

Table IV.4 *Tube-shell reactor dimensions*

	Inner diameter, cm	*External diameter, cm*	*Lenght, cm*
TUBE	*1.9*	*2.2*	*35*
SHELL	*3.1*	*3.4*	*36.5*

IV.3.1.2 Tubular reactor

For the Propane dehydrogenation tests, the same experimental apparatus (IV.2) tubular reactor (IV.2.1) and electrical oven (IV.2.2) setup for the SR tests was used.

IV.3.2 Analysis section

The products stream analysis is assured by a Hiden Analytical mass spectrometer (Figure IV.11). This device assures a continuous stream scanning, with a composition response every 15 seconds. Moreover, this instrument is able to import the reaction temperature signal, so obtaining a very comprehensive outlook of the system behavior.

Figure IV.11 *HPR7 Hiden Analytical mass spectrometer*

The Hiden Analytical mass spectrometer is equipped with a detector able to detect up to 200 AMU. Therefore, in order to analyze the composition of all possible products stream components, a wide analysis of produced hydrocarbons mass spectra was carried out, in order to define the most suitable characteristic mass for each compound, as summarized in Table IV.5.

Table IV.5 *Mass spectrometer AMU correspondence in PDH reaction analysis*

AMU	Compound
2	H_2
4	He
15	CH_4
26	C_2H_4
30	C_2H_6
41	C_3H_6
44	C_3H_8

In the case of water dilution, the mass spectrometer was coupled by a NDIR Uras 14 supplied by ABB Company, to monitor CO and CO_2 content. Before the analysis section, products stream passes through a cold trap to remove water.

IV.3.3 Catalysts

Several catalytic formulations were tested in PDH conditions. According to Ca.Re.N.A. directives, chromium free catalysts should be considered; as highlighted by literature, Pt-based catalysts seems the most promising for this kind of reaction. Since the role of the support could result crucial in catalyst performances, both in terms of catalytic activity and selectivity, as well as in terms of catalyst lifetime, several catalysts were prepared by fixing the active phase (0.3 wt% of platinum) and the catalytic stabilizer (0.9 wt% of tin) and by varying the support (Al_2O_3, CeO_2, $Ce_xZr_{1-x}O_2$).

The three catalysts were prepared by subsequent wet impregnation-precipitation of the support with tin in a first step, and platinum as a final step, in order to allow the Pt dispersion promoted by Sn layer. $PtCl_4 \cdot 2H_2O$ and $SnCl_2 \cdot 2H_2O$ delivered by Sigma-Aldrich were used as platinum and tin precursors respectively. Commercial γ-Al_2O_3 (*PURALOX® NWa155*) supplied by *Sasol*, and CeO_2, $Ce_xZr_{1-x}O_2$ powders supplied by Rhodia were used as supports.

The support was firstly impregnated with tin precursor; the obtained compound was dried at 120°C overnight and then calcined at 600°C for 3 hours. Then the Sn/support powder was impregnated with platinum precursor, the compound was treated with the same drying-calcination procedure. Within the Ca.Re.N.A. project accordance, two catalytic samples were supplied by SINTEF and Johnson Matthey for PDH tests. The main samples characteristics are summarized in Table IV.6.

Table IV.6 *Tested catalysts in Porpane DeHydrogenation*

Sample NAME	Producer	Pt (wt%)	Sn (wt%)	Support

$PtSn/Al_2O_3$	Homemade	0.3	0.9	Al_2O_3
$PtSn/CeO_2$	Homemade	0.3	0.9	CeO_2
$PtSn/CeO_2$-ZrO_2	Homemade	0.3	0.9	CeO_2-ZrO_2 (1:1 mol)
S-01	SINTEF	0.3	1.2	Mg(Al)O
S-02	Johnson Matthey	0.5	0.5	Mg(Al)O

All catalysts were "pelletized" in grain with a diameter of 180-355 μm and diluted (1:1 vol) with quartz grains (510-700 μm) to reduce pressure drop and to avoid catalyst packing. The catalyst was then inserted in the reactor and locked between 2 quartz wool disks. In order to avoid sire-reactions in products stream, the reactor volume downstream the catalyst was filled by raw quartz grains, aimed to reduce residence time of process stream out of catalytic bed.

IV.3.4 Experimental procedure

PDH tests were carried out in isothermal conditions, by fixing operating temperature and pressure and by feeding propane (purity 99.5%, supplied by SOL S.p.a.) alone, or diluted with steam, carbon monoxide and carbon dioxide. The propane mass rate was controlled by a BROOKS mass flow controller, and was determined by fixing the Weight Hourly Space Velocity (WHSV) defined as the ratio between mass rate of main reactant (in this case propane) and the mass of the:

$$WHSV = \frac{W_{C_8H_8}}{m_{cat}}$$

Chapter V
Methane reforming

V.1 Auto-Thermal Reforming (ATR)

V.1.1 Preliminary tests on reaction system

In order to evaluate the auto-thermal reformer performances, preliminary tests are performed on Commercial BASF catalyst. The aim of this phase is to evaluate the start-up times and the transitory phase, as well as to understand the experimental capability to host activity tests.

V.1.1.1 System start-up

The start-up procedure is a crucial step in reforming processes: the reactor must be started as soon as possible, and temperatures must remain within the working range of the catalyst. In this phase, an excessive increase of temperature may bring to the melting of monolith walls, so creating by-pass phenomena and then a massive drop in hydrocarbon conversion. The start-up was conducted by activating the electrical resistance, and feeding into the reactor an air-methane current with a feed ratio $O_2/C=1.37$ and a space velocity of 15000 h^{-1}. As the reactor temperature reached high levels, the air flow is reduced to obtain a feed ratio $O_2/C = 0.56$ and then water is delivered with a feed ratio of $H_2O/C = 0.49$: this operating condition was held until a steady-state condition is reached.

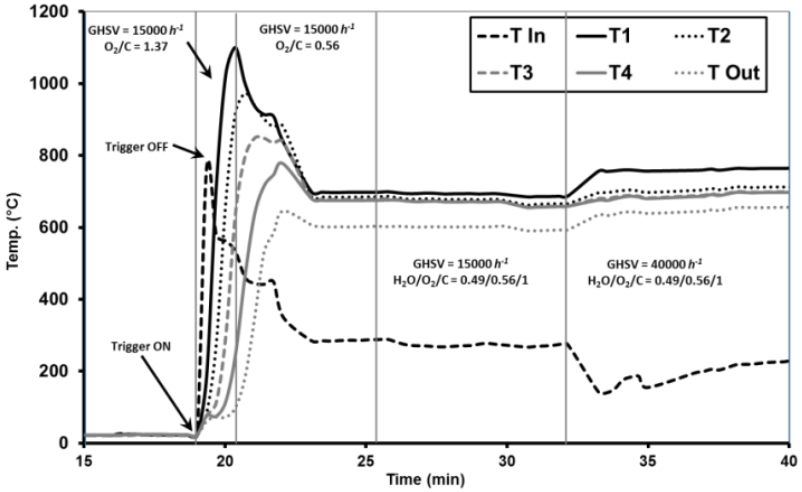

Figure V.1 *Temperature trend along catalyst in start-up phase*

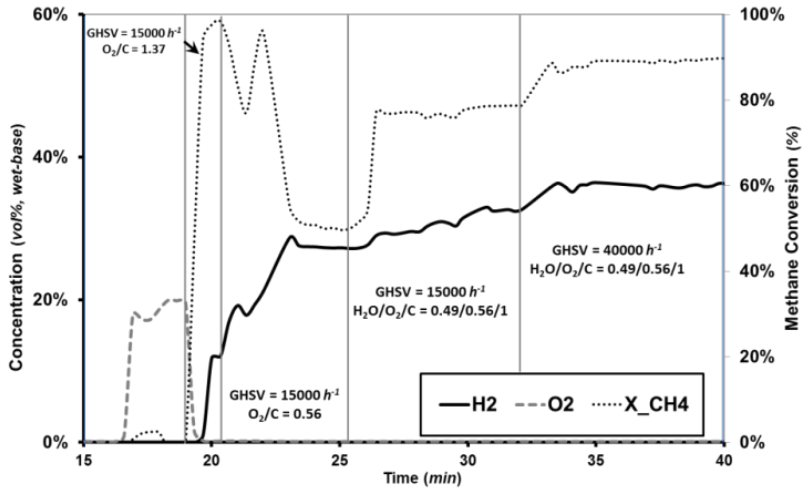

Figure V.2 *Product composition and methane conversion downstream catalyst in start-up phase*

Figure V.1 shows how in start-up phase very high temperatures along catalytic bed were reached within 1 minute and half. When reactants rates were switched in ATR conditions, stationary conditions were achieved within 10 minutes. In this conditions an H_2 concentration of 20% was quickly reached, and raised up 30% in a few of minutes (Figure V.2).

When steady-state condition was reached, reactants space velocity was raised to GHSV = 40000 h^{-1}, by holding feed ratio to $H_2O/O_2/C$ = 0.49/0.56/1.

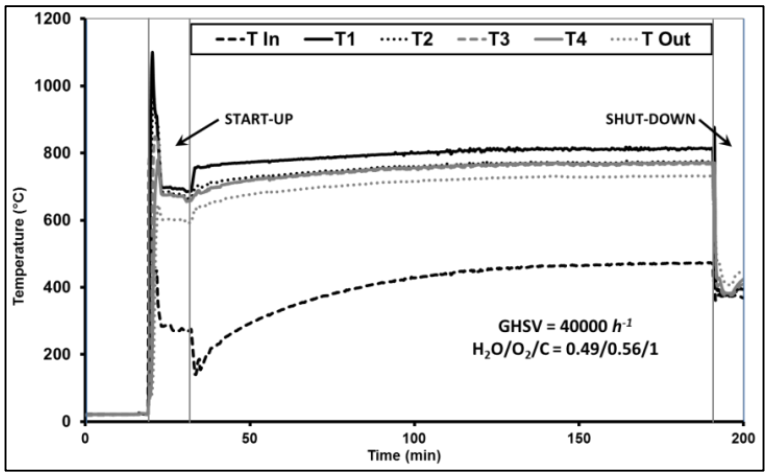

Figure V.3 *Temperature trend during the test (GHSV = 40000 h^{-1}, $H_2O/O_2/C$ = 0.49/0.56/1)*

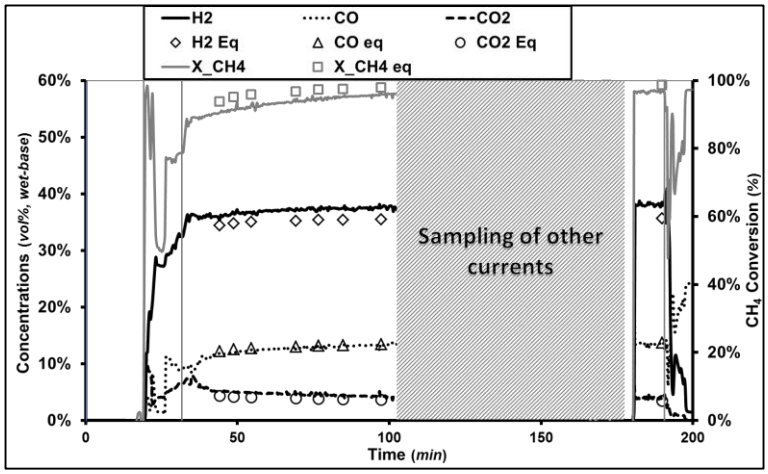

Figure V.4 *Composition and methane conversion during the test (GHSV = 40000 h^{-1}, $H_2O/O_2/C$ = 0.49/0.56/1)*

A very quick response in thermal profile along the whole catalytic bed was obtained, with a temperature raising after each catalytic brick (Figure V.3). During the whole test, reactor temperatures slowly increased: this was due to the global warm-up of the reactor, that reached a fully steady-state condition in very long times. However, temperature increases were within 10-15%, while hydrogen concentration quickly reached a value of 36%, and during test increased of about 6% (Figure V.4). Inlet gas temperature (T_{IN}) increasing was very more evident, due to the high thermal inertia of heat exchange module, that due to its greater thermal capacity requires much more time to reach

steady operation. In fact, only after 1 hour and half, temperatures reached values similar to the final ones.

V.1.1.2 System test

After start-up, the ATR operating conditions was held in order to evaluate the system performances.

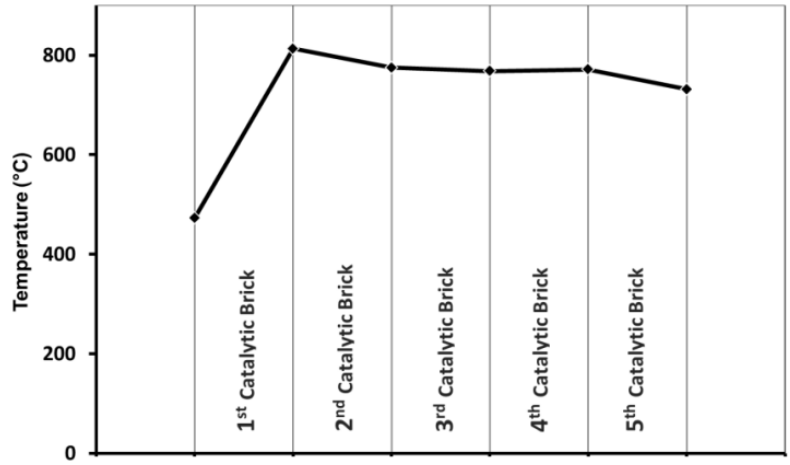

Figure V.5 *Temperature profile along catalyst (GHSV = 40000 h^{-1}, $H_2O/O_2/C$ = 0.49/0.56/1*

By analyzing thermal profile along catalytic bed (Figure V.5), it's very interesting to observe that all temperatures were within a range of 80°C, and neglecting the outside temperature (T_{OUT}), the temperature range was reduced to 40°C. A very flat temperature profile was thus realized along catalytic bed in the operating condition: in one hand, thermal transport along catalytic bed was very high, on the other hand the equilibrium condition was reached just after the second catalytic brick. The lower temperature after the last brick of the catalyst may be due to an error in temperature reading, caused to the presence of vortices in the heat exchange module: therefore, for thermodynamic equilibrium values the temperature after 4th brick was considered.

Figure V.4 shows concentration values during the whole test. It's easy to note that achieved product concentration were very close to thermodynamic equilibrium values. While H_2 concentration may be considered constant during test, an increase of CO coupled with a decrease of CO_2 was noted: this may be due to a slowdown in the WGS reaction, caused by the increasing in temperature along the catalytic bed. The consequent H_2 reduction was not observed, because temperature increasing lead to a growing of methane conversion, and then to a further H_2 production.

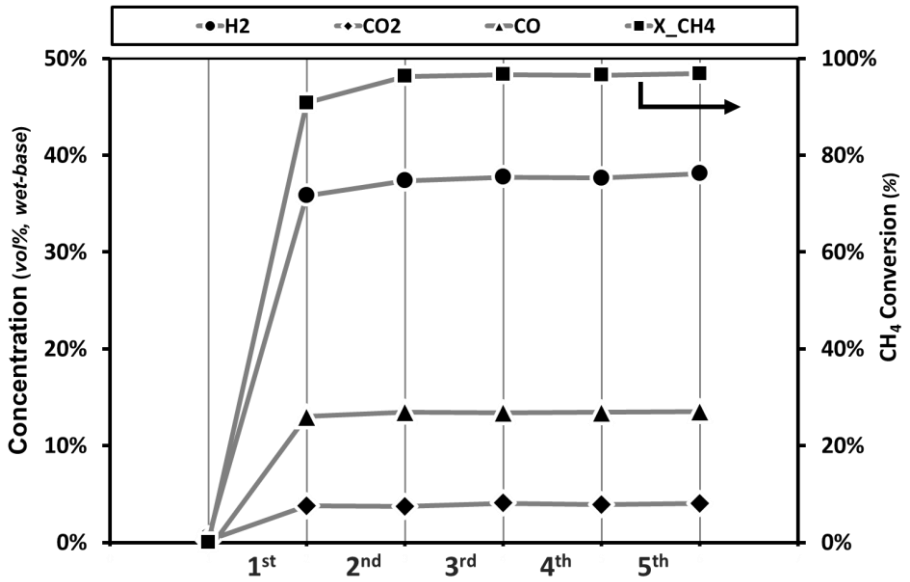

Figure V.6 *Composition and conversion profile along catalyst (GHSV = 40000 h^{-1}, $H_2O/O_2/C$ = 0.49/0.56/1)*

In Figure V.6 concentration profile along catalytic bed is reported. It's interesting to observe that just after the 2nd catalytic brick negligible changes were detected in product concentration, similarly to what was observed in temperature profile. The comparison with thermal equilibrium values demonstrated that just after the 3rd brick the system reached equilibrium condition.

Table V.1 *Reaction trend by varying GHSV ($H_2O/O_2/C$ = 0.49/0.56/1)*

GHSV (h^{-1})	*H_2 (vol%, w.b.)*	*X_{CH4} (%)*	*η (%)*	*Temperature (°C)*
40000	38.1%	96.9%	63.4%	732
50000	37.6%	96.6%	63.2%	771
66667	37.7%	96.7%	63.1%	768
100000	37.4%	96.3%	63.2%	775
200000	35.8%	90.8%	58.4%	814

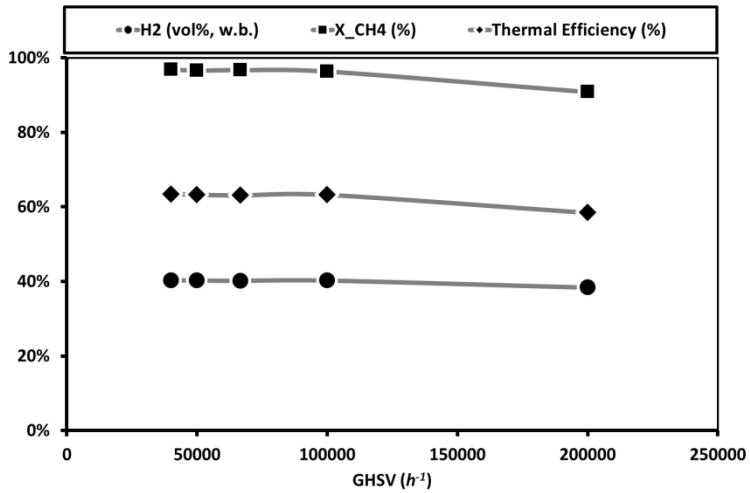

Figure V.7 *Reaction trend by varying GHSV ($H_2O/O_2/C$ = 0.49/0.56/1)*

Figure V.7 and Table V.1 show the relationship between the space velocity and the reaction parameters (temperature, H_2 concentration, CH_4 conversion and thermal efficiency). Even if reaction values showed not relevant changes for the different GHSV conditions, a regime condition was obtained for space velocity lower than 100000 h^{-1}. Thermal efficiency reached the notable value of 63%, very close to the maximum value obtainable by thermodynamic calculations for an ATR reaction in the selected operating conditions.

ATR tests were realized on the prepared catalysts, in order to investigate catalyst performances in terms of both catalytic activity and thermal management. Performances analysis was completed by comparing obtained results with thermodynamic equilibrium values.

All tests are realized by feeding to the system methane, air and bidistilled water at room temperature. All catalytic tests are conducted at a pressure of 2.5 atm.

V.1.2 Preliminary tests on AL92 catalyzed foam

Preliminary tests were conducted on AL92 catalyzed foam, by6 fixing the GHSV value and by varying the feed ratios.

In Figure V.8 and Figure V.9 the main results are reported.

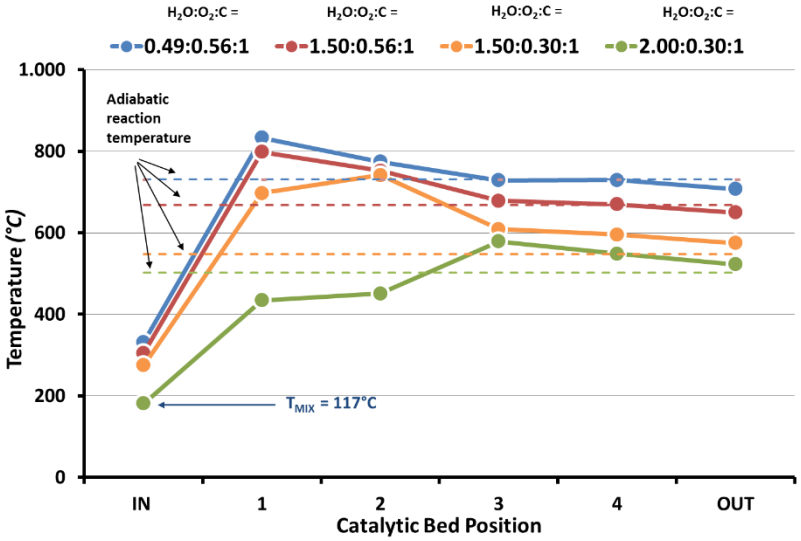

Figure V.8 *AL92 tests: thermal profiles (GHSV = 80,000 h^{-1}; p = 2.5 bar)*

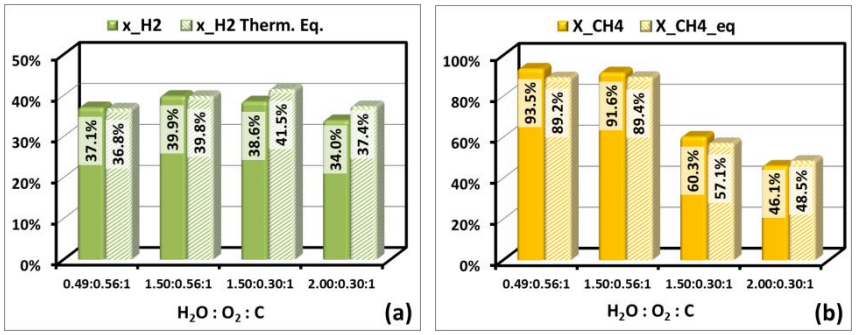

Figure V.9 *AL92 tests: Hydrogen concentration (a) and Methane conversion (b) (GHSV = 80,000 h^{-1}; p = 2.5 bar)*

As reported in Figure V.8 and Figure V.9, higher O_2/C ratio and lower S/C ratio led to higher temperatures and, as a consequence, at higher methane conversion values. However, all cases underlined the high activity of catalytic formulations, since gas composition and methane conversion appear very close to thermodynamic equilibrium values. The experimental conversion higher than the thermodynamic equilibrium one may be explained by the fact that the thermodynamic equilibrium values were evaluated at the T_{OUT} temperature; such temperature appears quite lower than T_3 and T_4, since it may be effected to the formation of vortex in the exit section of the catalytic bed in proximity of the heat recovery exchangers. Therefore, the T_{OUT} thermocouple may read a temperature of a quite cooled stream, that in turn causes an under-estimation of the thermodynamic equilibrium values. Moreover, performed tests underline that too extreme operating conditions (Case 4) were not sustainable by the system, since integrated steam generator seems not able to vaporize all the water, so resulting in the catalytic volume flooding. As a consequence, the adiabatic ATR reaction, evaluated in the selected operating conditions, seems to not be suitable for a membrane integrated process, since the temperature profile resulted higher than 550°C in a part of the catalytic bed.

V.1.3 Tests on catalyzed foams

ATR tests were performed on the catalyzed foams at several operating conditions by fixing feed ratios (H_2O:O_2:C = 0.49:0.56:1) and operating pressure (p = 2.5 bar), and by varying space velocity between 80,000/h and 120,000/h. In order to better understand the tested catalyst performances, the results are compared with catalytic performances of a commercial honeycomb monolithic catalyst noble metals based provided by BASF®.

The main results were summarized in Figure V.10, Figure V.11 and Figure V.12.

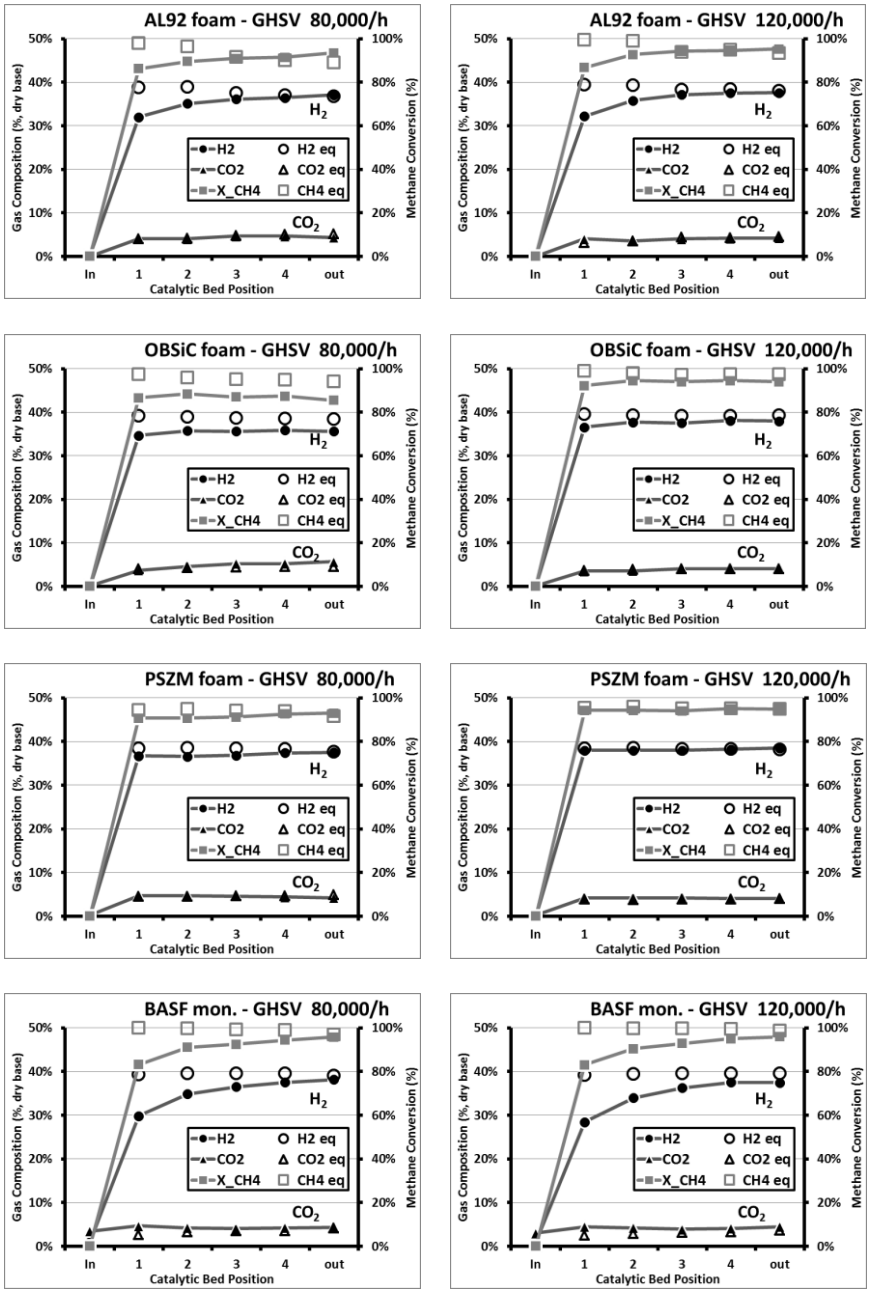

Figure V.10 *Gas composition and Methane conversion profiles (H_2O:O_2:C = 0.49:0.56:1; p = 2.5 bar)*

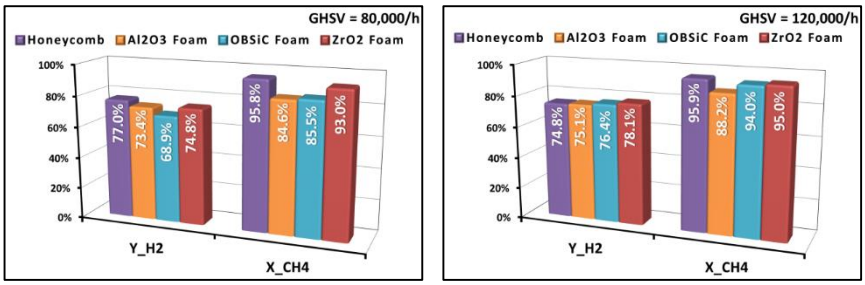

Figure V.11 *Hydrogen yield and methane conversion (H_2O:O_2:C = 0.49:0.56:1; p = 2.5 bar)*

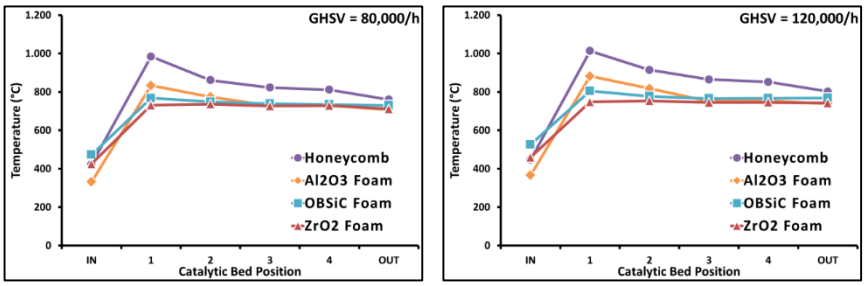

Figure V.12 *Temperature profiles (H_2O:O_2:C = 0.49:0.56:1; p = 2.5 bar)*

As a first result, the catalytic formulation seems highly active in all tested conditions and with all three different supports: gas composition and methane conversion appear very close to thermodynamic equilibrium values at the catalyst outlet section. By analyzing thermal profile, generally a very flat profile was observed for all foams, with best results obtained by ZrO_2 foam catalyst: the flat temperature profile results in a quicker approach to thermodynamic equilibrium, in terms of both hydrogen production and methane conversion. A similar behavior was obtained by OBSiC foam, where however a slightly higher thermal profile was recorded. It's relevant to underline that in each test, adiabatic reaction temperature was reached at the end of catalytic volume, to remark very low heat loss along catalyst.

As a strange behavior, by increasing GHSV value, in the honeycomb catalyst the gap between composition profiles and the corresponding equilibrium values seem so increase, while for the foams catalysts the effect seems to be the opposite. Of course, this phenomenon underlined that the BASF catalyst configuration was very close to its critical GHSV value, while foam catalysts may sustain higher reactants rate. Since the two catalysts have a similar catalytic formulation, the different behavior is due to the fluid dynamics along the monoliths: the continuous random structure of the foam catalysts in one hand assures very uniform temperature and composition radial profiles, in the other enhances mass solid-gas mass transfer. While the latter feature improved reactions kinetics, the former generated an uniform gas

condition that promotes the thermodynamic approach. For the foams, therefore, the highest reactants flow rate helped to reduce the heat losses relevance on system performances, resulting in an overall performances improvement.

V.2 Methane Steam Reforming

Steam reforming tests were carried out on foam catalyst. The methane conversion (Figure V.13) and hydrogen yield (Figure V.14) was monitored; furthermore, hydrogen productivity, in terms of moles of produced hydrogen per second per m^3 of catalyst, was evaluated.

As expected, the too low operating temperature played a crucial role in the catalysts overall performances: at atmospheric pressure, the methane conversion was clearly below 42%, resulting evidently far from the thermodynamic conversion; of course, the increasing of GHSV magnified the gap between obtained conversion and the thermodynamic value. Of course the highest S/C ratio weakly improves the methane conversion, however resulting in a worst approach to thermodynamic equilibrium.

The increasing in operating pressure obviously resulted in a reduction in methane conversion, as expected by thermodynamic predictions, but on the other hand reduced the gap between equilibrium and experimental values. In fact, to increase operating pressure resulted in an increasing of residence time, so producing a better approach to thermodynamic equilibrium.

In an overall context, in all tests PSZM catalyzed foam evidenced the worst conversion values and at higher GHSV catalyst performances were improved by increasing operating pressure. This behavior should be explained with a catalyst deactivation probably due to a lack of steam during test procedure.

The analysis of the results summarized in Figure V.13 and in Figure V.14 highlights the better performances of the alumina foam catalyst. In this analysis, a crucial role was covered by the heat transfer properties of the used foams, and in particular by the material thermal conductivity. The highest thermal conductive foam is characterized by a flatter radial and axial temperature profile, that results in a better solid-gas heat transfer. Since in the steam reforming reactions the heat transfer mechanisms plays a fundamental role on the overall reaction rate, the alumina foam, characterized by the highest bulk thermal conductivity, showed the best performances. The more the operating conditions stressed the heat transfer mechanisms (highest S/C ratio, highest GHSV values), the more the gain of the AL92 foam was more evident.

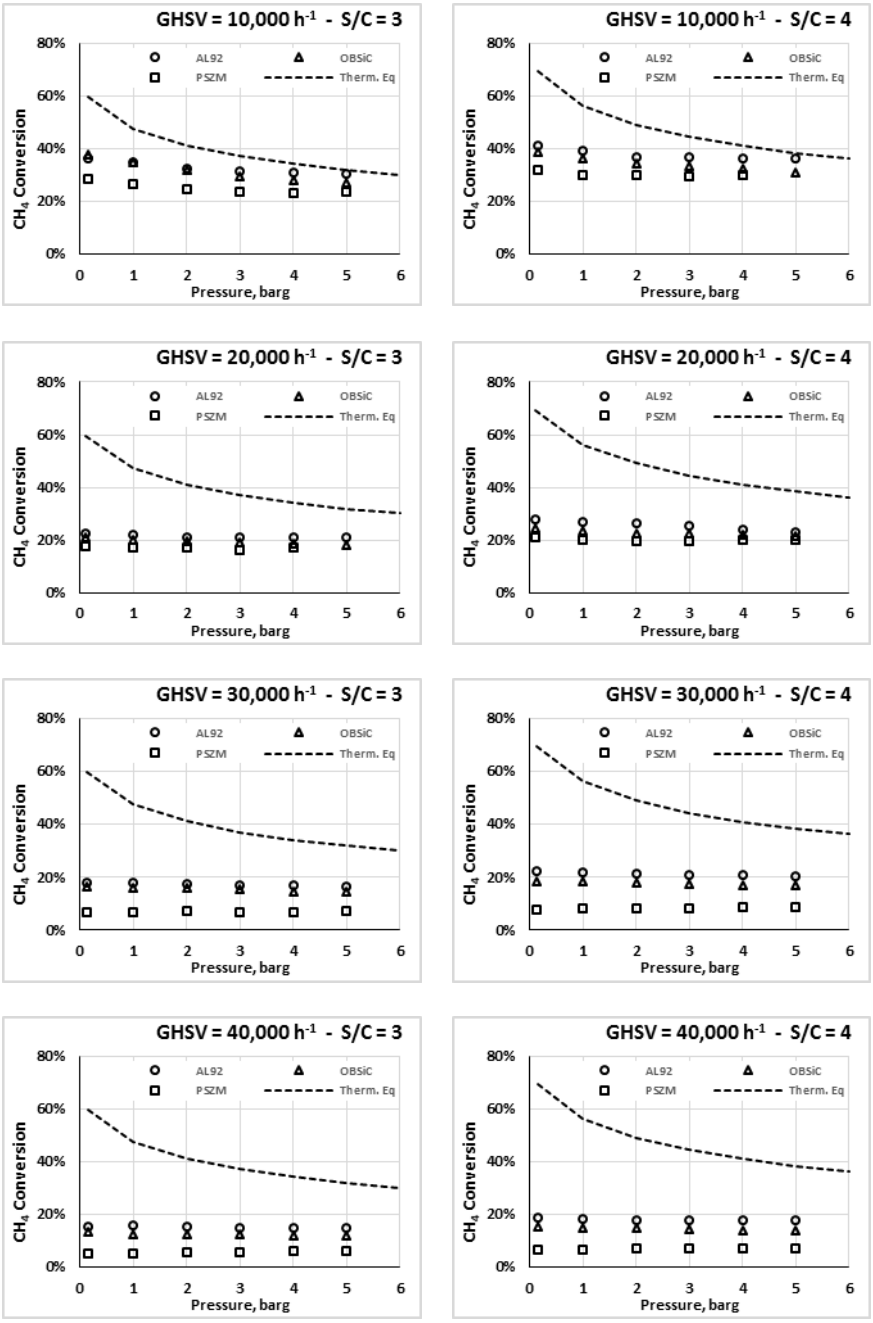

Figure V.13 *Methane conversion for the different catalytic foams (T = 550°C)*

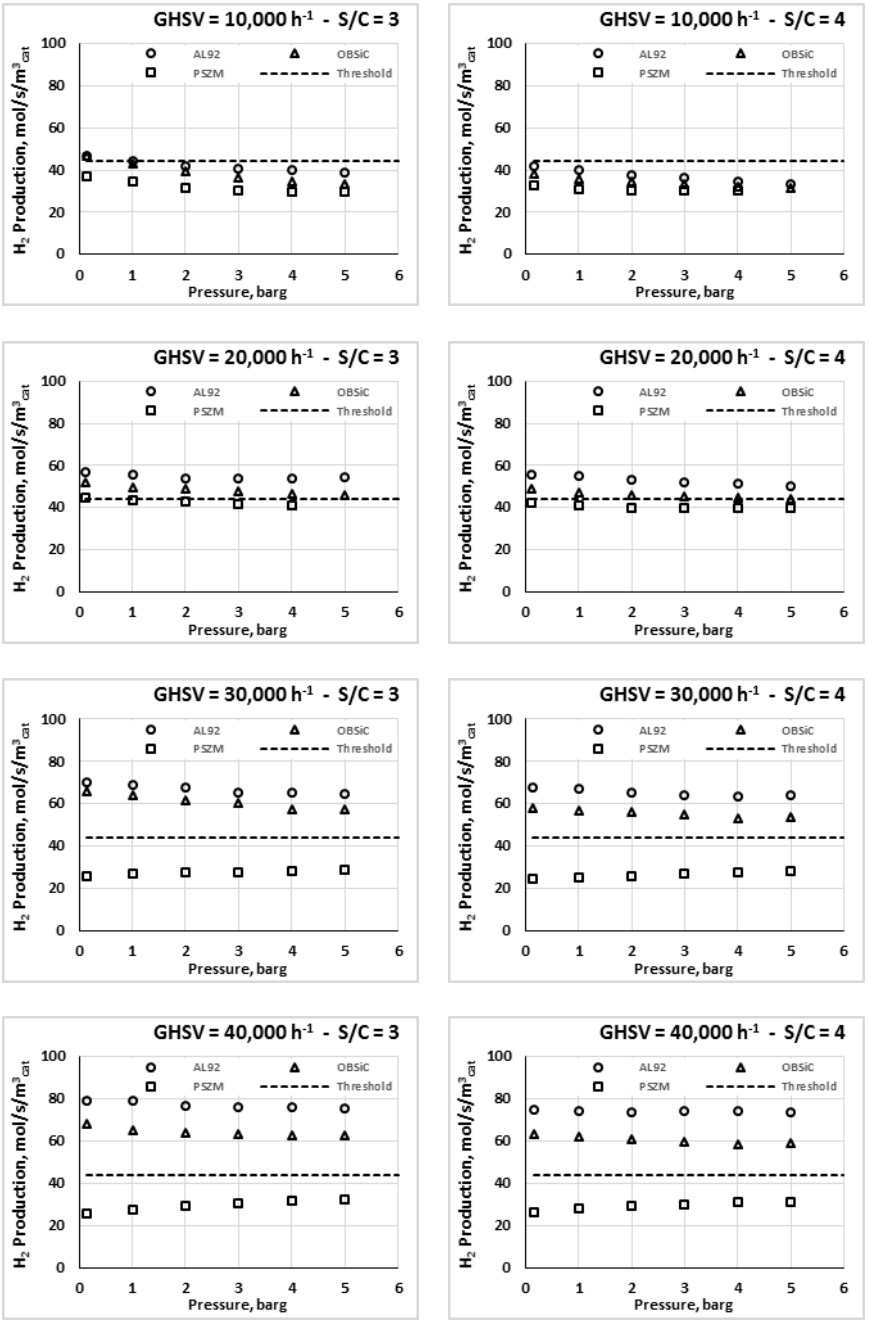

Figure V.14 *H_2 production for the different catalytic foams (T = 550°C)*

The CA.RE.N.A. project fixed a H_2 production target of 44 mol/s/m^3_{cat} at 40 barg, in order to have an useful coupling of selected catalysts with a membrane reactor. The use of a membrane reactor of course shift the focus away from the methane conversion; on the other hand, the high operating pressure becomes a requirement in order to maximize the hydrogen recovery. From this point of view, the AL92 catalyzed foam was candidate to have the best performances in terms of both hydrogen production and methane conversion. Despite catalytic tests at 40 barg in a lab-scale plant were not possible due to several safety limitations, evaluated H_2 production trend vs operating pressure and the progressive approach of the system by increasing operating pressure suggests that the proposed target is easily achievable by OBSiC and AL92 foams for a GHSV higher than 30,000 h^{-1}.

V.3 Discussion and conclusions

Catalytic tests were performed on 3 different kinds of catalyzed foams, in order to evaluate the influence of heat transfer mechanism in the system performances. All foams are activated by a catalytic coverage realized by Johnson Matthey within Ca.Re.N.A project. The catalytic tests were carried out in a thermally integrated ATR reactor, available in the ProCEED labs of the University of Salerno.

Preliminary tests were carried out, aimed to demonstrate the possibility to couple an H_2 perm-selective membrane to an ATR reactor. As expected, involved reactions generated a temperature peak in the first zone of the catalyst, depending on the feed ratio and the inlet temperature. The temperature was progressively reduced by increasing S/C ratio and decreasing O_2/C ratio, up to reach an inlet temperature of about 120°C (operative limitation due to the water condensing). The system appears able to reach thermodynamic equilibrium even in the more drastic conditions, however in several zones the catalyst temperature exceeded 540°C. Therefore, despite the appreciable performances of the catalytic system, the ATR process appears not suitable for the integration in a membrane reactor. It may be however considered an open architecture, in which catalytic stage and hydrogen removal stage are separated.

Activity were tested in ATR conditions, with very critical feed ratio (H_2O:O_2:C = 0.49:0.56:1). Performed tests underlines the high activity of the catalytic systems, that easily reached thermodynamic equilibrium. The use of thermally conductive catalyzed foams lead to a faster approach to thermodynamic equilibrium, as reported in the comparison with a commercial honeycomb monolithic catalyst. The complex foam structure in one hand promotes a continuous mixing of the reaction stream, in the other hand allows conductive heat transfer along the catalyst resulting in a flatter thermal profile.

The influence of the thermal profile along the catalyst was evidenced by comparing temperature and composition profile along the catalytic bed: the

more the temperature profile appears flat, the more the reaction stream quickly reaches a composition close to the final value. Therefore, by achieving a flat thermal profile, is possible in one hand to reduce hot-spot phenomena, that may causes local cracking phenomena, in the other hand to promote and then to accelerate the endothermic reforming reactions, so allowing to operate at higher GHSV values (both by increasing reactants rate or reducing catalytic volume).

In a first analysis, no correlations are found between material thermal conductivity and thermal profile: paradoxically, ZrO_2 has the lower thermal conductivity, but ZrO_2 foam results in the flatter thermal profile.

On the contrary, SR catalytic tests carried out on foam catalysts evidenced the relevance of heat transfer management on the catalytic performances. In particular, experimental results carried out at relatively low temperature (550°C) and different operating conditions, demonstrated that the samples characterized by the highest thermal conductivity showed the best results in terms of methane conversion and hydrogen yield. The beneficial effect was more evident in the more extreme conditions (higher S/C ratios, higher reactants rates), in which the heat transfer limitations are more evident. One of the most interesting effect resulting by the highest support thermal conductivity may be the possibility to obtain a flattening of the radial profile, that in one hand maximizes the heat transfer rate from the reactor walls to the catalyst.

Moreover, the random tridimensional structure of the foam catalyst, characterized by very high porosity and tortuosity, enhances the mass transfer and the mixing of the reacting mixture, obtaining a more uniform reaction condition along the whole catalytic bed, resulting in a more effective reaction system.

Chapter VI
Propane DeHydrogenation

VI.1 Catalyst components role

Catalytic performances of several catalysts are compared: Al_2O_3, Pt/Al_2O_3, $Pt\text{-}Sn/Al_2O_3$. Furthermore, the homogeneous reaction contribution was analyzed (empty reactor and quartz filled reactor). Catalytic tests were conducted at 600 °C, with a propane feed rate of 900 Ncc/min and a catalyst mass of 8.83 g.

As reported in Figure VI.1 and Figure VI.2, the catalytic system appears highly instable, since the conversion trend shows a clear and rapid deactivation over time. It is observed, moreover, a not negligible conversion of propane in the homogeneous phase, both with empty reactor and in the presence of quartz. It's reasonable that the residence time of the reactants in the reactor outside the catalytic bed is too much, enough to determine, in those thermal conditions, conversions of propane up to 8%. This phenomenon leads to the conclusion that in one hand the homogeneous reaction dramatically affects the results of the heterogeneous reaction, in the other hand, since the propane reacted not selectively in the reactor shell, the catalytic bed was fed by a current constituted not by pure propane, but by a mixture of different hydrocarbons of unknown composition. Furthermore, the homogeneous reaction was characterized by a selectivity of about 40% towards the propylene, to underline the main occurrence of side reactions.

Similarly, the alumina seems to be not completely inert to chemical reaction; however it exhausted most of its effect in less than 30 minutes of testing. The increased conversion of propane in the presence of alumina with respect to the homogeneous phase shows a not negligible catalytic activity of the support, on the contrary, the lower selectivity compared with homogeneous case suggests that the alumina, due to its acidic sites, promotes secondary reactions, such as cracking reactions. On the other hand, the catalytic effect fades within the first 30 minutes of testing due to the deposition of coke on the surface.

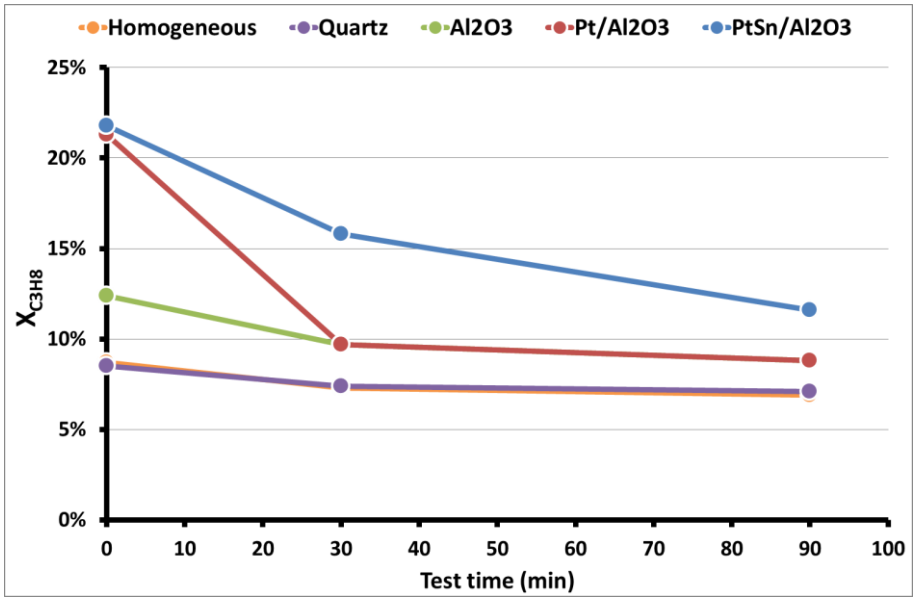

Figure VI.1 *Propane conversion vs time with and without catalyst and by varying catalytic formulation (WHSV = 12 h^{-1}; T = 600°C; p = 0 barg; tube-shell reactor)*

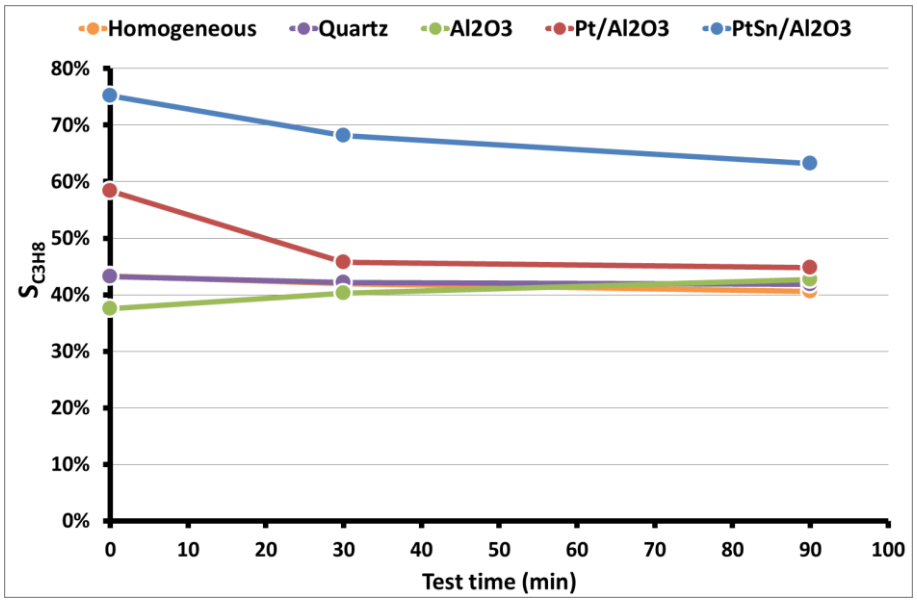

Figure VI.2 *Propylene selectivity vs time with and without catalyst and by varying catalytic formulation (WHSV = 12 h^{-1}; T = 600°C; p = 0 barg; tube-shell reactor)*

The effect of the platinum on the reaction is evident, bringing in the initial stages of the test the hydrocarbon conversion value up to 20%. The improvement led to the platinum sites had however a very short effect, since the propane conversion drop up to the pure alumina values in less than 30 minutes. In this phase, the Pt catalytic sites were completely covered by the coke deposition, so denying the platinum catalytic activity. On the other hand, the selectivity trend underlines that the main role of platinum is to promote the dehydrogenation reactions, so leading to a clearly higher selectivity. The gain in terms of propylene selectivity is quickly lost as the Pt sites were deactivated by coke deposition.

The graphs clearly show how tin improves catalyst performances in terms of activity but, above all, stability. The conversion trend shows how the presence of tin does not improve the propane conversion (conversion values of platinum and platinum-tin catalysts are initially the same), but it drastically improves the stability, thus weakening deactivation phenomena over time. It is also evident that the presence of tin increased selectivity to propylene: it can be deduced that tin inhibits the secondary reactions, thereby promoting the reaction of propane dehydrogenation. In other word, tin improve the platinum dispersion on the support resulting in a weaker accessibility to the acid sites of the support; so reactants mainly exploited the Pt catalytic activity, leading to a higher selectivity towards the desired products, reducing cracking reactions and as a consequence improving catalyst lifetime.

However, the homogeneous phase contribution dramatically effect also the performance of this catalyst: it takes into account that at 600°C is thermodynamically waiting a propane conversion of about 50%.

VI.2 Reaction temperature influence

In a second stage, Pt-Sn/Al_2O_3 catalytic activity at a reaction temperature of 550 °C was analyzed. In Figure VI.3 and Figure VI.4 propane conversion and propylene selectivity trends are reported; obtained data are compared with 600°C reaction data.

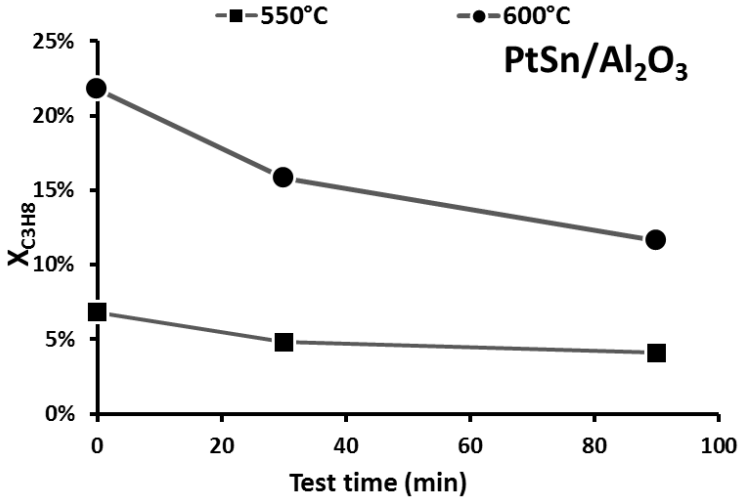

Figure VI.3 *Propane conversion vs time for 550°C and 600°C reactions (WHSV = 12 h^{-1}; p = 0 barg; tube-shell reactor)*

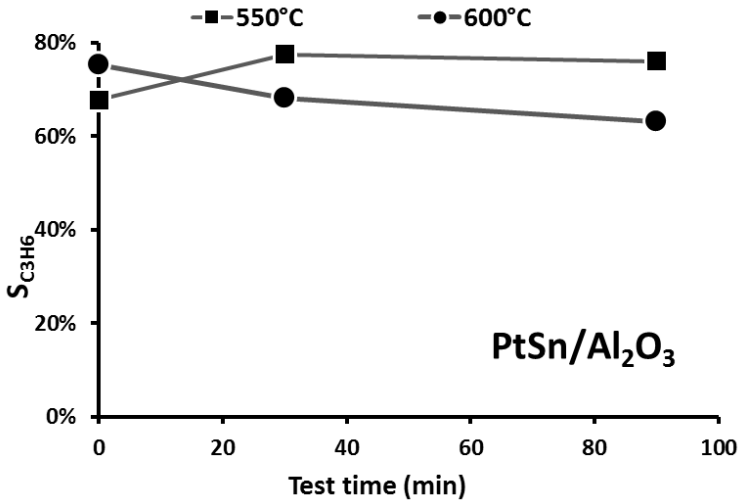

Figure VI.4 *Propylene selectivity vs time for 600°C and 550°C reactions (WHSV = 12 h^{-1}; p = 0 barg; tube-shell reactor)*

The reduction of test temperature dramatically deceased propane conversion values, in agreement with thermodynamic predictions. However, analyzing selectivity diagram, it is clear that, excluding the very first stage of reaction for which thermal transient might be relevant, the selectivity to propylene was favored at the lower reaction temperature. Moreover, the dehydrogenation is not the only involved reaction, but several other reactions occurs in the system. In particular, at lower temperatures the tested catalyst

appeared less active towards secondary reactions. To demonstrate this, it may be useful to report time trends of the molar fractions of the compounds in the products stream. In the case of reaction at 550°C (Figure VI.5) the presence of by-products (ethane, ethylene and methane) is less significant compared to the reaction at 600°C (Figure VI.6). Moreover, since at higher temperature the hydrogen signal is always higher than that of propylene, in contrast to what happens at a lower temperature, it is reasonable to suppose that at higher temperature the cracking phenomena are accentuated, resulting in a higher formation of hydrogen, together with the release of coke, due to the breaking of the hydrocarbon chain.

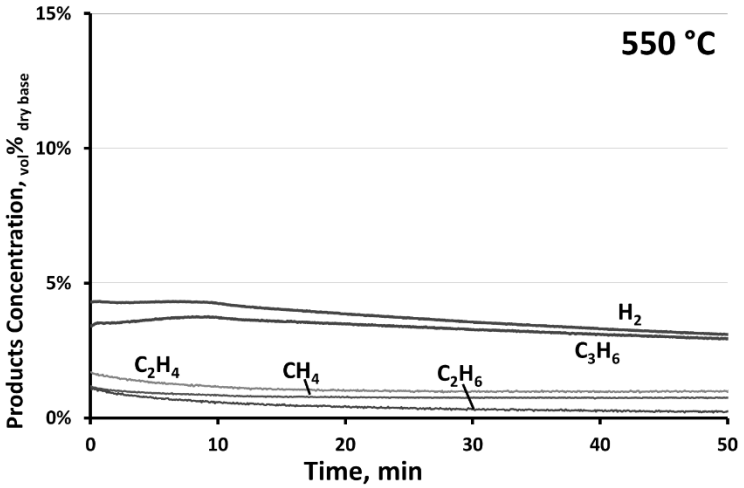

Figure VI.5 *Products trend (WHSV = 12 h^{-1}; T = 550°C; p = 0 barg; tube-shell reactor)*

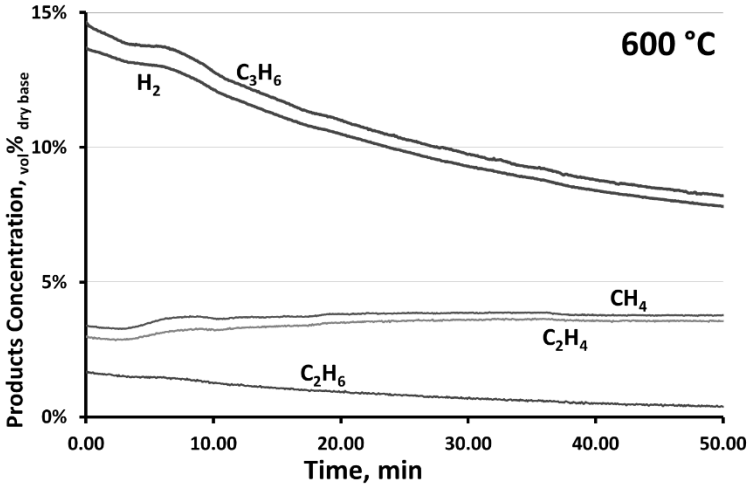

Figure VI.6 *Products trend (WHSV = 12 h^{-1}; T = 600°C; p = 0 barg; tube-shell reactor)*

Both graphs evidenced a parallelism of propylene-hydrogen and ethylene-methane concentrations, so remarking the two main reactions involved in the system:

$$C_3H_8 \rightleftarrows C_3H_6 + H_2$$
$$C_3H_8 \rightleftarrows C_2H_4 + CH_4$$

Moreover, by referring to the ethane trend, as well as to the gap propylene-hydrogen and methane-ethylene evidenced in the 550°C tests, its also reasonable to suppose the occurring of the propane hydro-cracking reaction:

$$C_3H_8 + H_2 \rightleftarrows C_2H_6 + CH_4$$

VI.3 Tubular reactor preliminary tests

Following the considerations on the contribution of the homogeneous reactions in the reaction system, a linear tubular reactor was designed and realized to minimize homogeneous reactions contributions.

In order to verify homogeneous reactions contribution, several tests were performed without catalyst: the catalyst packaging was simulated by replacing it with inert quartz having the same grain dimension. Tests were conducted for two different WHSV values, in order to verify stream rate influence. In Figure VI.7 propane conversion values vs temperature are reported, in a temperature range between 500°C and 600°C. WHSV = 6 h^{-1} value was obtained by using a 450 cm^3/min propane flow rate; WHSV = 12/h value was obtained by using a 900 cm^3/min propane flow rate.

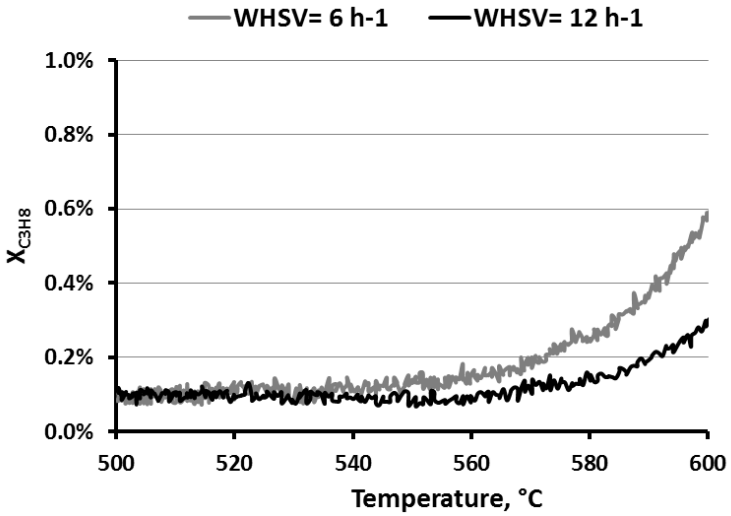

Figure VI.7 *Propane conversion vs temperature in homogenous conditions for WHSV = 6 h^{-1} and 12 h^{-1} (Tubular reactor; p = 0 barg)*

As evident by results, propane conversion remained lower than 1%; the temperature increasing results in an increasing of propane consumption, perhaps due to its decomposition to coke, however the values are very low. Moreover, by operating at WHSV = 12 h^{-1}, and then for a lower residence time, propane decomposition results lower than 0.3%.

Therefore, the tests demonstrated that the new reaction system was able to minimize homogeneous reactions contribution, and to study the effective catalyst activity and stability.

VI.4 Activity tests on $PtSn/Al_2O_3$ catalyst

In Figure VI.8 and Figure VI.9 propane conversion and selectivity to propylene trends are reported for the two reaction systems (tube shell reactor and stainless steel tubular reactor) in the 100% propane dehydrogenation reaction.

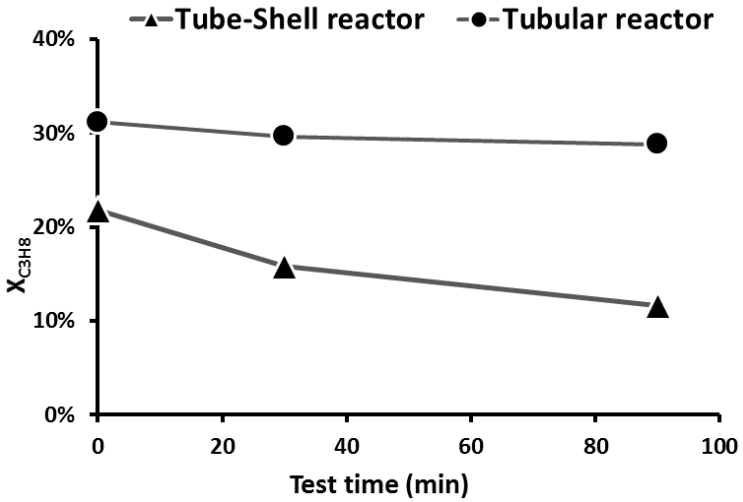

Figure VI.8 *Propane conversion trend for the two different reaction systems (WHSV = 12 h^{-1}; T = 600°C; p = 0 barg)*

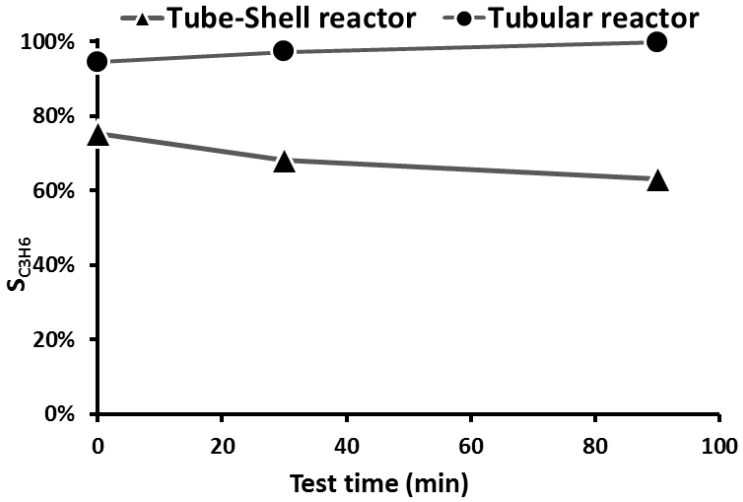

Figure VI.9 *Selectivity to propylene trend for the two different reaction systems (WHSV = 12 h^{-1}; T = 600°C; p = 0 barg)*

As a result, the tubular reactor results in better performances, both in terms of catalytic activity and selectivity to propylene, than tube-shell solution. The selectivity diagram suggests that in the new reaction system homogeneous phase contribution was dropped. Moreover, selectivity diagram underlines that the tubular reactor highly reduced side-reactions, so leading to a selectivity close to the 100% and as a consequence to a clear improving in catalyst stability, even if a not negligible deactivation was still recorded. On

the other hand, since the obtained conversion is evidently below the thermodynamic equilibrium values, it's reasonable to investigate different catalytic formulations and/or operating conditions.

VI.5 Catalytic support role

As a second step, the role of the catalytic support was investigated for Pt-Sn based catalysts. In particular, Al2O3, CeO2 and CeZrO2 were tested in the tubular reactor, by varying operating temperature from 400 to 600°C at atmospheric pressure. As a first step, catalysts were reduced in situ by a TPR procedure, the main results were reported in Figure VI.10.

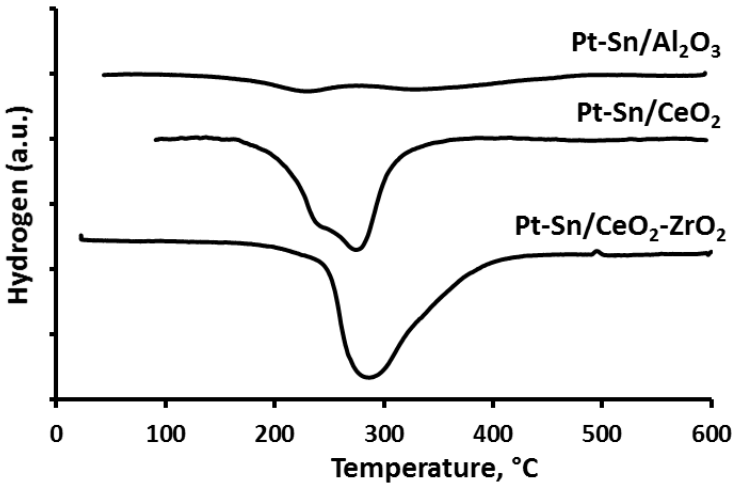

Figure VI.10 *TPR results for the Pt-Sn based catalysts*

As reported in the Figure VI.10, the ceria-based catalysts recorded a clearly higher hydrogen consumption: the phenomenon is due to the partial reduction of the support, as well as to the well note spill-over effect of the ceria, mainly due to the oxygen mobility of such support. It is also noticeable that the two peaks due to the Pt and Sn are welded between them, to constitute one peak with a broad closing curve. The effect, often reported in the literature, is attributed to the interaction between platinum and tin.

According with CARENA project directive, catalytic tests were carried out on a wet stream of propane, by adding 20% of steam. Activity tests were summarized in terms of propane conversion (Figure VI.11), and selectivity to propylene (Figure VI.12), coke (Figure VI.13) and reforming reactions (Figure VI.14), as well as propylene yield (Figure VI.15).

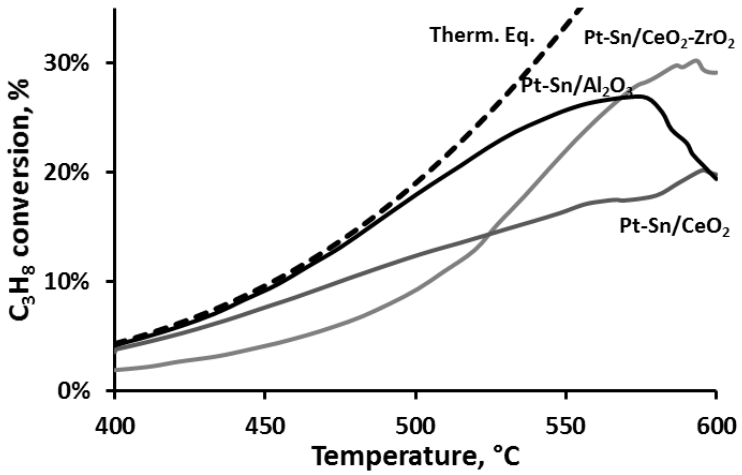

Figure VI.11 *Propane conversion trend for the different Pt-Sn based catalysts (WHSV = 8 h^{-1}; p = 0.2 barg; 20% fed steam)*

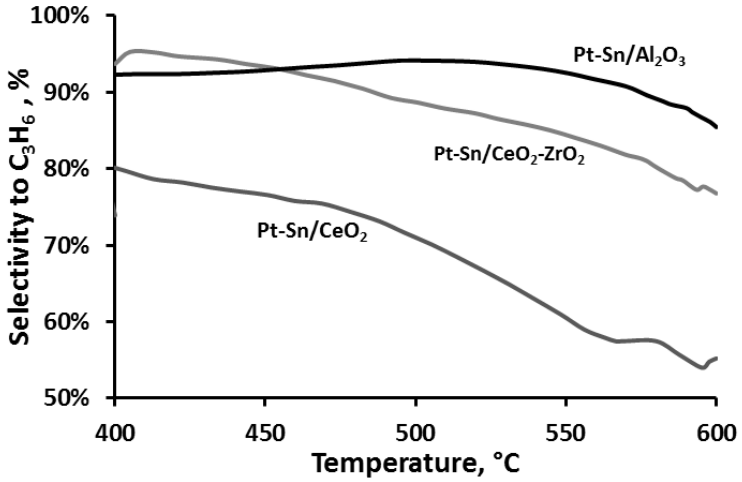

Figure VI.12 *Propylene selectivity trend for the different Pt-Sn based catalysts (WHSV = 8 h^{-1}; p = 0.2 barg; 20% fed steam)*

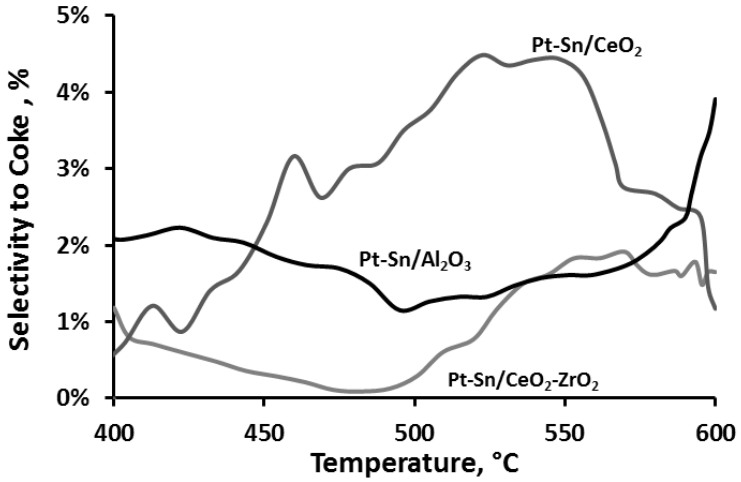

Figure VI.13 *Coke selectivity trend for the different Pt-Sn based catalysts (WHSV = 8 h^{-1}; p = 0.2 barg; 20% fed steam)*

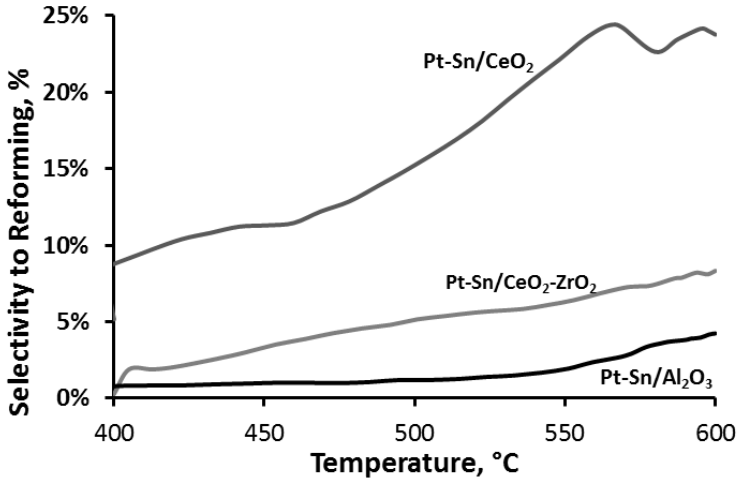

Figure VI.14 *Reforming selectivity trend for the different Pt-Sn based catalysts (WHSV = 8 h^{-1}; p = 0.2 barg; 20% fed steam)*

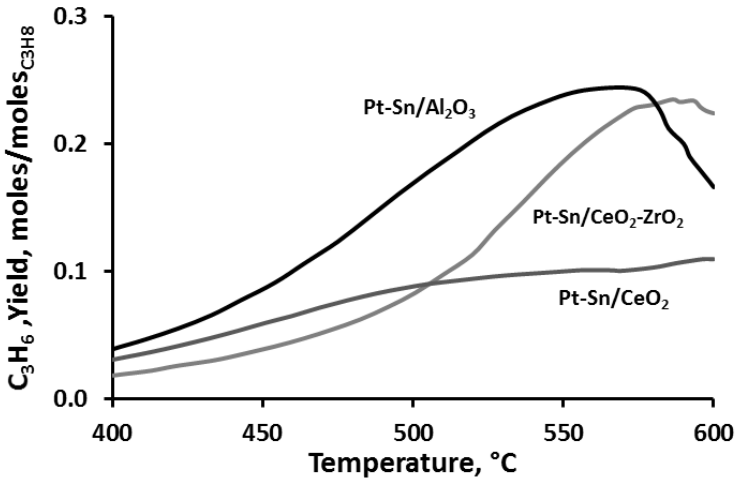

Figure VI.15 *Propylene yield trend for the different Pt-Sn based catalysts (WHSV = 8 h-1; p = 0.2 barg; 20% fed steam)*

Catalytic results evidenced the overall better performances of alumina based catalysts, that showed the highest conversion up to 580°C. However, the acid sites of the support promoted a constant coke deposition that caused the catalyst deactivation, as evidenced by the conversion drop at the high temperature. Up to 550°C, alumina catalyst showed a very low selectivity toward the reforming reactions so resulting in a selectivity to propylene higher than 90%. The selectivity propylene had an increasing trend up to 500°C, after that the coking and reforming reactions gave a sensible contribution.

Ceria based catalysts showed a marked activity towards reforming reactions. The CeO_2 based catalyst in particularly active in this direction, in addition a very high coke selectivity was observed. A reduced activity towards reforming reaction was shown by the $CeZrO_2$ catalyst, that was characterized by a very low coke deposition and as a consequence a weakest catalyst deactivation. The reducing characteristics of the support so were able to avoid (or at least to limit) cracking reactions, but also reduced the catalyst activity.

VI.6 Regeneration tests

In accordance with Ca.Re.N.A. PDH tests were carried out on S-01 and S-02 samples supplied by project partners. Catalyst producers propose to conduct tests at 600°C by diluting propane with 20% of water. The catalyst will be activated before testing by reducing-oxidizing-reducing procedure with a procedure suggested by SINTEF. The catalyst will be tested for 6 hours; at the end of the test, the catalyst will be regenerated by a oxidizing-reducing procedure. Globally, catalyst will be regenerated and re-tested for 2 times.

Table VI.1 *Regeneration tests procedure*

Step	Operation
Catalyst Activation	Reduction with 5% H_2 in He flux: Heating at 20°C/min up to 600°C + 2 hours at 600°C Oxidation • 1 hour at 600°C with 5% O_2 in N_2; • 1 hour at 600°C with AIR Reduction with 100% H_2 at 600°C for 1 hour
1° PDH Test	Feed: 80% C_3H_8 20% H_2O WHSV = 8-12 h^{-1} T = 540-600°C P = 1.5 Bar
1° Catalyst Regeneration	Oxidation • 1 hour at 600°C with 5% O_2 in N_2; • 1 hour at 600°C with AIR Reduction with 100% H_2 at 600°C for 1 hour
2° PDH Test	Feed: 80% C_3H_8 20% H_2O WHSV = 8-12 h^{-1} T = 540-600°C P = 1.5 Bar
2° Catalyst Regeneration	Oxidation: • 1 hour at 600°C with 5% O_2 in N_2; • 1 hour at 600°C with AIR Reduction with 100% H_2 at 600°C for 1 hour
3° PDH Test	Feed: 80% C_3H_8 20% H_2O WHSV = 8-12 h^{-1} T = 540-600°C P = 1.5 Bar

VI.6.1 S-01 sample

As a first step, S-01 formulation was tested by fixing the space velocity WHSV = 12 h^{-1} and the operating temperature T = 600°C, in order to investigate catalytic formulations in very stressing conditions. The main results in regeneration tests are summarized in Figure VI.16, Figure VI.17 and Figure VI.18.

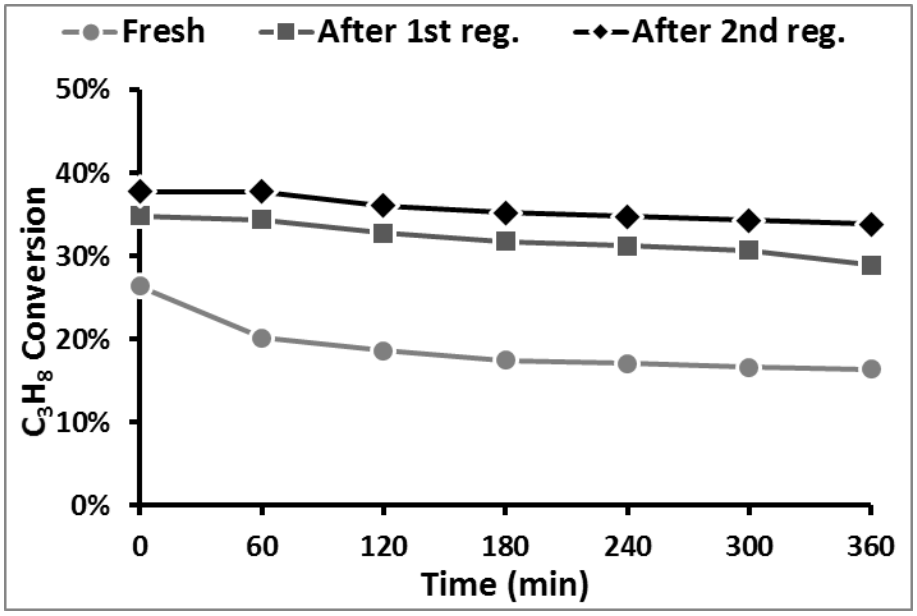

Figure VI.16 *Propane conversion trend for S-01 sample (WHSV = 12 h^{-1}; T = 600°C; p = 0.6 barg; 20% fed steam)*

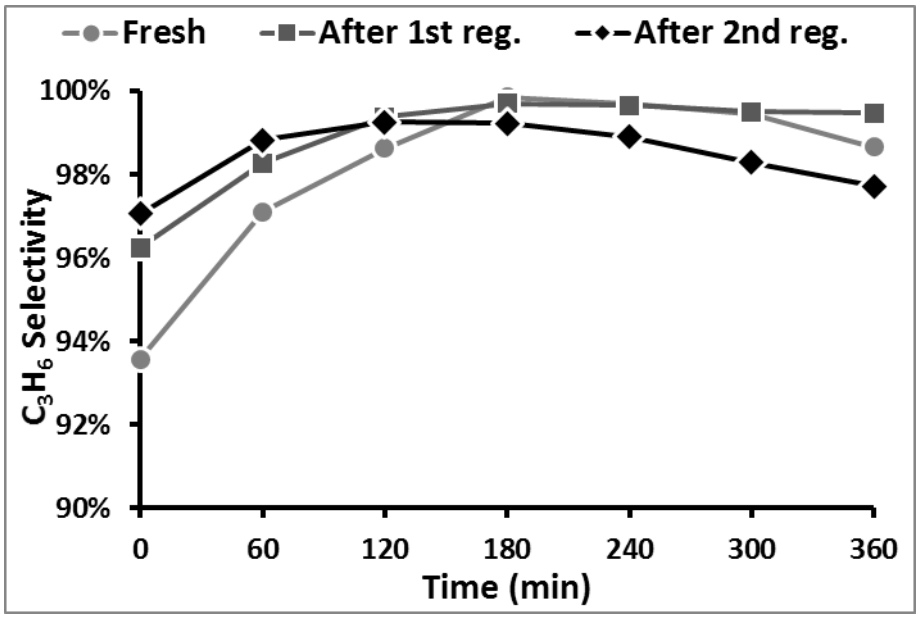

Figure VI.17 *Propylene selectivity trend for S-01 sample (WHSV = 12 h^{-1}; T = 600°C; p = 0.6 barg; 20% fed steam)*

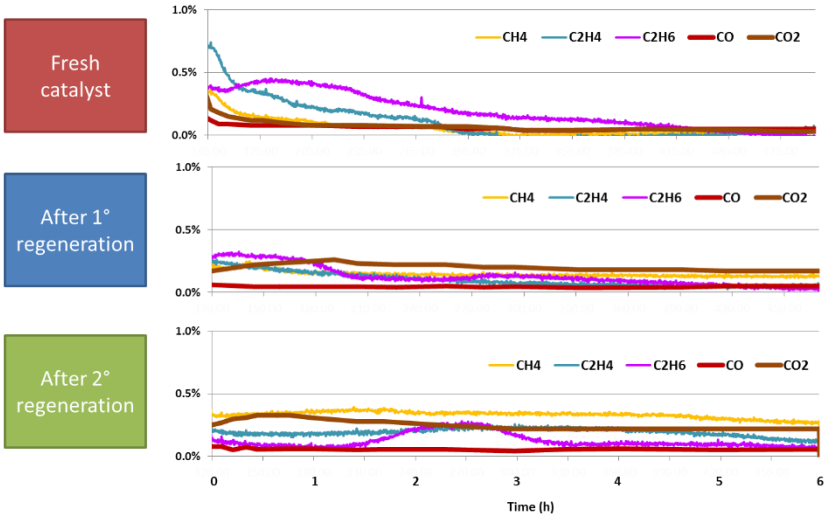

Figure VI.18 *Side-product content trend for S-01 sample (WHSV = 12 h^{-1}; T = 600°C; p = 0.6 barg; 20% fed steam)*

The obtained results show that S-01 sample take advantage by regeneration procedure, in particular for the first regeneration. The propane conversion after regeneration cycle appears at the same time higher and more stable. On the other side, catalyst selectivity appears very promising in all three tests, resulting in the whole tests higher than 90%, and becoming very close to 100% after 2 hours of test. This phenomenon underlines that, beside the water content in the reaction feed, reforming reactions are strongly limited, with a presence of CO and CO_2 lower than 0.5%. However, it's worth to note that the recorded conversion is significantly below the thermodynamic equilibrium value (close to 50%), and a sensible catalyst deactivation was recorded during the tests. Moreover, it's interesting to observe that the presence of CO_2 and methane seems to grow after each regeneration cycle, to remark some variations in the support nature.

VI.6.2 Ca.Re.N.A. partners catalysts comparison

The two catalytic formulations were then tested by reducing the space velocity WHSV = 8 h^{-1} and the operating temperature T = 540°C, in order to investigate catalytic formulations in more comfortable operating conditions.

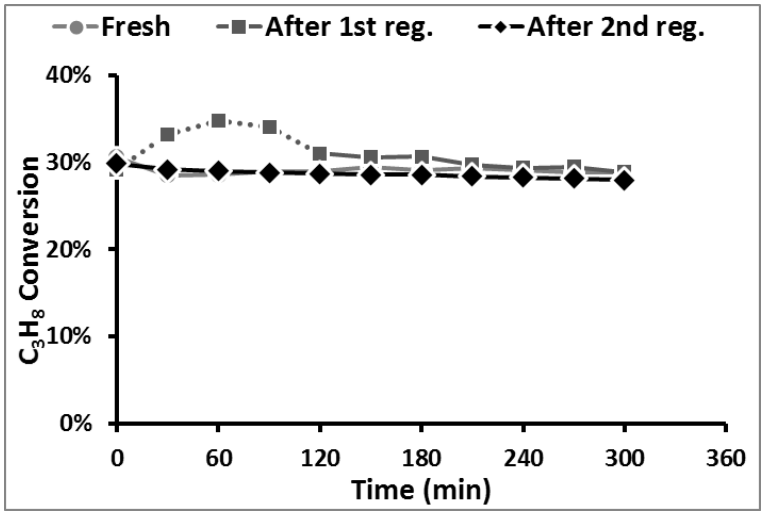

Figure VI.19 *Propane conversion in S-01 sample tests (WHSV = 8 h^{-1}; T = 540°C; p = 0.2 barg; H_2O/C_3H_8 = 0.25)*

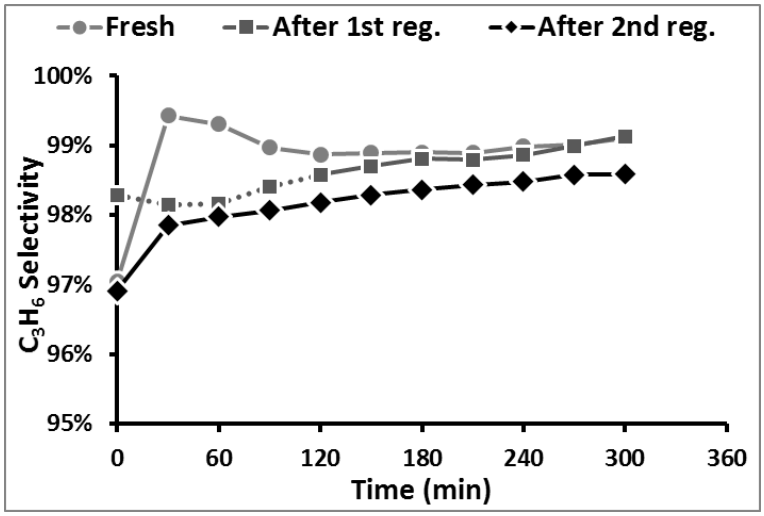

Figure VI.20 *Propylene selectivity in S-01 sample tests (WHSV = 8 h^{-1}; T = 540°C; p = 0.2 barg; H_2O/C_3H_8 = 0.25)*

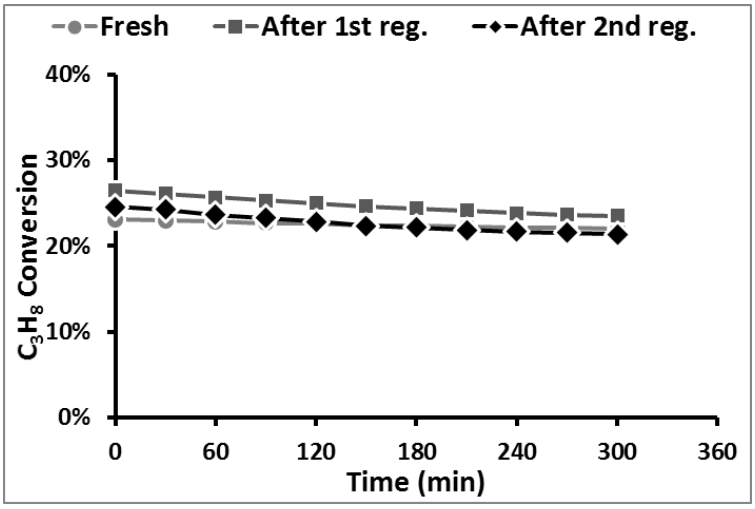

Figure VI.21 *Propane conversion in S-02 sample tests (WHSV = 8 h^{-1}; T = 540°C; p = 0.6 barg; H_2O/C_3H_8 = 0.25)*

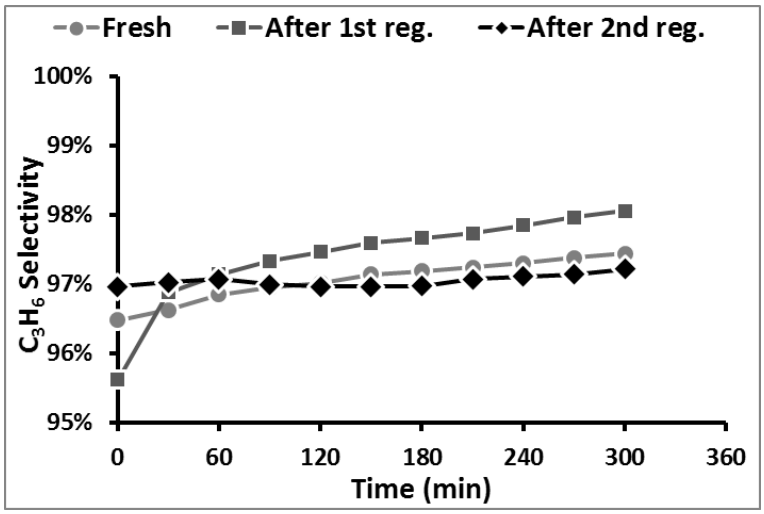

Figure VI.22 *Propylene selectivity in S-02 sample tests (WHSV = 8 h^{-1}; T = 540°C; p = 0.6 barg; H_2O/C_3H_8 = 0.25)*

The results underlined very promising performances for all the two formulations, since a quite stable conversion and an excellent selectivity was recorded with each sample. Moreover, the regeneration steps seems to not modify the catalytic performances: for the two catalyst, the first regeneration weakly improved the propane conversion, while the second regeneration didn't lead to further modifications (Figure VI.19, Figure VI.21). As a first outlook, the S-01 sample seems to show best performances in terms of both reactant conversion and propylene selectivity. It's also worth to note that during catalytic tests a coke selectivity of 0.3% was evaluated for S-01 sample,

while it was 1.0% for S-02 sample. It's however worth to underline that in the S-02 sample tests the operating pressure was slightly higher (0.6 barg) than S-01 (0.2 barg): this weak pressure difference may justify the lower propane conversion and the higher selectivity to coke for the S-02 sample. As a final consideration, the approach to thermodynamic equilibrium was quite the same for the two catalysts, by considering the different operating pressure.

VI.6.3 Feed steam content

The fed steam content effect was studied with both catalysts by varying the feed composition from 20% vol. steam content up to pure propane (0% steam content). The results are represented in Figure VI.23 and Figure VI.24. Propane conversion and selectivity to propylene seem not to significantly change, in particular on the S-02 sample. However, the pure propane feeding resulted the worse operating condition because of the coke formation. Furthermore, while the S-02 sample seems to be less affected by the steam content reduction, on the other hand by focusing on CO_2 concentration in products, the increasing in carbon dioxide at higher steam content in the feed stream to the reactor suggests a more evident sensibility towards reforming reaction.

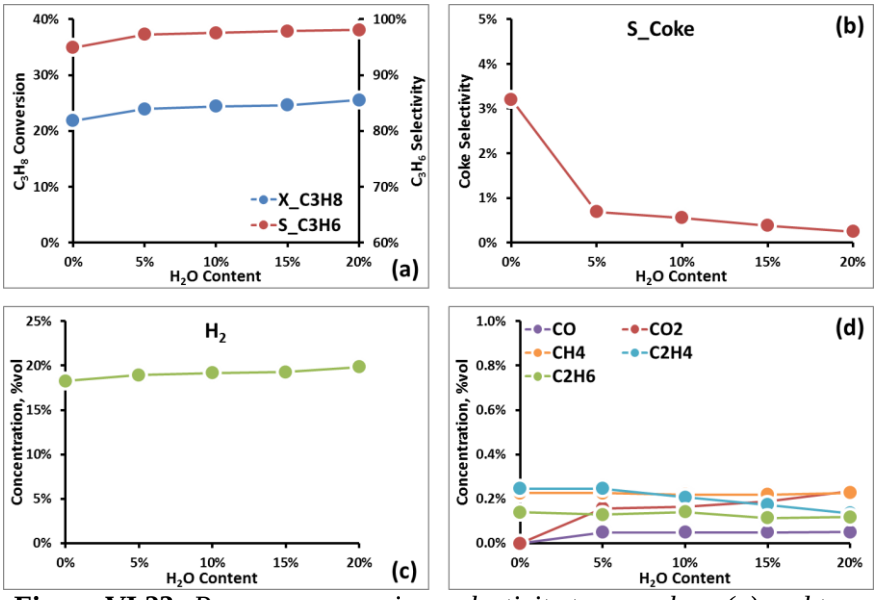

Figure VI.23 *Propane conversion, selectivity to propylene (a) and to coke (b), hydrogen (c) and side-products (d) distribution on fed steam content for the S-01 sample (T = 540°C; p = 0.4 barg; WHSV = 8 h^{-1})*

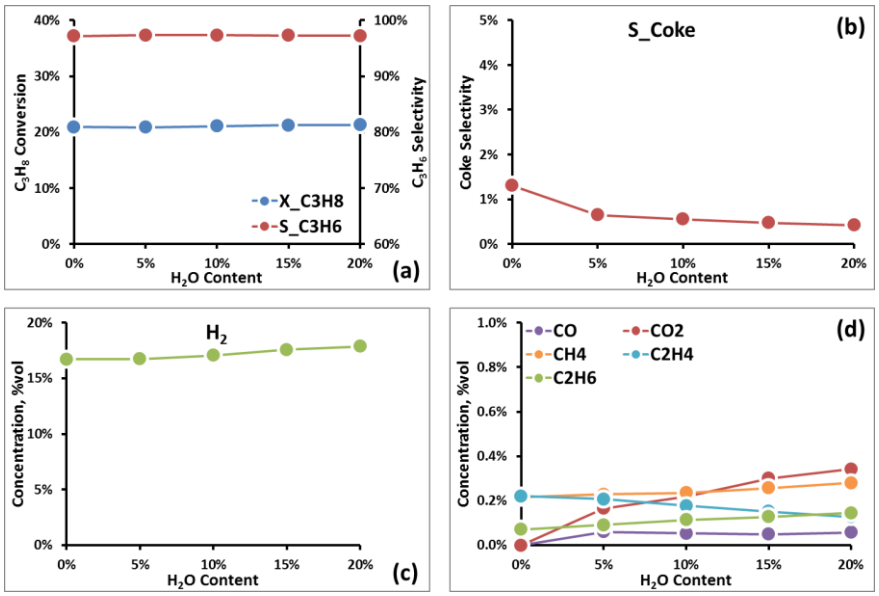

Figure VI.24 *Propane conversion, selectivity to propylene (a) and to coke (b), hydrogen (c) and side-products (d) distribution on fed steam content for the S-02 sample (T = 540°C; p = 0.2 barg; WHSV = 8 h^{-1})*

VI.6.4 Pressure effect

The pressure effect was also considered, and catalytic tests from about 0 up to 5 barg were carried out (Figure VI.25 and Figure VI.26). To increase pressure thermodynamically disadvantaged reactant conversion, as reported in propane conversion and hydrogen concentration trends. On the other hand, at high pressures hydrocarbon cracking was favored as highlighted by the selectivity to coke graph with the consequent decreasing in selectivity to propylene. S-02 sample was characterized by a less sensitivity toward pressure variation; however, the conversion values were lower than the S-01 one.

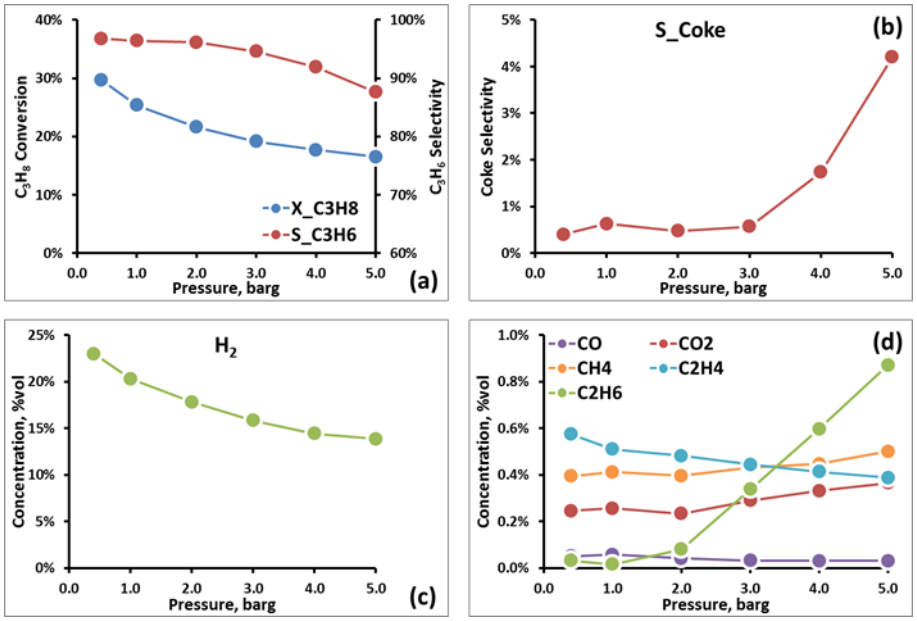

Figure VI.25 *Propane conversion, selectivity to propylene (a) and to coke (b), hydrogen (c) and side-products (d) distribution on fed steam content for the S-01 sample (T = 540°C; H_2O/C_3H_8 = 0.25; WHSV = 8 h^{-1})*

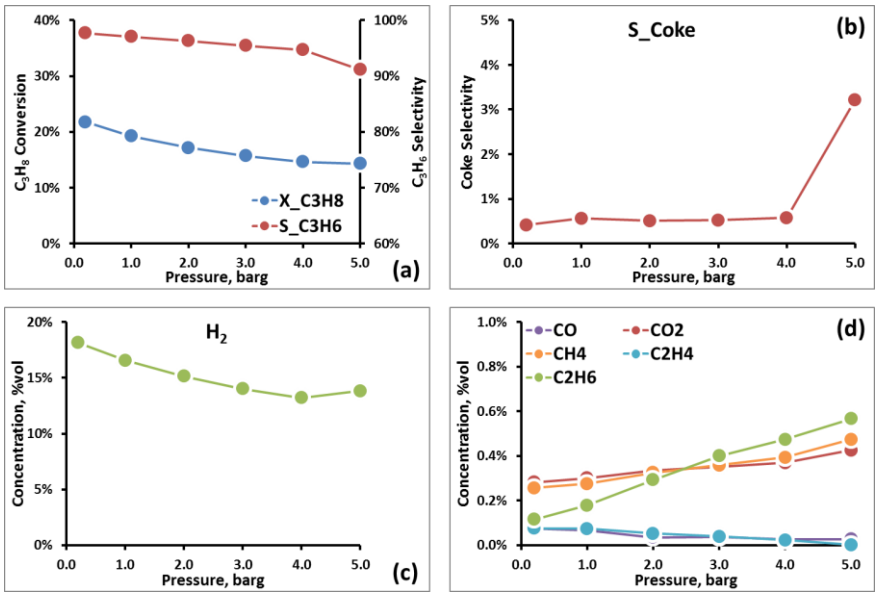

Figure VI.26 *Propane conversion, selectivity to propylene (a) and to coke (b), hydrogen (c) and side-products (d) distribution on fed steam content for the S-02 sample (T = 540°C; H_2O/C_3H_8 = 0.25; WHSV = 8 h^{-1})*

VI.6.5 CO – CO_2 effect

The effect of carbon monoxide and carbon dioxide content on catalytic performance was studied with S-02 sample formulation, by fixing the molar ratio H_2O/C_3H_8 = 0.25 and varying the CO and CO_2 content in the feed composition from $0\%_{vol}$ up to $10\%_{vol}$; the effects of CO and CO_2 were studied individually. Experimental tests were conducted at 540°C and 0.24 barg at WHSV = 8 h^{-1}.

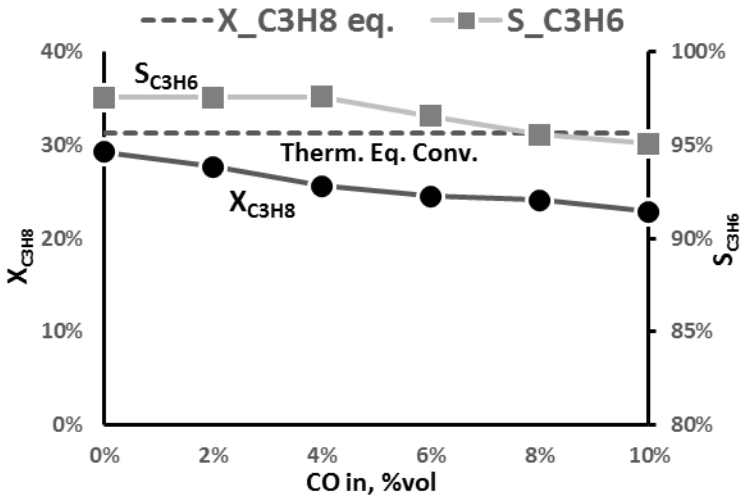

Figure VI.27 *Propane conversion and selectivity to propylene dependences on fed CO content for the S-02 sample (T = 540°C; p = 0.25 barg; H_2O/C_3H_8 = 0.25; WHSV = 8 h^{-1})*

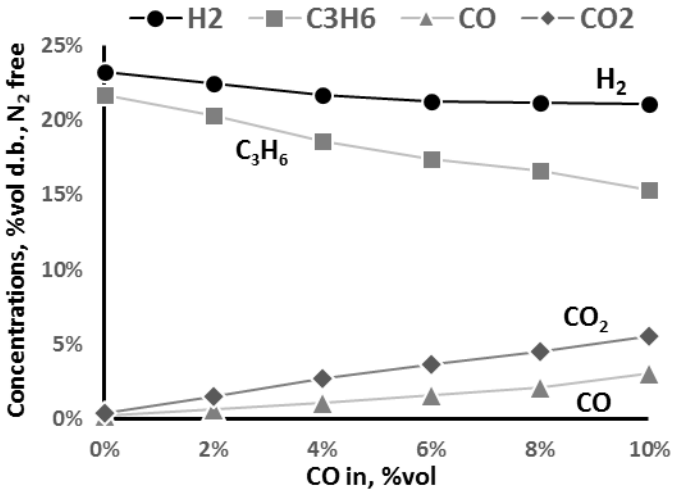

Figure VI.28 *H_2,C_3H_6, CO and CO_2 distribution dependence on fed CO content for the S-02 sample (T = 540°C; p = 0.25 barg; H_2O/C_3H_8 = 0.25; WHSV = 8 h^{-1})*

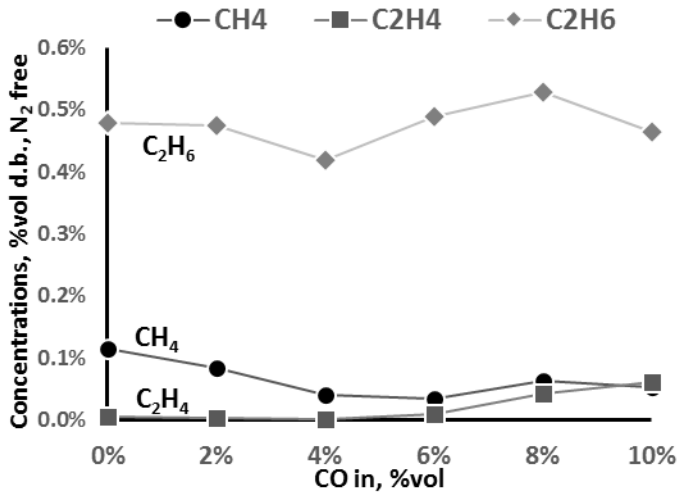

Figure VI.29 *CH_4, C_2H_4, and C_2H_6, distribution dependence on fed CO content for the S-02 sample (T = 540°C; p = 0.25 barg; H_2O/C_3H_8 = 0.25; WHSV = 8 h^{-1})*

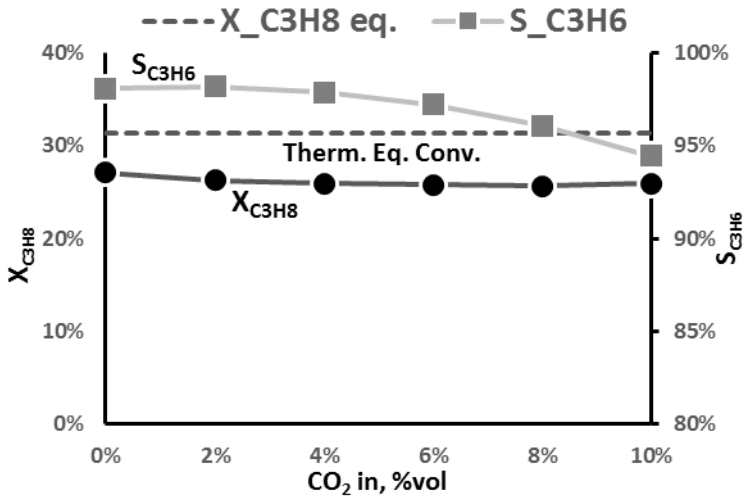

Figure VI.30 *Propane conversion and selectivity to propylene dependences on fed CO_2 content for the S-02 sample (T = 540°C; p = 0.25 barg; H_2O/C_3H_8 = 0.25; WHSV = 8 h^{-1})*

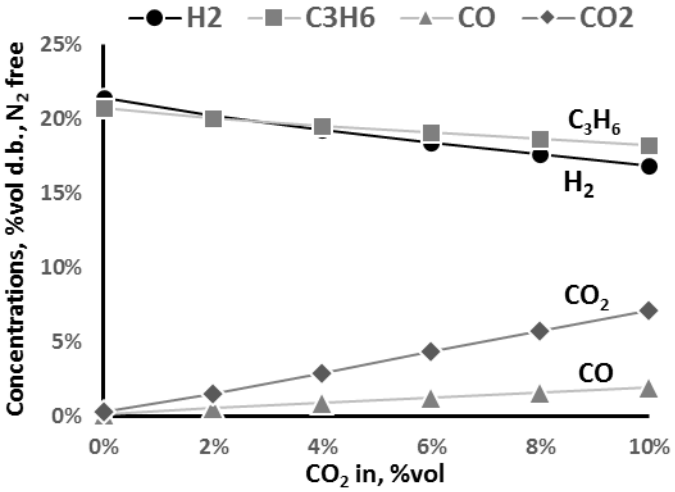

Figure VI.31 *H_2,C_3H_6, CO and CO_2 distribution dependence on fed CO_2 content for the S-02 sample (T = 540°C; p = 0.25 barg; H_2O/C_3H_8 = 0.25; WHSV = 8 h^{-1})*

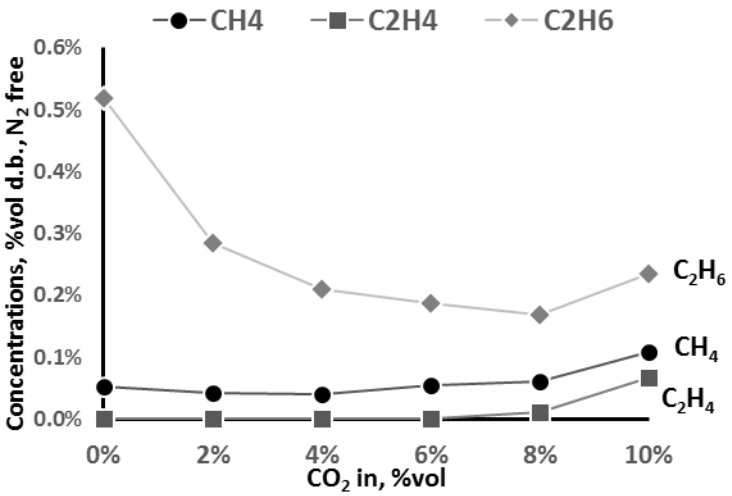

Figure VI.32 *CH_4, C_2H_4, and C_2H_6, distribution dependence on fed CO_2 content for the S-02 sample (T = 540°C; p = 0.25 barg; H_2O/C_3H_8 = 0.25; WHSV = 8 h^{-1})*

It can be seen (Figure VI.27) that the presence of CO causes a progressive reduction of propane conversion and for the highest CO concentration a weak reduction of selectivity towards propylene. The gap between H_2 and C_3H_6 concentrations (Figure VI.28) may be explained by the effect of WGS reactions, as highlighted by the massive presence of CO_2 in the products stream. However, since the more CO was fed, the more the carbon balance

diverges, the conversion to coke (or other undetected substances) could not be neglected.

The presence of CO_2 in the feeding reaction stream seems to lead to less evident effects: the propane conversion values are quite less sensible to carbon dioxide presence, while at highest dilution values the selectivity to propylene clearly decreased (Figure VI.30). Since the main by-products didn't increase with CO_2 dilution (Figure VI.32), it's reasonable to link this worsen performance to coke (or other undetected compounds) formation. The higher reduction of hydrogen yield with respect to propylene (Figure VI.31) was due to the reverse-WGS reaction (as confirmed by CO presence in products) as well as CO_2 hydrogenation reactions.

Tests were repeated at similar conditions, increasing the operating pressure up to 5 barg.

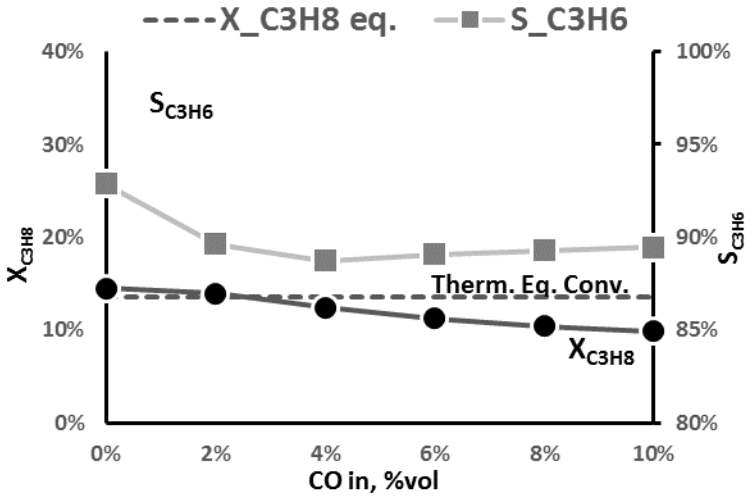

Figure VI.33 *Propane conversion and selectivity to propylene dependences on fed CO content for the S-02 sample (T = 540°C; p = 5 barg; H_2O/C_3H_8 = 5; WHSV = 8 h^{-1})*

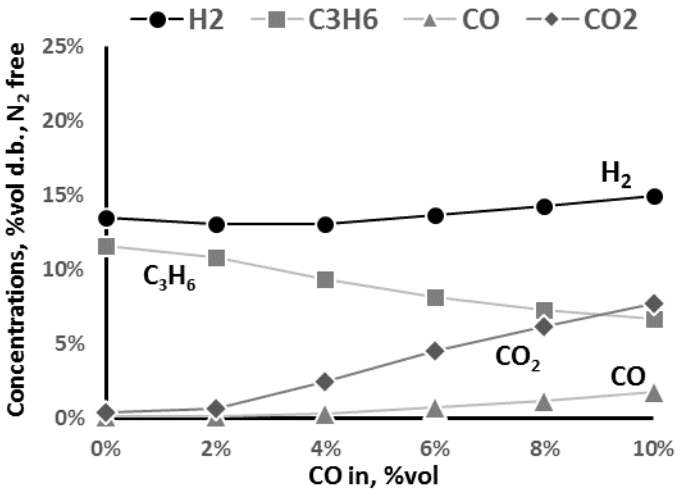

Figure VI.34 *H_2,C_3H_6, CO and CO_2 distribution dependence on fed CO content for the S-02 sample (T = 540°C; p = 5 barg; H_2O/C_3H_8 = 0.25; WHSV = 8 h^{-1})*

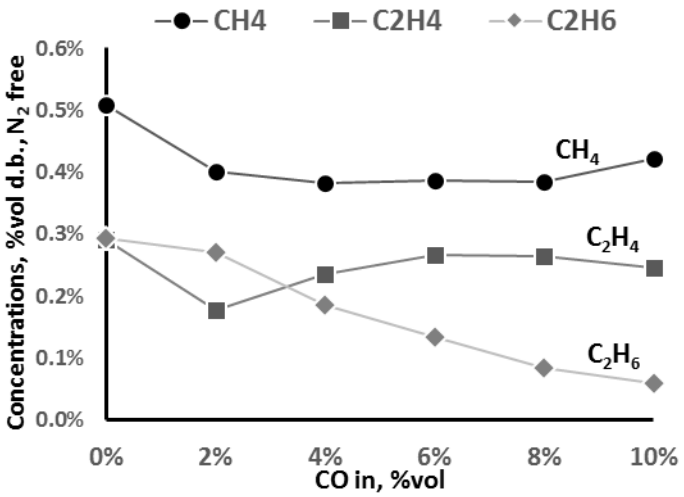

Figure VI.35 *CH_4, C_2H_4, and C_2H_6, distribution dependence on fed CO content for the S-02 sample (T = 540°C; p = 5 barg; H_2O/C_3H_8 = 0.25; WHSV = 8 h^{-1})*

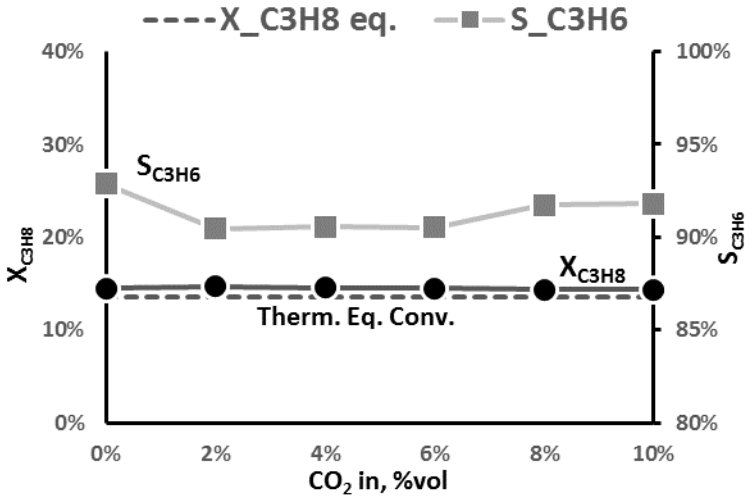

Figure VI.36 *Propane conversion and selectivity to propylene dependences on fed CO_2 content for the S-02 sample (T = 540°C; p = 5 barg; H_2O/C_3H_8 = 0.25; WHSV = 8 h^{-1})*

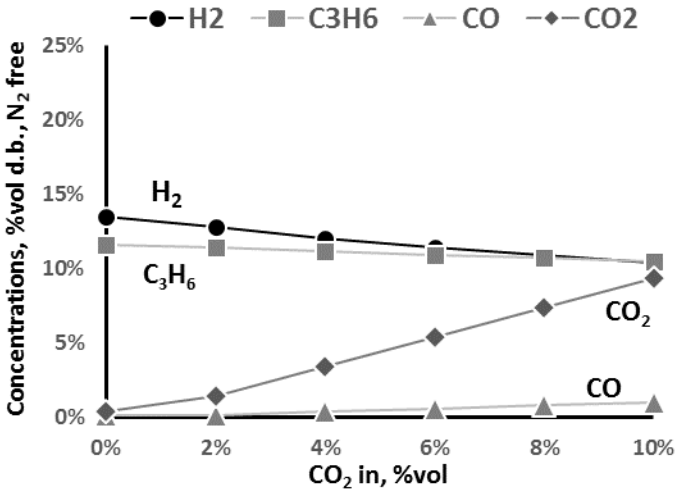

Figure VI.37 *H_2,C_3H_6, CO and CO_2 distribution dependence on fed CO_2 content for the S-02 sample (T = 540°C; p = 5 barg; H_2O/C_3H_8 = 0.25; WHSV = 8 h^{-1})*

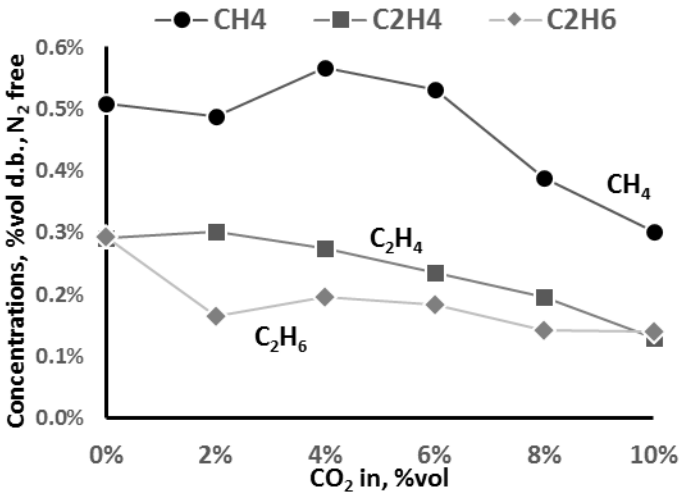

Figure VI.38 *CH_4, C_2H_4, and C_2H_6, distribution dependence on fed CO_2 content for the S-02 sample (T = 540°C; p = 5 barg; H_2O/C_3H_8 = 0.25; WHSV = 8 h^{-1})*

The results obtained at the highest pressure seem to confirm the trend evidenced in the earlier tests: the presence of carbon monoxide in the fed stream was detrimental for the catalyst activity (Figure VI.33). The phenomenon may be explained with the interaction of CO with Pt: carbon monoxide adsorbed on Pt site inhibits its catalytic activity. Of course, this behavior doesn't occur by feeding CO2 (Figure VI.36). On the other hand, the catalyst seems to have some activity towards the Water-Gas Shift reaction, since by adding CO to the feeding stream a significant amount of CO_2 was found in the reaction products (Figure VI.34). The WGS activity, increasing at increased pressure, enhances the hydrogen formation, in the products, therefore hindering the propane conversion of PDH reaction. The reverse-WGS reaction was also noticed in the test with CO_2-containing feed (Figure VI.37), but its contribute is clearly very lower, while the removal of H_2 from the process stream pushes the system towards further propane conversion. Finally, at the highest pressure some contribute of methanation reaction was observed (Figure VI.35, Figure VI.38).

VI.7 Durability tests

Stability tests of S-02 sample were performed. The following test procedure was planned:

- Catalyst activation
  - TPR: 600 cc/min 5% H_2 in He from 25°C to 600°C, heating rate 20°C/min
  - Reduction: 600 cc/min 5% H_2 in He at 600°C
  - Oxidation: 600 cc/min 5% O_2 in N_2 at 600°C
  - Reduction: 600 cc/min 100% H_2 at 600°C
- PDH
  - 750 Ncc/min 80% C_3H_8 + 20% H_2O (WHSV = 8 h^{-1}) at 540°C, 4.5 barg (for 6-7 hours)
- Quenching
  - Quick cooling (from 540 to 40°C in 10 minutes)of the system with 1800 cc/min of He
  - Overnight at room temperature, 50 cc/min He
- PDH …
- Quenching ...
- PDH …

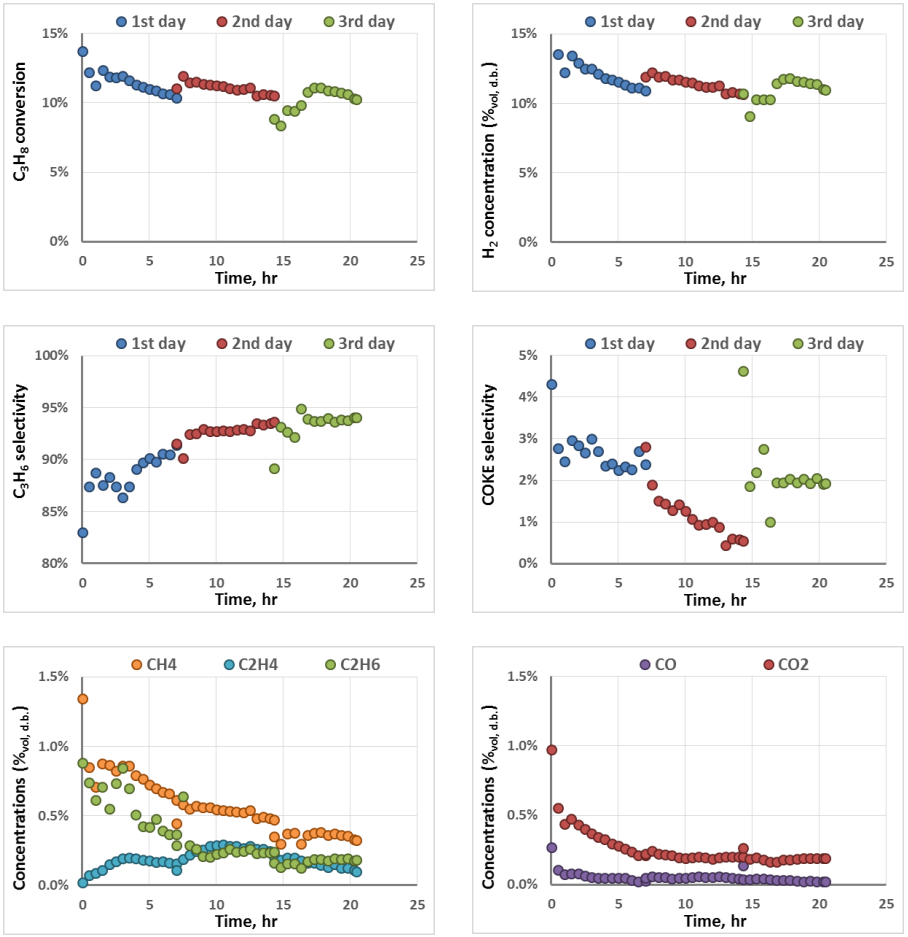

Figure VI.39 *Durability tests results on S-02 sample (T = 540°C; p = 4.5 barg; H_2O/C_3H_8 = 0.25; WHSV = 8 h^{-1})*

The regeneration tests results are summarized in Figure VI.39. As first, the catalyst recorded a sensible activity reduction during the test: by referring to the propane conversion, it drops from about 13% up to 10%. It's also noticeable that after each day, the catalyst recovered a little amount of activity. The phenomenon may be due to the cooling procedure: the steam of helium used in the cooling and warm up steps effected in a weak catalyst regeneration, that however didn't recovered completely the initial activity. It suggests that the helium removed some compound adsorbed on the catalytic surface, that caused the active sites inhibition, but of course is not able to remove deposed coke. Therefore is reasonable to think that catalyst deactivation (or at least active site locking) was caused by both catalyst coverage by coke deposition and inhibitor adsorption on catalytic site. To confirm this hypothesis, the deactivation rate (the propane conversion slope vs time) appears very similar for the 3 days tests, since coke selectivity was quite constant. It's worth to note

that hydrogen concentration follows the propane conversion behavior, presenting the same overall reduction along the test. On the other hand, the selectivity to propylene showed an homogeneous trend during the test, following an asymptotic curve; of course, in the first hours of activity, the system highlighted a relevant selectivity towards the side reactions, as demonstrated by the concentration of CO, CO_2 and the other hydrocarbons. All the side-products seems to reach a stationary value after 10 hours of overall test; on the contrary, the methane content showed a decreasing trend during the whole test, however the trend seems to reduce the slope in the time.

VI.8 Discussion and conclusions

The selective propane dehydrogenation is attracting the scientific research attention due to the growing worldwide propylene demand. Despite the traditional technologies diffused for the PDH reaction, innovative routes are required, aimed to the process intensification for the yield maximizing and as a consequence for the reduction of operating costs.

CARENA project focused on membrane reactors applications, and so on the catalyst-membrane integration, as key feature for a process intensification route.

Since in the CARENA project guideline the reactants recycling was adopted, reaction selectivity and catalyst lifetime are crucial parameters for the performances evaluations. Moreover, the membrane integration perspective constrains the operating condition choice, in terms of temperature and pressure, even penalizing the hydrocarbon conversion.

The literature pointed on Pt or Cr based catalysts as the most active and selective catalysts.

Since CARENA project points on Cr-free catalysts, the attention was shifted on Pt catalysts, by focusing on the role of promoters (or stabilizers) and catalytic support.

In the propane dehydrogenation, usually high attention is paid on the operating parameters (temperature, pressure, dilution, contact time) and catalytic formulation, but also the reactor geometry play an important role due to the possibility of side-reactions also in the homogeneous phase. Too high residence time of the reactants and products at high temperature outside the catalytic volume may result in uncontrolled reactions of the process stream, resulting in a dramatic drop of process selectivity. Specific tests demonstrated that non-optimized reactants pre-heating step led to a partial feed decomposition due to uncontrolled homogeneous gas phase reactions, that causes a sensible feed loss. Furthermore, due to homogeneous reactions, in the catalytic volume could be delivered a process stream completely different to the fed mixture. Therefore some components generated in the homogeneous phase may in one hand block the catalyst active sites, in the other hand

promote the coke formation, resulting in a catalytic surface coverage and then in the catalyst deactivation. Also at the catalyst outlet section attention must be played due to the possibility to obtain side-reactions in the product stream, particularly in the case of the PDH reaction where the higher propylene reactivity. Based on the achieved consideration, a specific lab-scale reactor was designed in order to minimize the unwanted side-reactions in the homogeneous gas phase.

From the catalyst point of view, the role of each component of the catalytic formulation was also investigated. The choice of a proper support is a crucial step, since the chemical properties of a support may affect catalyst performances by controlling unwanted side-reactions. As the most common catalytic support, alumina acid sites promotes cracking phenomena, for this reason as a widely used solution an alumina-modified support was used, in order to not affect the high specific surface of the Al_2O_3, and to neutralize acid site. Platinum have a fundamental role in the PDH reaction, maximizing the propane conversion and addressing the process selectivity toward the production of propylene. Unfortunately, the pure Pt was quickly deactivated by coke deposition, and the enhancement led to the platinum addition could be completely erased in less than one hour. In this aim, tin demonstrated to have a promotion effect on Pt/Al_2O_3 catalyst, improving Pt dispersion on the catalytic surface and stabilizing the catalytic sites, that in this way are able to weaken support acid properties. As a consequence, the selectivity towards propylene and the catalyst lifetime are improved.

In order to further increase catalyst life, steam addition in fed propane resulted an appropriate solution, on the other hand reforming reactions may occurs. In this sense, the role of the support was investigated, highlighting that ceria-based catalysts promotes reforming reactions, that lead to a relevant decreasing in process selectivity. On the other hand, the operating temperature also play a crucial role in the process, and to operate at too high temperature may results in an increasing in propane conversion but also in side-reaction contribute, that lead to a faster catalyst deactivation.

Specific tests carried out on S-01 sample evidenced that an appropriate modification of alumina support may lead to higher selectivity. Moreover, at higher temperature the catalyst regeneration may result in a slight improving of catalytic performances. On the other hand, a lower temperature, compatible to a membrane coupling, still led to appreciable conversion values, offering in addition a very low catalyst deactivation and an excellent selectivity to propylene. The gain linked to a quite low temperature was also confirmed by activity tests on the S-02 sample, also based on an alumina-modified support. The two formulations demonstrated to be not much sensible to reforming reaction, while the fed steam amount help to minimize the selectivity to coke. Since the catalytic system should be designed to be used in a membrane reactor, the operating pressure is also a crucial parameter for the membrane but also for the catalyst. Of course the increasing in the operating pressure

promotes cracking phenomena, decreasing the selectivity to propylene and enhancing the coke formation. However, the S-02 sample, despite a less weakly pronounced catalytic activity, showed to be the less sensible to the extreme operating conditions, so resulting the best candidate to the membrane integration.

Since in the CARENA project the PDH process is inserted in a wide process scheme, by which the PDH stage may be fed by a stream containing a little amount of CO and CO_2, the role of these compounds was investigated. The carbon monoxide resulted the most detrimental compound, leading to an overall performances worsening. In one hand the CO affinity with Pt sites led to a partial reduction of catalytic activity, on the other hand the not negligible contribution of WGS reaction resulted in an hydrogen production outside the PDH reaction, so partially reducing the propane conversion. On the contrary, the CO_2 presence didn't lead to relevant effect, acting as a diluent for the reaction. Moreover, the weak amount of reverse-WGS reaction remove a little amount of hydrogen produced by PDH reaction, so leading to further propane conversion. On the other hand, the reverse-WGS produces CO that, as demonstrated, has a detrimental effect on performances.

Finally, durability tests evidenced that the high pressure promotes the catalyst deactivation in the investigated operating temperature, so suggesting to change some parameters (temperature, dilution) in order to maximize catalyst lifetime without dramatically effect on membrane operating conditions.

Chapter VII
Conclusions

The research activity was carried out within the involving of the ProCEED lab of the University of Salerno within the CARENA project. The CARENA project focused on the process intensification of some productive scheme by catalytic membrane reactor; the role of UNISA within CARENA was to test and study catalysts for methane reforming and propane dehydrogenation formulated by partners, and to address suppliers towards catalytic formulations able to maximize selectivity and catalyst lifetime.

VII.1 Methane reforming

An auto-thermal reformer thermally integrated was designed and setup in order to test structured catalysts. Catalytic tests were performed on 3 different kinds of catalyzed foams, in order to evaluate the influence of heat transfer mechanism in the system performances. All foams are activated by a catalytic coverage realized by Johnson Matthey within the Ca.Re.N.A project.

Catalytic foams showed excellent activity in terms of both methane conversion and hydrogen yield, resulting able to reach thermodynamic equilibrium in very short residence time.

Preliminary tests, demonstrated that due to the temperature peak in the catalytic bed the ATR process appears not suitable for the integration in a membrane reactor. It may be however considered an open architecture, in which catalytic stage and hydrogen removal stage are separated.

The use of thermally conductive catalyzed foams lead to a faster approach to thermodynamic equilibrium, as reported in the comparison with a commercial honeycomb monolithic catalyst. The complex foam structure in one hand promotes a continuous mixing of the reaction stream, in the other hand allows conductive heat transfer along the catalyst resulting in a flatter thermal profile. As a result, the more the temperature profile appears flat, the more the reaction stream quickly reaches a composition close to the final value. In addition, by achieving a flat thermal profile, is possible in one hand to reduce hot-spot phenomena, that may causes local cracking phenomena, in the other hand to promote and then to accelerate the endothermic reforming

reactions, so allowing to operate at higher GHSV values (both by increasing reactants rate or reducing catalytic volume).

In a first analysis, no simply direct correlations are found between material intrinsic thermal conductivity and thermal profile measured in the foam: paradoxically, ZrO_2 has the lower thermal conductivity, but ZrO_2 foam results in the flatter thermal profile. The unexpected result is due to the very complex solid-gas system, and a very large amount of parameters should be considered. As a final consideration, the overall heat exchange rates in both solid-gas and solid-solid phases play a crucial role in this kind of catalytic system, and the optimal thermal management may improve system performances.

On the contrary, SR catalytic tests carried out on foam catalysts evidenced the relevance of heat transfer management on the catalytic performances. In particular, experimental results carried out at relatively low temperature (550°C) and different operating conditions, demonstrated that the samples characterized by the highest thermal conductivity showed the best results in terms of methane conversion and hydrogen yield. The beneficial effect was more evident in the more extreme conditions (higher S/C ratios, higher reactants rates), in which the heat transfer limitations are more evident. One of the most interesting effect resulting by the highest support thermal conductivity may be the possibility to obtain a flattening of the radial profile, that in one hand maximizes the heat transfer rate from the reactor walls to the catalyst.

Moreover, the random tridimensional structure of the foam catalyst, characterized by very high porosity and tortuosity, enhances the mass transfer and the mixing of the reacting mixture, obtaining a more uniform reaction condition along the whole catalytic bed, resulting in a more effective reaction system.

VII.2 Propane DeHydrogenation

In the propane dehydrogenation, usually high attention is paid on the operating parameters (temperature, pressure, dilution, contact time) and catalytic formulation, but also the reactor geometry play an important role due to the possibility of side-reactions also in the homogeneous phase. Too high residence time of the reactants and products at high temperature outside the catalytic volume may result in uncontrolled reactions of the process stream, resulting in a dramatic drop of process selectivity. Specific tests demonstrated that non-optimized reactants pre-heating step led to a partial feed decomposition due to uncontrolled homogeneous gas phase reactions, that causes a sensible feed loss. Furthermore, due to homogeneous reactions, in the catalytic volume could be delivered a process stream completely different to the fed mixture. Therefore some components generated in the homogeneous phase may in one hand block the catalyst active sites, in the other hand promote the coke formation, resulting in a catalytic surface coverage and then

in the catalyst deactivation. Also at the catalyst outlet section attention must be played due to the possibility to obtain side-reactions in the product stream, particularly in the case of the PDH reaction where the higher propylene reactivity. Based on the achieved consideration, a specific lab-scale reactor was designed in order to minimize the unwanted side-reactions in the homogeneous gas phase.

From the catalyst point of view, the role of each component of the catalytic formulation was also investigated. Performed tests demonstrated the chemical properties of a support may affect catalyst performances by promoting unwanted side-reactions. Platinum played a fundamental role in the PDH reaction, maximizing the propane conversion and addressing the process selectivity toward the production of propylene. Unfortunately, the pure Pt was quickly deactivated by coke deposition: in this regard, tin demonstrated to have a promotion effect on Pt/Al_2O_3 catalyst, improving Pt dispersion on the catalytic surface and stabilizing the catalytic sites. As a consequence, the selectivity towards propylene and the catalyst lifetime are improved.

If in one hand steam addition in fed propane increases catalyst life, on the other hand reforming reactions may occur. In this sense, the role of the support was investigated, highlighting that ceria-based catalysts promotes reforming reactions, leading to a relevant decrease in process selectivity.

Catalytic formulation was addressed to use alumina-modified support, in order to not affect the high specific surface of the Al_2O_3, and to neutralize its surface acidity. CARENA partners provided Pt-Sn based catalysts on modified alumina. Specific tests carried out on S-01 sample evidenced that an appropriate modification of alumina support may lead to higher selectivity. Moreover, at higher temperature the catalyst regeneration may result in an improving in catalytic performances. On the other hand, a lower temperature, compatible to a membrane coupling, still led to appreciable conversion values, offering in addition a very low catalyst deactivation and an excellent selectivity to propylene. The gain linked to a quite low temperature was also confirmed by activity tests on the S-02 sample, also based on an alumina-modified support. The two formulations demonstrated to be not much sensible to reforming reaction, while the fed steam amount help to minimize the selectivity to coke. Since the catalytic system should be designed to be used in a membrane reactor, the operating pressure is also a crucial parameter for the membrane but also for the catalyst. Of course the increasing in the operating pressure promotes cracking phenomena, decreasing the selectivity to propylene and enhancing the coke formation. However, the S-02 sample, despite a less weakly pronounced initial catalytic activity, resulted the less sensible to the extreme operating conditions, so resulting the best candidate to the membrane integration.

According to the PDH stage exploit in the CARENA project, the effect of the presence of CO and CO_2 in the fed stream was investigated. The carbon monoxide resulted the most detrimental compound, leading to an overall

performances worsening. In one hand the CO affinity with Pt sites led to a partial reduction of catalytic activity, on the other hand the not negligible contribution of WGS reaction resulted in an hydrogen production outside the PDH reaction, so partially reducing the propane conversion. On the contrary, the CO_2 presence didn't lead to relevant effect, acting as a diluent for the reaction. Moreover, the weak amount of reverse-WGS reaction remove a little amount of hydrogen produced by PDH reaction, so leading to further propane conversion. On the other hand, the reverse-WGS produces CO that, as demonstrated, has a detrimental effect on performances.

Finally, durability tests evidenced that the high pressure promotes the catalyst deactivation in the investigated operating temperature, so suggesting to change some parameters (temperature, dilution) in order to maximize catalyst lifetime without dramatically effect on membrane operating conditions.

Chapter VIII **References**

BAI, L., ZHOU, Y., ZHANG, Y., LIU, H., SHENG, X. & XUE, M. 2011. Influence of the Competitive Adsorbates on the Catalytic Properties of PtSnNaMg/ZSM-5 Catalysts for Propane Dehydrogenation. *Industrial & Engineering Chemistry Research,* 50**,** 4345-4350.

BARGHI, B., FATTAHI, M. & KHORASHEH, F. 2012. Kinetic modeling of propane dehydrogenation over an industrial catalyst in the presence of oxygenated compounds. *Reaction Kinetics, Mechanisms and Catalysis*, 107**,** 141-155.

BERG, R. C. & VORA, B. V. 1982. Detergent alkylate. *Encyclopedia of Chemical Processing and Design.* New York: Marcel Dekker.

BHARADWAJ SS, S. L. 1995. Catalytic partial oxidation of natural gas to syngas. 42, 109-127.

BLOCH, H. S. 1969. *and other patents on the catalytic*. U.S. patent application.

CHEN, M., XU, J., LIU, Y.-M., CAO, Y., HE, H.-Y. & ZHUANG, J.-H. 2010. Supported indium oxide as novel efficient catalysts for dehydrogenation of propane with carbon dioxide. *Applied Catalysis A: General***,** 35-41.

CRACIUN R, D. W., KNOZINGER H. 2002. The effect of CeO2 structure on the activity of supported Pd catalysts used for methane dteam reforming. 230, 153-168.

D.C.R.M. SANTOS, L. M., F.B. PASSOS 2009. The effect of the addition of Y2O3 to Ni/a-Al2O3 catalysts on the autothermal reforming of methane. (articolo in stampa).

DAVANNEY, M. 2009. Marketing Research Report: Propylene. *In:* CONSULTING, S. (ed.) *Chemical Economics Handbook.*

DHAMMIKE DISSANAYAKE, M. P. R., KARL C. C. KHARAS2 AND JACK H. LUNSFORD 1991. Partial oxidation of methane to carbon monoxide and hydrogen over a Ni/Al2O3 catalyst 132, 117-127

DIDENKO, L. P., SAVCHENKO, V. I., SEMENTSOVA, L. A., CHIZHOV, P. E. & BYKOV, L. A. 2013. Dehydrogenation of propane in a combined membrane reactor with hydrogen-permeable palladium module. *Petroleum Chemistry,* 53**,** 27-32.

DINSE, A., FRANK, B., HESS, C., HABEL, D. & SCHOMACKER, R. 2008. Oxidative dehydrogenation of propane over low-loaded vanadia catalysts: Impact of the support material on kinetics and selectivity. *Journal of Molecular Catalysis A: Chemical***,** 28-37.

DONSÌ, F., CIMINO, S., DI BENEDETTO, A., PIRONE, R. & RUSSO, G. 2005. The effect of support morphology on the reaction of oxidative dehydrogenation of ethane to ethylene at short contact times. *Catalysis Today***,** 551-559.

DUAN, Y., ZHOU, Y., ZHANG, Y., SHENG, X. & XUE, M. 2010. Effect of Sodium Addition to PtSn/AlSBA-15 on the Catalytic Properties in Propane Dehydrogenation. *Catalysis Letters,* 141**,** 120-127.

DUAN, Y., ZHOU, Y., ZHANG, Y., SHENG, X., ZHOU, S. & ZHANG, Z. 2012. Effect of aluminum modification on catalytic properties of PtSn-based catalysts supported on SBA-15 for propane dehydrogenation. *Journal of Natural Gas Chemistry,* 21**,** 207-214.

EGOY, M. 2012. *European propylene sellers face a tough fourth quarter market* [Online].

FARJOO, A., KHORASHEH, F., NIKNADDAF, S. & SOLTANI, M. 2011. Kinetic modeling of side reactions in propane dehydrogenation over Pt - Sn/γ - Al2O3 catalyst. *Scientia Iranica,* 18**,** 458-464.

FATTAHI, M., KHORASHES, F., SAHEBDELFAR, S., TAHRIRI ZANGENEHB, F., GANJI, K. & SAEEDIZAD, M. 2011. The effect of oxygenate additives on the performance of Pt–Sn/γ-Al2O3 catalyst in the propane dehydrogenation process. *Scientia Iranica C ( ) ( ),* –.

GRAIG, R. G. & SPENCE, D. C. 1986. Catalytic dehydrogenation of liquefied petroleum gas by the Houdry Catofin and Catadiene processes. *Handbook of Petroleum Refining Processes.* New York: McGraw-Hill.

HAENSEL, V. 1952. *and other patents on catalytic reforming with Pt catalysts assigned to UOP*. U.S. patent application.

HUANG, L., XU, B., YANG, L. & FAN, Y. 2008. Propane dehydrogenation over the PtSn catalyst supported on alumina-modified SBA-15. *Catalysis Communications***,** 2593-2597.

J. GAO, J. G., D. LIANG, Z. HOU, J. FEI, X. ZHENG 2008. Production of syngas via autothermal reforming of methane in a fluidized-bed reactor over the combined CeO2–ZrO2/SiO2 supported Ni catalysts. 33, 5493-5500.

JR-ROSTRUP-NIELSEN 1975. Steam reforming catalyst - an investigation of catalyst for tubolar steam reforming of hydrocarbons.

JR-ROSTRUP-NIELSEN 1993. Production of syntesis gas. 18, 305-324.

KLEY, I. & TRAA, Y. 2012. Influence of acid sites on the propene selectivity during propane dehydrogenation on zeolite Pt/Zn,Na-MCM-22. *Microporous and Mesoporous Materials,* 164**,** 145-147.

KUMAR, M. S., CHEN, D., HOLMEN, A. & WALMSLEY, J. C. 2009. Dehydrogenation of propane over Pt-SBA-15 and Pt-Sn-SBA-15: Effect of Sn on the dispersion of Pt and catalytic behavior. *Catalysis Today*, 17-23.

LEMOS, W. 2011. *NPRA supplement: Propylene on a rocky upward trend* [Online]. ICIS Chemical Business. Available: http://www.icis.com/resources/news/2011/03/28/9446613/npra-supplement-propylene-on-a-rocky-upward-trend/.

LI, Q., SUI, Z., ZHOU, X., ZHU, Y., ZHOU, J. & CHEN, D. 2011. Coke Formation on Pt–Sn/Al2O3 Catalyst in Propane Dehydrogenation: Coke Characterization and Kinetic Study. *Topics in Catalysis,* 54**,** 888-896.

LÖFBERGA, A., ESSAKHI, A., PAUL, S., SWESI, Y., ZANOTA, M. L., PITAULT, I. & SUPIOT, P. 2011. Use of catalytic oxidation and dehydrogenation of hydrocarbons reactions to highlight improvement of heat transfer in catalytic metallic foams. *Chemical Engineering Journal*, 49-56.

M. M.V.M. SOUZA, M. S. 2005. Autothermal reforming of methane over Pt/ZrO2/Al2O3 catalysts. 281, 19-24.

M. NURUNNABI, Y. M., S. KADO, B. LI, K. KUNIMORI, K. SUZUKI, K. FUJIMOTO, K. TOMISHIGE 2006. Additive effect of noble metals on NiO-MgO solid solution in oxidative steam reforming of methane under atmospheric and pressurized conditions. 299, 145-156

MEDRANO, J. A., JULIÁN, I., GARCÍA-GARCÍA, F. R., LI, K., HERGUIDO, J. & MENÉNDEZ, M. 2013. Two-Zone Fluidized Bed Reactor (TZFBR) with Palladium Membrane for Catalytic Propane Dehydrogenation: Experimental Performance Assessment. *Industrial & Engineering Chemistry Research*, 130304122611001.

NAWAZ, Z., TANG, X., ZHANG, Q., WANG, D. & FEI, W. 2009. SAPO-34 supported Pt–Sn-based novel catalyst for propane dehydrogenation to propylene. *Catalysis Communications*, 1925-1930.

NEXANT 2009. Alternative Routes to Propylene. *ChemSystem PERP Program.* New York, USA.

OVSITSER, O., SCHOMAECKER, R., KONDRATENKO, E. V., WOLFRAM, T. & TRUNSCHKE, A. 2012. Highly selective and stable propane dehydrogenation to propene over dispersed VOx-species under oxygen-free and oxygen-lean conditions. *Catalysis Today,* 192**,** 16-19.

PALMA, V., PALO, E., RICCA, A. & CIAMBELLI, P. 2011. Compact Multi-fuel Autothermal Reforming Catalytic Reactor for H2 Production. *Chemical Engineering Transactions,* 25**,** 641-646.

PAVLOVA, S. N., SADYKOV, V. A., FROLOVA, Y. V., SAPUTINA, N. F., VEDENIKIN, P. M., ZOLOTARSKII, I. A. & KUZMIN, V. A. 2003. The effect of the catalytic layer design on oxidative

dehydrogenation of propane over monoliths at short contact times. *Chemical Engineering Journal***,** 227-234.

REN, Y., ZHANG, F., HUA, W., YUE, Y. & GAO, Z. 2009. ZnO supported on high silica HZSM-5 as new catalysts for dehydrogenation of propane to propene in the presence of CO2. *Catalysis Today***,** 316-322.

ROH, H. S., JUN, K. W., DONG, W. S., CHANG, J. S., PARK, S. E. & JOE, Y. I. 2002. Highly active and stable Ni/Ce–ZrO2 catalyst for H2 production from methane 181, 137-142

RUCKENSTEIN, E. & HU, Y. H. 1999. Methane partial oxidation over NiO/MgO solid solution catalysts 183, 85-92.

S. AYABE, H. O., T. UTAKA, R. KIKUCHI, K. SASAKI, Y. TERAOKA, K. EGUCHI 2003. Catalytic autothermal reforming of methane and propane over supported metal catalysts. 241, 261-269.

S. BEDRANE, C. D., D. DUPREZ 2002. Investigation of the oxygen storage process on ceria- and ceria–zirconia-supported catalysts. 75, 401-405

SAMAVATI, A., FATTAHI, M. & KHORASHEH, F. 2013. Modeling of Pt-Sn/γ-Al2O3 deactivation in propane dehydrogenation with oxygenated additives. *Korean Journal of Chemical Engineering,* 30**,** 55-61.

SANFILIPPO, D., BUONOMO, F., FUSCO, G. & MIRACCA, I. 1998. Paraffins Activation through Fluidized Bed Dehydrogenation: the Answer to Light Olefins Demand Increase. *Stud. Surf. Sci. Catal***,** 919-924.

SHISHIDO, T., SHIMAMURA, K., TERAMURA, K. & TANAKA, T. 2012. Role of CO2 in dehydrogenation of propane over Cr-based catalysts. *Catalysis Today,* 185**,** 151-156.

SOKOLOV, S., STOYANOVA, M., RODEMERCK, U., LINKE, D. & KONDRATENKO, E. V. 2012. Comparative study of propane dehydrogenation over V-, Cr-, and Pt-based catalysts: Time on-stream behavior and origins of deactivation. *Journal of Catalysis,* 293**,** 67-75.

SUN, P., SIDDIQI, G., VINING, W. C., CHI, M. & BELL, A. T. 2011. Novel Pt/Mg(In)(Al)O catalysts for ethane and propane dehydrogenation. *Journal of Catalysis,* 282**,** 165-174.

TROVARELLI, A. 1996. Catalytic Properties of Ceria and CeO_2-Containing Materials 38, 439-520.

VU, B. K. & SHIN, E. W. 2010. Influence of Oxygen Mobility over Supported Pt Catalysts on Combustion Temperature of Coke Generated in Propane Dehydrogenation. *Catalysis Letters,* 141**,** 699-704.

VU, B. K., SHIN, E. W., AHN, I. Y., HA, J.-M., SUH, D. J., KIM, W.-I., KOH, H.-L., CHOI, Y. G. & LEE, S.-B. 2012. The Effect of Tin–Support Interaction on Catalytic Stability over Pt–Sn/xAl–SBA-15

Catalysts for Propane Dehydrogenation. *Catalysis Letters*, 142**,** 838-844.

VU, B. K., SONG, M. B., AHN, I. Y., SUH, Y.-W., SUH, D. J., KIM, J. S. & SHIN, E. W. 2011a. Location and structure of coke generated over Pt–Sn/Al2O3 in propane dehydrogenation. *Journal of Industrial and Engineering Chemistry*, 17**,** 71-76.

VU, B. K., SONG, M. B., AHN, I. Y., SUH, Y.-W., SUH, D. J., KIM, W.-I., KOH, H.-L., CHOI, Y. G. & SHIN, E. W. 2011b. Pt–Sn alloy phases and coke mobility over Pt–Sn/Al2O3 and Pt–Sn/ZnAl2O4 catalysts for propane dehydrogenation. *Applied Catalysis A: General***,** 25-33.

VU, B. K., SONG, M. B., AHN, I. Y., SUH, Y.-W., SUH, D. J., KIM, W.-I. L., KOH, H.-L., CHOI, Y. G. & SHIN, E. W. 2011c. Propane dehydrogenation over Pt–Sn/Rare-earth-doped Al2O3: Influence of La, Ce, or Y on the formation and stability of Pt–Sn alloys. *Catalysis Today*, 164**,** 214-220.

WADDAMS, A. L. 1980. *Chemicals from Petroleum - 4th edition,* Houston, Gulf Publishing Company.

WANG, J., ZHANG, F., HUA, W., YUE, Y. & GAO, Z. 2012. Dehydrogenation of propane over MWW-type zeolites supported gallium oxide. *Catalysis Communications*, 18**,** 63-67.

WEISS, A. H. 1970. The manufacture of propylene (158th Meeting of the American Chemical Society, 10–12 September 1969). *Refining Petroleum for Chemicals, Advances in Chemistry Series.* Washington DC: American Chemical Society.

X. DONG, X. C., Y. SONG, W. LIN 2007. Effect of Transition Metals (Cu, Co and Fe) on the Autothermal Reforming of Methane over Ni/Ce0.2Zr0.1 Al0.7 Oδ Catalyst. 16, 31-36.

X. WU, L. X., D. WENG 2004. The thermal stability and catalytic performance of Ce-Zr promoted Rh-Pd/g-Al2O3 automotive catalysts. 221, 375-383.

YU, C.-L., XU, H.-Y., CHEN, X.-R., GE, Q.-J. & LI, W.-Z. 2010. Preparation, characterization, and catalytic performance of PtZn-Sn/SBA-15 catalyst for propane dehydrogenation. *JOURNAL OF FUEL CHEMISTRY AND TECHNOLOGY*, 38 (3)**,** 308-312.

YU, C., XU, H., GE, Q. & LI, W. 2007. Properties of the metallic phase of zinc-doped platinum catalysts for propane dehydrogenation. *Journal of Molecular Catalysis A: Chemical***,** 80–87.